



JRC Testing and Demonstration Hub for the GNSS Component of the EU Space Programme

Inventory of GNSS Testing Capabilities

Piccolo, A., Cucchi, L., Gioia, C., Tegedor Navarro, F., Damy, S., Motella, B., Menzione, F., Bonenberg, L., Zoccarato, P., Picchi, O., Bonavitacola, F., Basso, M., Sgammini, M., Paonni, M., Fortuny Guasch, J.

2024



This document is a publication by the Joint Research Centre (JRC), the European Commission's science and knowledge service. It aims to provide evidence-based scientific support to the European policymaking process. The contents of this publication do not necessarily reflect the position or opinion of the European Commission. Neither the European Commission nor any person acting on behalf of the Commission is responsible for the use that might be made of this publication. For information on the methodology and quality underlying the data used in this publication for which the source is neither Eurostat nor other Commission services, users should contact the referenced source. The designations employed and the presentation of material on the maps do not imply the expression of any opinion whatsoever on the part of the European Union concerning the legal status of any country, territory, city or area or of its authorities, or concerning the delimitation of its frontiers or boundaries.

Contact information

Name: Joaquim Fortuny-Guasch
Address: Via Enrico Fermi, 2749, I-21027 Ispra (VA), Italy
Email: Joaquim.Fortuny-Guasch@ec.europa.eu
Tel.: +39 0332 785104

EU Science Hub
<https://joint-research-centre.ec.europa.eu>

JRC137126

EUR 31883 EN

Print	ISBN 978-92-68-13852-6	ISSN 1018-5593	doi:10.2760/171198	KJ-NA-31-883-EN-C
PDF	ISBN 978-92-68-13853-3	ISSN 1831-9424	doi:10.2760/726940	KJ-NA-31-883-EN-N

Luxembourg: Publications Office of the European Union, 2024

© European Union, 2024



The reuse policy of the European Commission documents is implemented by the Commission Decision 2011/833/EU of 12 December 2011 on the reuse of Commission documents (OJ L 330, 14.12.2011, p. 39). Unless otherwise noted, the reuse of this document is authorised under the Creative Commons Attribution 4.0 International (CC BY 4.0) licence (<https://creativecommons.org/licenses/by/4.0/>). This means that reuse is allowed provided appropriate credit is given and any changes are indicated.

For any use or reproduction of photos or other material that is not owned by the European Union permission must be sought directly from the copyright holders.

All content © European Union 2024, unless otherwise specified.

How to cite this report: European Commission, Joint Research Centre, Piccolo, A., Cucchi, L., Gioia, C., Tegedor Navarro, F., Damy, S., Motella, B., Menzione, F., Bonenberg, L., Zoccarato, P., Picchi, O., Bonavitacola, F., Basso, M., Sgammini, M., Paonni, M. and Fortuny Guasch, J., JRC Testing and Demonstration Hub for the GNSS Component of the EU Space Programme, Publications Office of the European Union, Luxembourg, 2024, JRC137126.

Document Change Record

Reason for the Change	Issue	Revision	Date
First issue of the document.	1	0	July 2021
<p>Second issue of the document integrating new testing capabilities and updating existing ones. The main changes are summarized below with new or modified sections with respect to the previous document issue.</p> <p>§ 3.1.5 GNSS Antennas PCO/PCV Characterization. § 3.2.2 Performance Assessment of SBAS-enabled Maritime Receivers § 3.3.4 Highly degraded GNSS environment - Test Drive in Milan § 3.4 Galileo High Accuracy Service § 3.5 Galileo Timing Service § 3.6 Galileo OSNMA Service § 3.7 Galileo ACAS Service § 3.8 Galileo I/NAV Improvement Testing Capability § 3.9 ARAIM Service § 3.10 Galileo Space Service § 3.11 Complementary Position, Navigation and Timing (C-PNT) § 3.12 GNSS Signal Record & Replay Testing § 3.13.3 JRC GNSS simulated attacks library § 4 Future Update of the Inventory of GNSS Testing Capabilities with reference to the future updates <ul style="list-style-type: none"> - LEO-PNT Test Bench - Norway Jammer Test Scenarios - Radio Frequency Interference from Space - CRPA Antenna Testing - GNSS Data Library </p>	2	0	April 2024

Contents

Abstract	1
Acknowledgements	2
1 Introduction.....	3
1.1 Scope of the Document.....	3
1.2 Structure of the Document	4
2 General Terms and Conditions	5
2.1 Preparatory Activities	5
2.2 General Conditions	6
2.3 Contact Points for General Inquiries and logistics.....	6
3 Testing Capabilities Catalogue	7
3.1 Antenna Measurements and Characterisation.....	7
3.1.1 The EMSL Laboratory	7
3.1.2 Antenna measurements with a Vector Network Analyser	9
3.1.3 Antenna measurements with a GNSS simulator	11
3.1.4 Antenna array measurements.....	12
3.1.5 GNSS Antennas PCO/PCV Characterization	15
3.2 Standardization and Conformance Testing.....	18
3.2.1 Conformance testing of eCall devices	18
3.2.2 Performance Assessment of SBAS-enabled Maritime Receivers.....	19
3.2.3 Performance assessment of Galileo-enabled ship-borne GNSS receivers.....	22
3.2.4 Assessment of Galileo HAS performance for vehicle in urban scenario.....	25
3.2.5 Performance assessment of smartphones exposing raw measurements	28
3.2.5.1 Smartphones testing using live signals in space	29
3.2.5.2 Smartphone testing using a GNSS simulator	29
3.3 Retrieval of Reference Trajectory Solutions	32
3.3.1 GNSS/IMU based reference solution: an agriculture case study	32
3.3.2 GNSS based reference solution: a drone case study	34
3.3.3 Total station based surveying.....	36
3.3.3.1 Static survey: a 5G case study	36
3.3.3.2 Robotic Tracking Station	37
3.3.4 Highly Degraded GNSS Environment – Test Drive in Milan	38
3.4 Galileo High Accuracy Service	39
3.4.1 Reference HAS User Algorithm	39
3.4.2 HAS User Algorithm Testbed	40
3.4.3 Testing of HAS Performance	41
3.5 Galileo Timing Service	43
3.5.1 UTC Time Scale Transfer	43
3.5.1.1 UTC(IT) Calibration.....	44

3.5.2	Timing testing via Record & Replay	45
3.6	Galileo OSNMA Service	47
3.6.1	Generation of the Galileo OSNMA data stream.....	47
3.6.1.1	I/NAV data streams	47
3.6.1.2	OSNMA record and replay	47
3.6.2	Set-up for OSNMA testing	47
3.6.2.1	OSNMA-enabled receivers	47
3.6.2.2	Test set-up.....	47
3.6.3	OSNMA Post Processing.....	48
3.6.4	Examples of supported projects.....	49
3.6.4.1	BANSHEE.....	49
3.6.4.2	ASGARD	49
3.7	Galileo ACAS Service	51
3.7.1	Paula User Terminal	52
3.8	Galileo I/NAV Improvements Testing Capability	54
3.8.1	Testing strategy.....	54
3.8.2	Test Conditions	55
3.9	ARAIM User Algorithm Implementation	56
3.10	Galileo for Space Applications	58
3.10.1	An Integrated SSV Test Bench.....	59
3.10.1.1	User Mission Definition	60
3.10.1.2	RF Calibration.....	60
3.10.1.3	Antenna Patterns Implementation.....	61
3.10.1.4	Reference GNSS COTS Receiver	62
3.10.2	JRC-ISSVTB Configuration	63
3.10.3	GNSS Spaceborne Receiver Testing Capability	64
3.10.4	GASPER P2OD Test Setup	66
3.11	Complementary Position, Navigation and Timing (C-PNT)	67
3.11.1	JRC Ispra site as C-PNT Demonstrator (Living Labs).....	67
3.11.2	C-PNT Demonstration – Precise Time Transfer.....	67
3.11.3	C-PNT Demonstration – Indoor and Outdoor Positioning.....	69
3.12	GNSS Signal Record & Replay Testing	71
3.12.1	SDR (Software Defined Radio) Record & Replay System	71
3.12.2	LabSat-3 platform.....	74
3.13	Laboratory testing with RFI and spoofing signals	76
3.13.1	Testing of GNSS receivers with RFI signals	76
3.13.2	Testing of GNSS receivers with spoofing signals.....	79
3.13.3	JRC GNSS simulated attacks library	80
3.13.3.1	Nominal Scenario	80

3.13.3.2 Meaconer	82
3.13.3.3 Synchronized RFCS-like Spoofers	83
3.13.3.4 Advanced Spoofers	84
3.13.3.5 Security Code Estimation and Replay	86
3.14 Testing at JRC Campus	88
3.14.1 JRC Ispra Campus Description	88
3.14.2 JRC Living Labs	89
3.14.3 Test Cases	90
3.14.3.1 SARA drone flight trials in the JRC Campus	90
3.14.3.2 Testing of an indoor navigation app on a smartphone	90
3.14.3.3 VALOUR project	92
4 Future Updates on the Inventory of GNSS Testing Capabilities	94
4.1 LEO-PNT Test Bench	94
4.2 Norway Jammer Tests Scenarios	95
4.3 Radio Frequency Interference Detection from Space	96
4.4 CRPA Antenna Testing	97
4.5 GNSS Data Library	98
5 Conclusions	99
References	101
List of abbreviations and definitions	108
List of figures	114
List of tables	118

Abstract

The European Commission (EC) Joint Research Centre (JRC), in the frame of a scientific and technical support activity with the Satellite Navigation Unit of the EC Directorate General Defence Industry and Space (DEFIS) and the European Union Agency for the Space Programme (EUSPA), has agreed to facilitate testing and demonstrations activities of Research and Development (R&D) Actions under the European Union (EU) Global Navigation Satellite System (GNSS) Programmes. In this context, Horizon Europe and Galileo Fundamental Elements project consortia are invited to come to the JRC and access the GNSS testing facilities based in its Ispra Site. With the aim to promote this testing activities, a reference document providing an up-to-date inventory of the GNSS testing capabilities was published in July 2021 and now, with the present inventory, is updated and extended. From the first release of the inventory, the JRC keeps on improving its GNSS laboratory testing capabilities, addressing in the best manner the new challenges and evolving user needs in the GNSS domain, all with a clear focus on Galileo. Since the declaration of the initial services in 2016, Galileo has enriched its portfolio of services, introducing clear differentiators with respect to other GNSS systems. In particular, the Galileo Open Service (OS) has been upgraded with an improved navigation message, acting as a boost of the robustness and time to first fix, the High Accuracy Service (HAS) enables a decimetre-level accuracy through real-time corrections broadcast by Galileo satellites, the OS Navigation Message Authentication (OSNMA) strengthens the security and resilience against spoofing attacks, the Safety-of-Life (SoL) service enables the implementation of horizontal ARAIM service, responding the requirements of civil aviation. This report is structured as follows. Firstly, it sets the general terms and conditions to request the access to the testing facilities, and secondly, it provides a comprehensive summary of the GNSS testing capabilities that are currently available at the JRC. In many occasions, a reference to past testing campaigns is made to illustrate the typical testbeds and results that were produced. With this reference document at hand, interested project consortia should be able to specify an initial test plan with the required level of detail.

Acknowledgements

The development of the testing capabilities and associated laboratory infrastructures subject of this report has only been possible thanks to the constant support and trust from the colleagues at the Satellite Navigation Unit of the European Commission (EC) Directorate General Defence Industry and Space (DEFIS), and the European Union Agency for the Space Programme (EUSPA). Over the last few years, thanks to this fruitful cooperation, the JRC has established a scientific and technical team that is actively supporting the implementation of the EU Global Navigation Satellite System (GNSS) Components of the EU Space Programme Galileo and EGNOS.

Likewise, the support from the colleagues at the Strategy, Work Programme and Resources (JRC.A) and the Technologies for Space, Connectivity and Economic Security (JRC.E2) Directorates of the JRC is also acknowledged.

Authors

Andrea Piccolo, Luca Cucchi, Ciro Gioia, Javier Tegedor, Sophie Damy, Beatrice Motella, Francesco Menzione, Lukasz Bonenberg, Paolo Zoccarato, Ottavio Picchi, Fausto Bonavitacola, Marco Basso, Matteo Sgammini, Matteo Paonni, Joaquim Fortuny-Guasch

European Commission, Joint Research Centre
Directorate E, Societal Resilience and Security
Unit E2, Technologies for Space, Connectivity and Economic Security, Italy

1 Introduction

1.1 Scope of the Document

The scope of the document is to provide an overall description of the portfolio of Global Navigation Satellite System (GNSS) testing capabilities currently available at the European Commission's Joint Research Centre (JRC), at the premises of its Ispra site. In particular, this document issue is the result of a major revision and extension of the laboratory testing capabilities with respect to those reported in a previous document issue [1].

The facilitation of testing and demonstration activities in the context of R&D Actions under the European Union (EU) GNSS Programmes at the JRC started back in 2012, with the EUSPA FP7 Project DETECTOR [2]. Since then, JRC's testing capabilities have been kept continuously up-to-date and upgraded in relation with the evolution of the GNSS Programmes and, more specifically, that of Galileo and EGNOS. This reviewed catalogue of the testing capabilities is, as the previous release, rich and covers numerous domains. Some examples of testing capabilities that have been kept and improved are the detection and characterisation of radio-frequency interference (RFI) to protect and increase the use of GNSS in critical mass market applications (i.e. road, maritime, drones and aviation), and the development of GNSS Receivers with integrity monitoring capabilities for vehicular and pedestrian platform through several EC R&D actions [1].

The scientific support activity behind the portfolio of GNSS testing capabilities was consolidated and led to a formal agreement with the Directorate General Defence Industry and Space (DG DEFIS) of the European Commission (EC), in charge of the management of the EU GNSS Programmes, and the European Union Agency for the Space Programme (EUSPA). Over the last years, the scientific team at the JRC has kept on strengthening the range of testing capabilities on the user-segment of GNSS and, more recently, has integrated new capabilities ad-hoc for GNSS receivers used in space on-board satellites. The main upgrades and additions integrated in this inventory can be summarized as follows:

- A new capability to characterize the phase center variation (PCV) and phase center offset (PCO) of GNSS antennas is introduced. These parameters are crucial for high-precision applications, particularly for satellite GNSS antennas in LEO and above.
- A dedicated test bench designed and thoroughly tested to assess ship-borne SBAS (Satellite-Based Augmentation System) receivers against a new IEC standard. This development aligns with the planned deployment of the EGNOS Maritime Service.
- An improved GNSS performance assessment in an urban scenario. Data collection in Milan using a reference navigation system and multiple GNSS receivers on-board a vehicle is reported. The resulting datasets and reference trajectory aid in assessing the Galileo High Accuracy Service (HAS) in urban environments.
- A reference Galileo HAS implementation. This capability is introduced to facilitate the implementation and assessment of the Galileo HAS on GNSS receivers. Notably, a dedicated HAS testbed evaluates user algorithm performance across various configurations.
- A Galileo timing service testbed and procedures to assess timing receivers' conformity against the requirements specified in the CEN/CENELEC Galileo Timing Receiver Standard. This preparation aligns with the planned introduction of the Galileo Timing Service.
- Developed under the PAULA project and later handed over to the JRC, the ACAS (Assisted Commercial Authentication Service) testbed is showcased. Interestingly, the PAULA testbed serves as a multi-purpose platform, aiding the assessment of Galileo OSNMA and HAS performance.
- A testing capability to verify GNSS receivers implementing Galileo I/NAV improvements, where some example results from a recent test campaign, coordinated by EUSPA, are included.
- A novel horizontal ARAIM service test capability based on the JRC's ARTEX ARAIM testbed is reported. This implementation complies with civil aviation requirements and the safety-of-life (SoL) service.
- A new integrated space service volume test bench (ISSVTB) for space GNSS Receivers is presented, reporting illustrative results from the H2020 GASPER project, the first IOV/IOD mission exploiting real-time precise orbit determination and Galileo HAS.

- New testing capabilities developed for the demonstrations of Complementary PNT (C-PNT) technology platforms at the JRC Ispra Campus in 2021 and 2022, which include timing and indoor and outdoor positioning technologies not solely reliant on GNSS.
- An extension of the record and replay testing capabilities of GNSS signals based on different HW platforms depending on the requirements on the sampling rate, number of simultaneous frequency bands, and bit depth of the recorded samples, is introduced.
- A library of GNSS jamming, meaconing, and spoofing scenarios specifically designed for drones. This library can serve other use-cases, such as those relevant in the automotive or civil aviation domains.

Project consortia potentially interested in conducting tests and demonstrations at the JRC need to have access to a reference document where the testing capabilities available are thoroughly reported, possibly with use case examples and results from test campaigns facilitated in the past. This document is aimed at addressing specifically this need and provide a comprehensive set of information that can set the potential users in the position to specify a test plan with the required level of detail at the submission of a project proposal. At a later stage, project consortia that were successful in the evaluation process and planned the tests and demonstrations at the JRC will be asked to share the test plan. This is required to assess the feasibility in terms of the equipment needed and the temporal availability of the laboratory sufficiently in advance.

Finally, the evolution of the support activity with DG DEFIS and the EUSPA will entail the development of new testing capabilities at the JRC. Consequently, to integrate these changes, this document is expected to be reviewed and updated on a regular basis in the coming years.

1.2 Structure of the Document

This document has been structured as follows

- Section 1 is this introduction which provides the scope of the document and an overview of the JRC testing and demonstration capability at Ispra premises.
- Section 2 provides the general terms and conditions to access to the GNSS testing facilities of the JRC, during the entire process of preparation, execution, and finalisation of the requested tests.
- Section 3 describes the testing capabilities available to date at the JRC thorough 14 main categories which includes:
 - GNSS antenna measurements and characterisation
 - GNSS receiver testing, measurement of reference trajectories, GNSS timing receiver characterisation and integrity monitoring
 - new Galileo services testing capabilities (i.e. High Accuracy Service (HAS), Galileo Open Service Navigation Message Authentication (OSNMA), Assisted Commercial Authentication Service (ACAS), I/NAV Improvements)
 - Space Service Volume testing capabilities
 - Complementary PNT demonstration capabilities
 - Radio frequency interference testing, radio frequency signal record and replay, and the outdoor facilities of the JRC Living Labs.
- Section 4 includes a summary of the planned upgrades and extensions currently under development, which will be integrated in future release of the inventory.

2 General Terms and Conditions

2.1 Preparatory Activities

For the preparation of a verification and validation test phase at JRC laboratory facility, a project consortium can refer to the actions timeline of Table 1, where T_v denotes the date of the event to be held at the JRC premises. The scheduling made in this table is to be considered as indicative only, and therefore, modifications to the proposed timeline are expected to be agreed on a case by case with the Project Consortium.

Table 1. Typical interactions between JRC and the project consortium requesting the facilitation of testing and demonstration activities.

Start Event	End Event	Actions
$T_v - 3m$	$T_v - 2.5m$	JRC expects to receive the following items: <ul style="list-style-type: none"> - Test plan with test cases description including: objectives, overall description, test facility, test set-up, step-by-step procedure, pass/fail criteria if applicable - Control software/Drivers/Datasheet/user manual of relevant hardware (HW) equipment under test from Project Consortium.
$T_v - 2.5m$	$T_v - 2m$	JRC examines the documentation and provides feedback. Possible interactions between JRC and consortium via email exchanges and/or teleconference might be arranged to agree pending issues such as the test plan, logistics, the booking of test facilities and the readiness of the equipment under test.
$T_v - 2m$	$T_v - 1m$	JRC expects to receive the Device Under Test (DUT) and the necessary HW equipment at the Reception & Shipment of Goods Desk of JRC's Ispra Site.
$T_v - 1m$	$T_v - 0.5m$	JRC is in charge of setting up the test bed and facilitating a preparatory dry-run. In case of need, during these preparatory phase, remote access to the test equipment can be granted to the consortium. Log data and analysis results are exchanged and verified. Meetings with consortium are scheduled at regular basis to assess that the results are in line with the expectations.
T_v	$T_v + 3d$	Execution of the test campaign or demonstration event at the JRC premises in Ispra. Typical duration of the test campaign is 2 to 3 days.
$T_v + 3d$	$T_v + 5d$	JRC collects and shares the data logs and tests results other than those already gathered directly by the consortium during the test campaign.
$T_v + 5d$	$T_v + 10d$	The Project Consortium arranges the pick-up of the test equipment from the Reception & Shipment of Goods Desk of JRC's Ispra Site. The test equipment is returned to the Consortium.

2.2 General Conditions

The access to the JRC laboratory facility is driven by the following conditions:

- JRC facilities and support from the technical staff are available to facilitate testing and demonstration activities under EC initiatives as Horizon Europe and Galileo Fundamental Elements R&D Actions.
- This document is intended to be used as a guideline during the preparation of the test plan, which is under the responsibility of the Project Consortium requesting the access to the JRC testing facilities.
- The facilitation of the testing and demonstration activities proposed by the Project Consortium is subject to the feasibility of the test plan and the availability of required testing facilities and equipment. Although there is no specific limit on the duration of the test campaign, since the test facilities are made available to multiple project consortia, for obvious reasons, it is suggested to keep the duration to a minimum.
- In case of testing activities to be carried out in the JRC premises, it is worth underlining that the final test campaign or demonstration event represents just the last step of a set of preparatory activities aimed at defining and configuring the test environment properly.

2.3 Contact Points for General Inquiries and logistics

The contact point details for any inquiries regarding the access to the GNSS testing facilities of the JRC is as follows:

Head of the Galileo Sector
e-mail: JRC-GALILEO@ec.europa.eu
Phone: +39 0332 785104
Via Enrico Fermi, 2749
I-21027 Ispra, Italy
EC Joint Research Centre
Direktorat E Societal Resilience and Security
Unit E2 Technologies for Space, Connectivity and Economic Security

Any shipments of equipment needed for the testing campaigns at the JRC shall be addressed to:

e-mail: JRC-ISPRA-RICEVIMENTO-MERCI@ec.europa.eu
Phone: +39 0332 786164
EC Joint Research Centre
Reception & Shipment of Goods Service
Via Enrico Fermi, 2749
I-21027, Italy

It is important to keep in mind that all parcels shall arrive accompanied with a pro-forma invoice listing the items shipped to the JRC and a note stating that "All the goods are entering the JRC Ispra Site temporarily for testing purposes". In the absence of the pro-forma invoice, please be aware that parcels might be rejected at the JRC Customs and returned to the sender.

3 Testing Capabilities Catalogue

This section gives a comprehensive overview of the GNSS receiver testing capabilities that are currently available at the JRC and are considered relevant in the frame of the EU R&D Actions under the EU GNSS Component of the EU Space Programme. A total of nine different categories of the testing capabilities are presented, illustrated with a description the test set-ups, the test procedures and a selection of the results that were obtained.

3.1 Antenna Measurements and Characterisation

This section provides a description of the main testing facility in the GNSS laboratory of the JRC, the European Microwave Signature Laboratory (EMSL), and the different measurement configurations aimed at characterising GNSS antennas and GNSS antenna arrays in an anechoic room.

3.1.1 The EMSL Laboratory

The main testing facility to conduct antenna measurements at the JRC is EMSL. The overall structure of the EMSL anechoic chamber is the conjunction of a hemi-spherical and a cylindrical dome, with a diameter of 20 meters. The centre of the hemi-spherical dome is located at 5 meters above the floor. The Devices Under Test (DUTs) are positioned on top of a rotating tower that can move in and out the dome. An interesting feature of the EMSL is that, in the gap between the hemi-spherical and cylindrical domes, it has two separate antenna sleds with transmit and receive antennas that can move independently along a circular rail on the dome of the anechoic chamber, maintaining its pointing at the centre or focal point. The high load capacity of the rotating tower, it can hold a maximum load is 3.0 tons, allows the testing of antennas integrated in vehicles. A 3-D sketch of the exploded view of the EMSL along with a photograph of the rotating tower inside the anechoic chamber are shown in Figure 1.

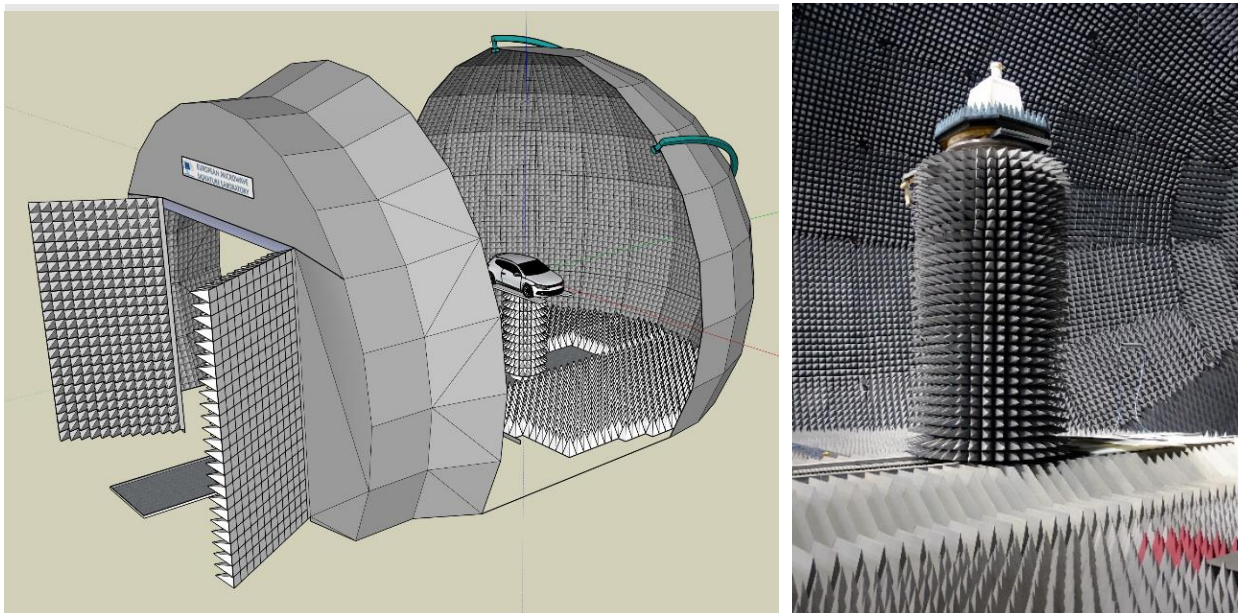


Figure 1. 3-D sketch of an exploded view of the EMSL with a car on top of the rotating tower (left). A photograph of the rotating tower with an antenna under test (right).

The EMSL laboratory was built in 1992 and was originally designed for antenna and electromagnetic scattering measurements. Since its inauguration and until 2008, the testing activities were focused on the fields of radar remote sensing and, more in particular, on polarimetric Synthetic Aperture Radar (SAR) to support the development of new applications of spaceborne SAR missions [3], [4], [5] and [6]. More recently, in 2008, the EMSL was upgraded to initiate the current testing activity on GNSS receivers and, more precisely, those integrating Galileo and EGNOS. The first main upgrade made at that time was the integration of a GNSS simulation platform in the laboratory, such that over-the-air measurements to assess the performance of GNSS receivers with their antennas could be carried out in a controlled, automated, and repeatable manner.

[7]. These measurements are conducted with one of the probe antennas that can be moved along the circular rail transmitting the signals from the GNSS simulator. The second main upgrade was that of adding a new set of antennas on the sled A to be used in antenna measurements in the frequency range from 700 MHz up to 4.0 GHz. A close view of the antennas, video cameras, and laser pointer currently installed in the sleds A and B of the EMSL is shown in Figure 2.

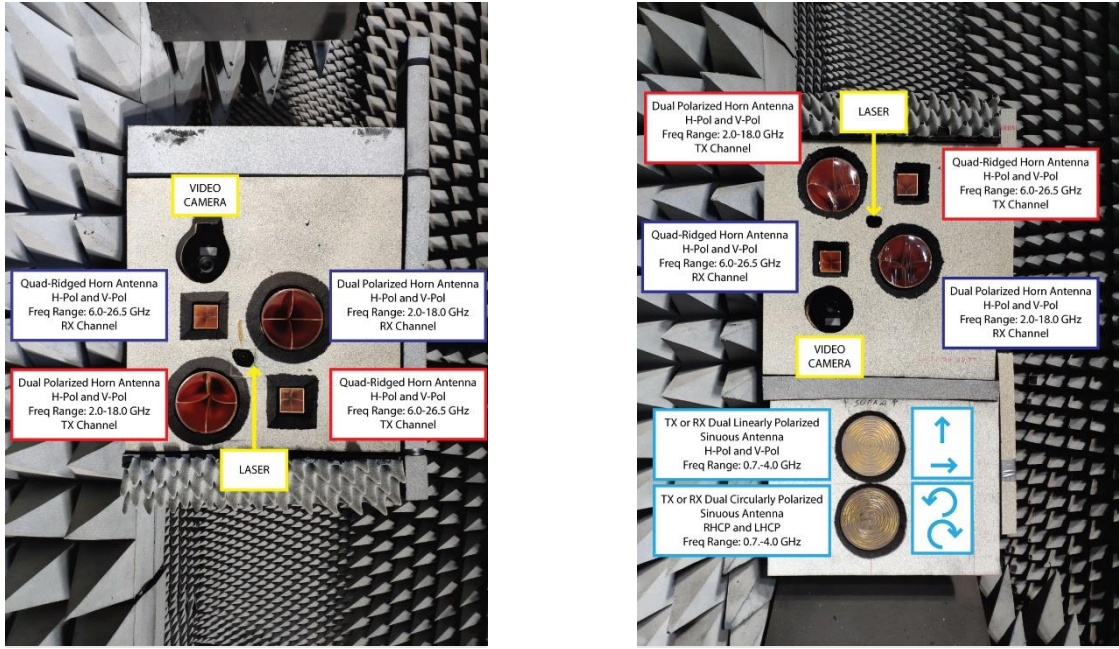


Figure 2. Close view of the antennas, video camera and laser pointer in the sleds A (left) and B (right) of the EMSL laboratory.

The electromechanical sub-system of the EMSL consists of four brushless DC motors that actuate the movement of four mechanical axes individually (i.e., sled A, sled B, linear axis of the tower, and rotation of the tower). A dedicated control software interfaces with a Programmable Logic Controller (PLC) over the network such that the antenna measurements can be conducted in a fully automated manner. The positioning ranges and accuracy of the four mechanical axes of the EMSL are summarised in Table 2.

Table 2. Specification of the positioning ranges and accuracies of the four mechanical axes of the EMSL.

Axis	Positioning Range	Accuracy
Linear axis of measurement tower	$-8500 \text{ mm} \leq L \leq +2500 \text{ mm}$	$\pm 0.5 \text{ mm}$
Azimuth Scan Angle of measurement tower	$-20^\circ \leq \phi \leq +360^\circ$	0.05°
Zenith Scan Angle of Sleds A and B	$-112^\circ \leq \theta \leq +112^\circ$	0.005°

The EMSL laboratory has three Radio Frequency (RF) signal paths, two identical paths routed to each one of the antenna sleds plus a third one that is routed to the measurement tower. The RF paths routed to the antenna sleds include four RF cables: one Transmitting (TX) channel, two Receiving (RX) channels and one return channel for the external reference. The third RF path to the measurement tower includes just one RF cable that can be used on TX and RX modes depending on what is the device under test. The routing of the RF signal paths and that in the sleds to the probe antenna is managed with a network of 32 electromechanical microwave switches. The configuration of the routing of the three RF paths can be programmed and is remotely controlled with a microwave switch driver instrument interfaced over the intranet of the laboratory.

A common measurement set-up for the characterisation of a GNSS antenna is that of combining a 180 degree zenith scan of the probe antenna with a 180 degree azimuth scan of the measurement tower, as it is depicted in Figure 3. This combination allows to have a set of measurement points uniformly sampled in the azimuth and zenith angles, covering the entire upper hemisphere.

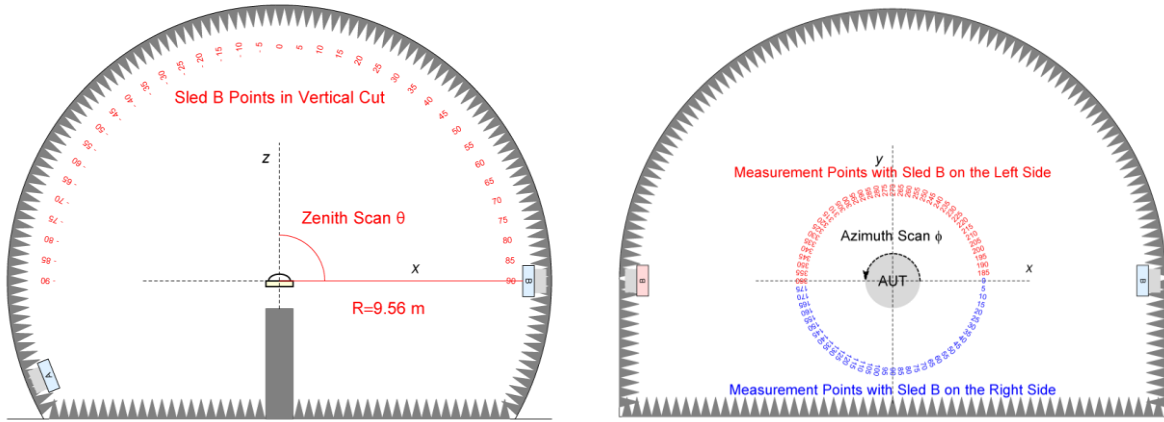


Figure 3. Sketch of the side view (left) and top view (right) of the two circular scans in an antenna measurement in the EMSL, which correspond to the zenith and azimuth angles.

Two 3D sketches identifying the four mechanical axes of the EMSL and the measurement points in an antenna measurement with combined zenith/azimuth scans are shown in Figure 4.

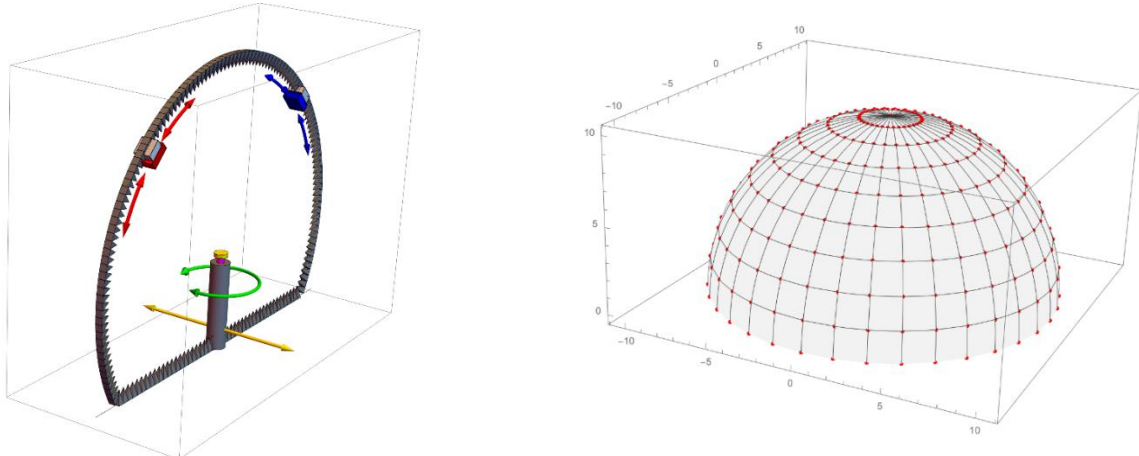


Figure 4. 3D sketches identifying the four mechanical axes of the EMSL (left) and the spherical grid of measurement points in an antenna measurement with combined azimuth/zenith scans (right).

At present, the two core RF instruments of the EMSL that can be used to characterise a GNSS antenna are a vector network analyser and the GNSS simulator. Measurements with the vector network analyser can be carried out in two configurations, depending whether the antenna to be tested integrates a low noise amplifier on reception (i.e., as it is the case in many GNSS antenna systems) or not. A third configuration that can be used is that where the source of the RF signals received by the antenna under test is that coming either from the GNSS simulator or a rooftop geodetic antenna installed in the building hosting the EMSL.

3.1.2 Antenna measurements with a Vector Network Analyser

A sketch of the set-ups for the antenna measurements with the Vector Network Analyser (VNA), in the configuration to characterise a passive or an active reference antenna, are shown in Figure 5. More precisely, it shows the set-up of a calibration measurement with a reference antenna with gain vs frequency characteristic known from a previous measurement or has been provided by an accredited laboratory.

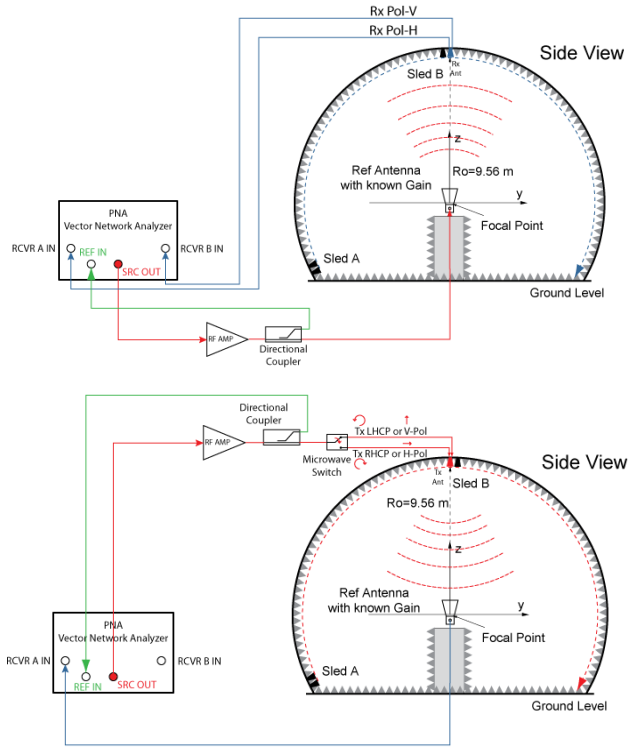


Figure 5. Sketches of the set-up of a calibration measurement with the vector network analyser: reference antenna with known gain on transmit (left) and receive (right) modes.

There is commonality in the two configurations of the measurements with the VNA that is important to underline. In both set-ups there is an amplifier in the RF transmit path with a directional coupler located right after. This coupled return path is routed to the external reference input of the VNA to filter out any variations of the amplifier amplitude and phase response during the measurement, improving the overall stability and accuracy of the system. This is particularly important when the characterisation made is that of estimating the variations of the phase centre and phase centre offset of the antenna under test. In these measurements, the entire RF chain of the measurement system excluding the device under test has to exhibit an extremely high phase and amplitude stability.

A VNA is an instrument that allows to characterise the scattering parameters (S-parameters) of a device under test. In the antenna measurements, it is then possible to characterise the gain by measuring the complex ratios A/R_1 and B/R_1 versus frequency, where A and B are the test port receivers of the VNA and R_1 is the external reference input of port 1. Measurements of the return loss or impedance matching versus frequency of the antenna under test can also be carried out. This measurement though requires a prior calibration of the VNA at the location of the RF port of the antenna, which must be carried out using an S-parameter calibration kit covering the frequency range of interest.

An illustrative example of the results obtained in the measurements of a Javad choke-ring GNSS antenna are given in Figure 6. The characterisation made on this antenna was that of measuring the gain in the Left Hand Circular Polarisation (LHCP) and Right Hand Circular Polarisation (RHCP) modes at two vertical cuts spaced 90 degrees. This is a measurement of the overall gain of the antenna plus filter and the low noise amplifier that has integrated. The vertical cuts of the measured antenna gain pattern correspond to the frequency of 1578.0 MHz.

Choke-Ring Antenna Elevation Cuts at L1 (1.578 GHz)

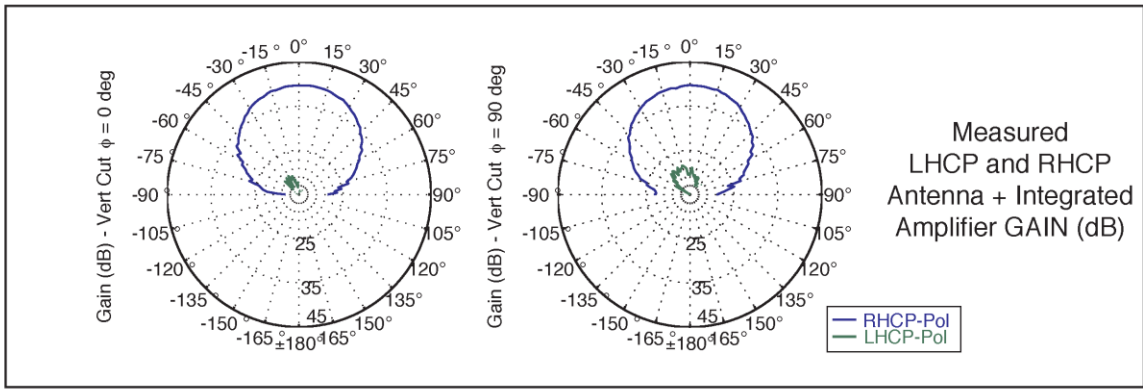


Figure 6. Two vertical cuts of the LHCP and RHCP gain of a Javad choke-ring antenna at the frequency of 1578.0 MHz: vertical cuts at azimuth 0 deg (left) and azimuth 90 deg (right).

A second batch of measurements on a second antenna, a Trimble Zephyr type 2, was made to characterize the frequency dependence of the gain in a frequency range covering entirely all the GNSS bands. A photograph of the antenna under test, and the RHCP gain versus the frequency at the boresight are shown in Figure 7, where the effects of the selective pass band filters integrated in the antenna are clearly noticeable.

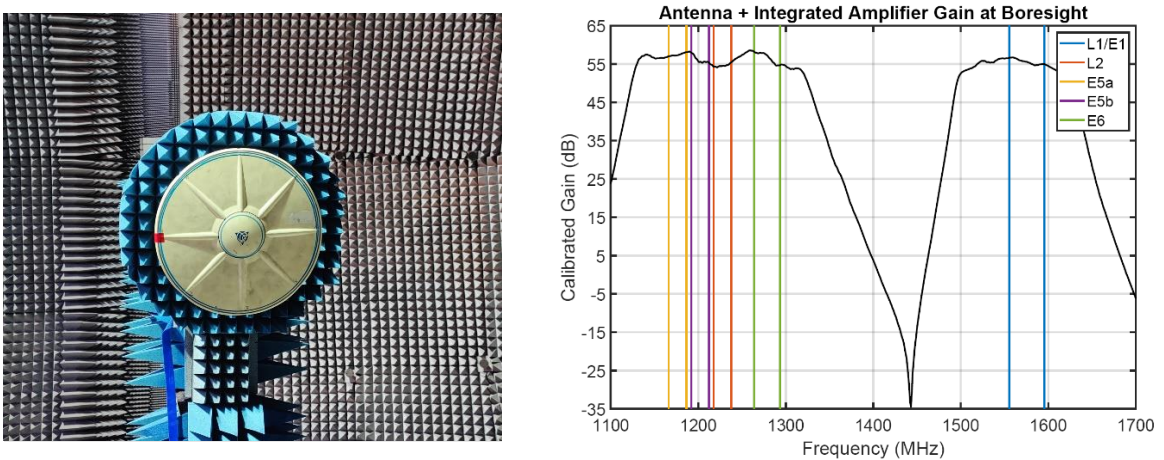


Figure 7. Photograph of the Trimble Zephyr Type 2 (left), and RHCP gain versus frequency of a Trimble Zephyr Type II antenna measured at boresight in the EMSL (right).

3.1.3 Antenna measurements with a GNSS simulator

A second modality of conducting the characterisation of an antenna is that of using a GNSS simulator as the signal source. The EMSL laboratory is equipped with a state-of-the-art GNSS simulator that is currently capable to generate Galileo E1/E5/E6, GPS L1/L2/L5, and Satellite Based Augmentation System (SBAS) signals [8]. A dedicated room behind the dome of the EMSL is the host of the GNSS simulation rack, which includes the simulator, its controller, an RF signal combiner, two vector signal generators, a Rubidium frequency standard, a GNSS timing receiver and Network Time Protocol (NTP) server, and a server station hosting Dynamic Host Configuration Protocol (DHCP), Domain Name System (DNS) and Network Attached Storage (NAS) services. A sketch of the configuration of the laboratory when the GNSS simulator is used as the signal source to characterise a GNSS antenna, and a photograph of the GNSS simulation rack are shown in Figure 8.

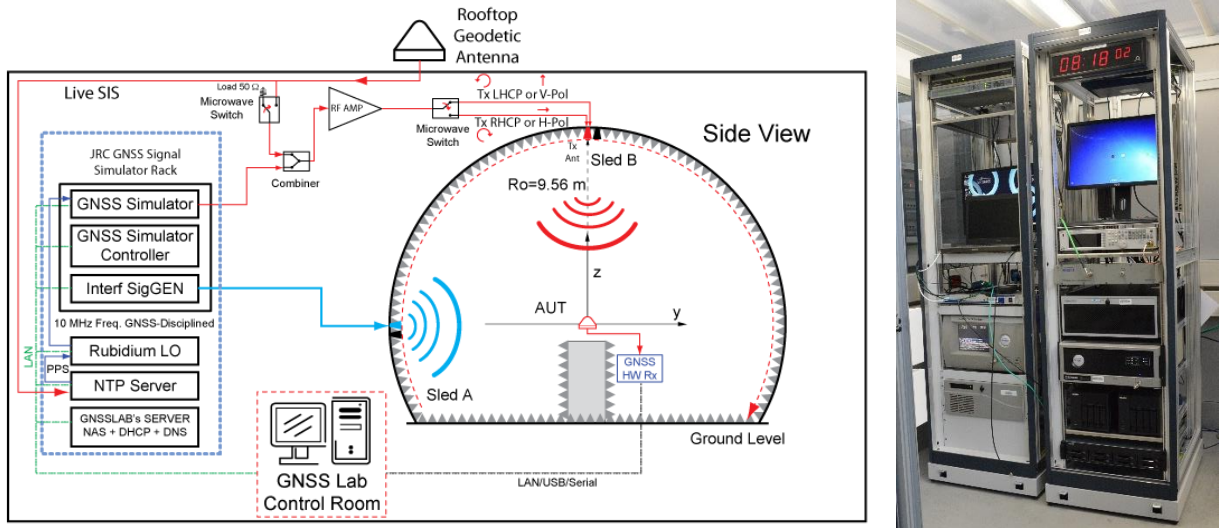


Figure 8. Sketch of the laboratory set-up to characterise an antenna using a GNSS simulator as a signal source (left) and photograph of the GNSS simulation rack behind the dome of the EMSL (right).

The use of the signal generator and RF combiner is an interesting option in case one wants to assess the performance of a GNSS receiver and its antenna when there are other signals present either in band or in adjacent bands (e.g., a GNSS jamming or spoofing signal). In this type of tests, it is possible to channel separately the signal from the GNSS simulator and that from the RF signal generator to the two antenna sleds, as illustrated in Figure 8.

An aspect that deserves special attention when conducting RF compatibility tests is the calibration of the power levels of the GNSS signals broadcast inside the anechoic chamber of the EMSL. Here, it is important to note that it is possible to calibrate the transmit power level at the probe antenna in the sled. This will ensure that the radiated power level at the position of the antenna under test is closely aligned with that specified in the Interface Control Document (ICD) of the GNSS systems enabled in the simulator.

A variant of the configuration of the test set-up using a GNSS simulator that is worth noting is the one using a GNSS playback platform as the signal source. In this test modality, the GNSS playback device broadcasts a signal that has been synthesised or recorded in advance. Just as it is done with a GNSS simulator, the power level of the GNSS playback device can be calibrated to obtain radiated power levels close to the antenna under test that are aligned with those specified in the ICD.

A last observation on the antenna measurements using a GNSS simulator as the signal source is that some of the KPIs that can be characterised are very close to those using a vector network analyser. Examples of these are the group delay and phase centre variation of the antenna under test. An investigation on the stability and cross-validity of this type of measurements with those using a vector network analyser is currently on-going at the JRC.

3.1.4 Antenna array measurements

The testing and characterisation of GNSS antenna arrays is an important capability of the anechoic chamber of the EMSL. Example Key Performance Indicators (KPIs) that one may want to assess are the performance of the antenna array to implement effectively null-steering or digital beamforming [9]. A possible approach to assess these KPIs is to characterise each antenna element separately. This characterisation can only be carried out when the RF port of all the elements of the antenna array are interfaceable with the vector network analyser. The EMSL laboratory is equipped with a microwave switch driver instrument and an 11-port microwave switch that have been specifically designed for antenna array measurements. This multi-port microwave switch device can be installed next to the antenna array under test and can be controlled remotely during the tests. For the sake of illustration, a sketch of the multi-port microwave switch and a photograph of a 7-element antenna array mounted on the measurement tower are shown in Figure 9. During the tests run on this antenna array, the radiation pattern of every antenna element was characterised sequentially, scanning all the elements with the multi-port switch at each position of the probe antenna in the sled and

rotation angle of the measurement tower. The current version of the control software used for the antenna measurements allows a fully automated switching across an arbitrary number of antenna elements, which at present is limited to 11.

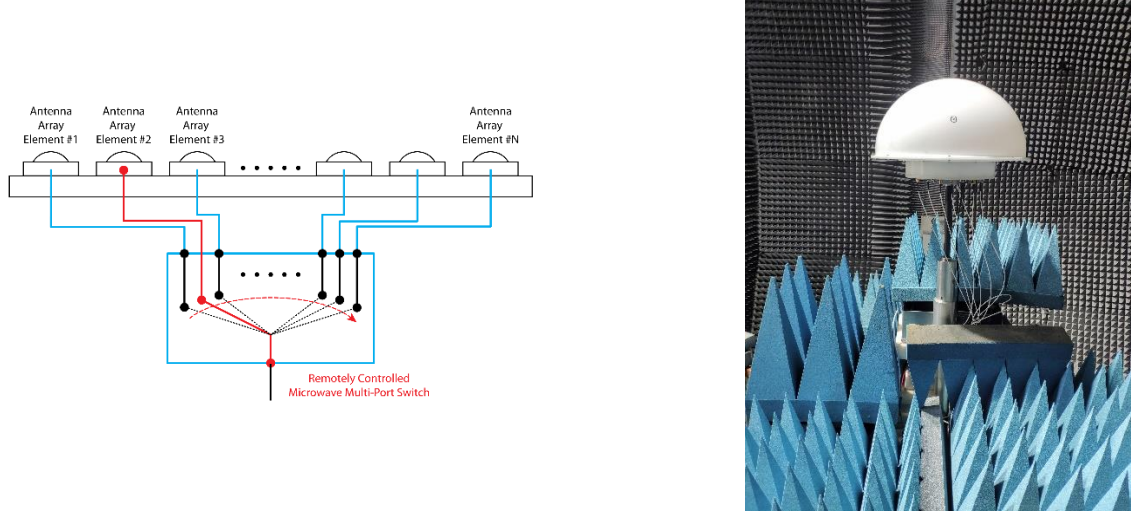


Figure 9. A sketch of the multi-port microwave switch (left) and a photograph of a 7-element antenna array mounted on the measurement tower of the EMSL (right).

A closer view of another 7-element array, this one with a circular ground plane, and the horizontal and vertical cuts of the RHCP measured gain pattern of the central element (blue lines) and one of the peripheral elements (red lines) are shown in Figure 10. These results correspond to an azimuth angle of the vertical cuts of 0 deg, and an elevation angle of the horizontal cuts of 40 deg. The elements of the array are active GNSS antennas with dual-polarisation (LHCP-RHCP) receive ports.

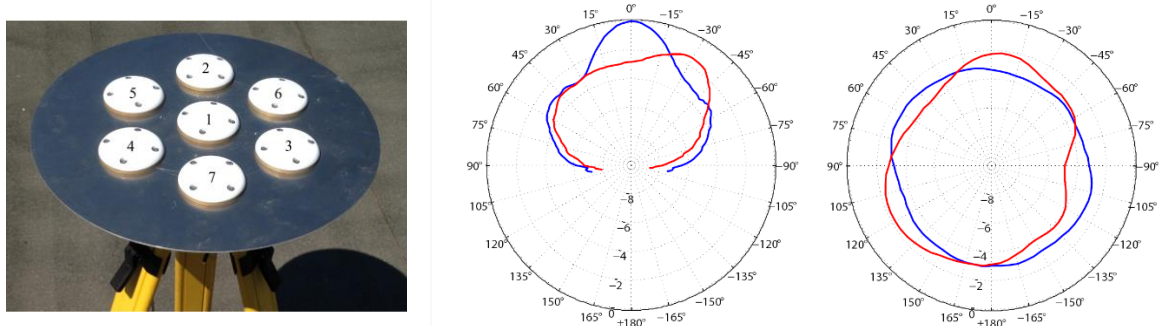


Figure 10. Close view of the 7-element antenna array and the ground plane (left); vertical cuts of the RHCP gain pattern of the central and a peripheral element at azimuth 0deg (center); horizontal cuts of the gain of the central and a peripheral element at 40 deg elevation (right).

An interesting and pretty unique feature of the EMSL anechoic chamber is that, in addition to the two sleds with the Tx/Rx probe antennas, it also has an array of 36 dual-polarised antennas that are distributed in a half of the hemi-spherical dome. These additional probe antennas are dual linearly polarised standard gain horns that can be used in the frequency range 1 to 18 GHz. This fixed antenna array was originally installed to conduct multi-static radar cross section measurements of targets under test. A dedicated network of a total of 7 six-port electromechanical microwave switches allows the routing of the Tx or Rx signals to/from any individual probe antenna. The entire set of multi-port switches can be interfaced remotely and the signal routing can be changed during the course of a measurement. A 3-D sketch of the RF signal routing network, with the 7 electromechanical switches on the dome of the EMSL, and a photograph of the interior of the EMSL, indicating the arrangement of the 36 probe antennas, are shown in Figure 11.

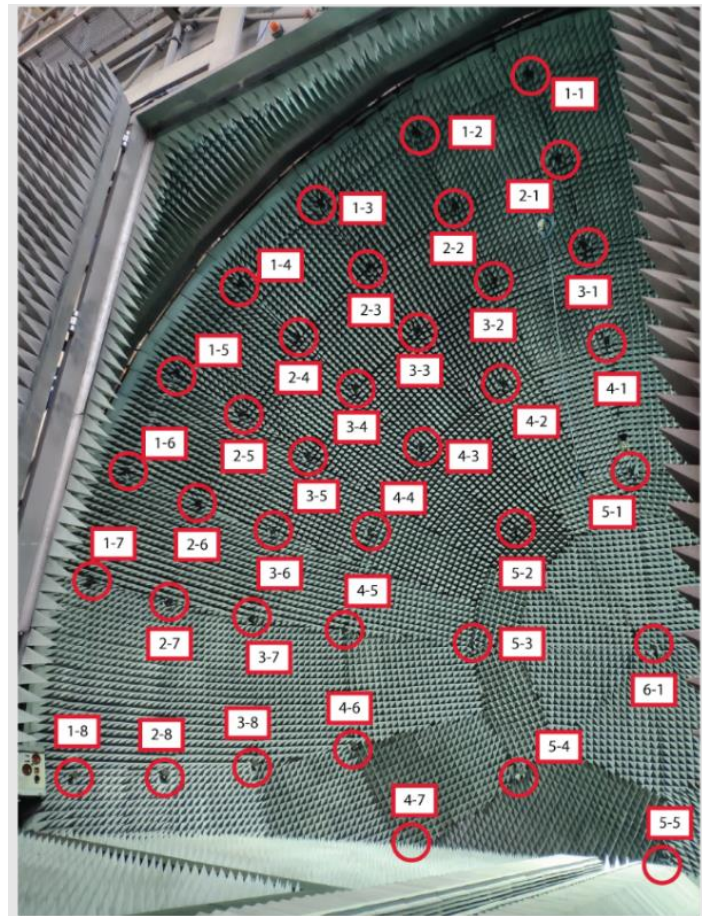
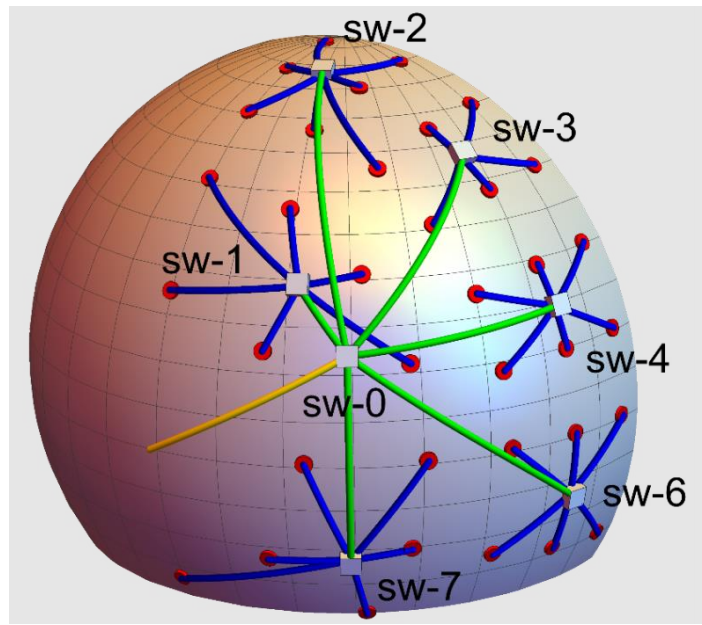


Figure 11. 3-D sketch of the signal routing network of the array of the 36 fixed antennas on the outer surface of the dome (top), and photograph showing the arrangement of the fixed probe antennas as seen inside the anechoic chamber (bottom).

3.1.5 GNSS Antennas PCO/PCV Characterization

The characterisation of the phase centre offset (PCO) and phase centre variation (PCV) of GNSS antennas represents a newest JRC laboratory testing capability realized through the integration of a dedicated pan-tilt antenna positioner FLIR D300-RF [10]. This positioner will be mounted on top of the measurement tower of the EMSL laboratory. The control software of the EMSL laboratory has already been upgraded to integrate the pan and tilt axes of the new positioner. This will allow the execution of automated tests to characterise the radiation pattern and the phase center variation of the antennas under test. A photograph of the pan-tilt positioner, which currently in it its final integration phase, is shown in Figure 12.

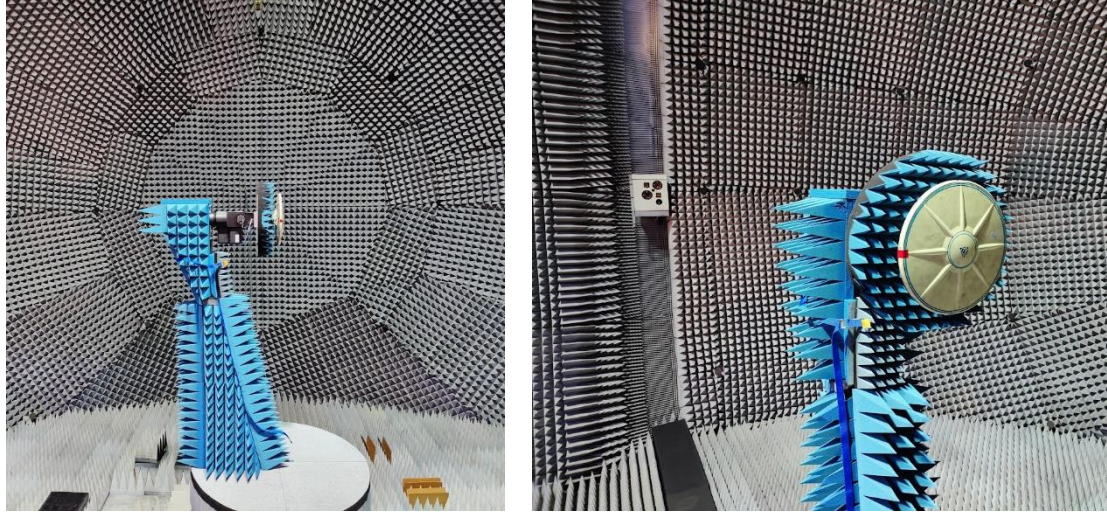


Figure 12. Photographs of the pan-tilt antenna positioner mounted on the measurement tower of the EMSL during one of the integration tests; (left) side and (right) front views of the pan-tilt antenna positioner.

This new antenna positioner will allow the characterisation of the phase centre variation as a function of the azimuth and elevation angles of the antenna under test. One interesting feature of the positioner is that integrates a pass-through RF rotary joint that exposes an RF connector next to the antenna under test. This pass-through connector allows a full 360 degrees rotation of the pan axis of the positioner without stressing mechanically the RF cable. Further, the pan-tilt positioner allows the mounting of an antenna under test on a circular ground plane, something that is potentially of interest to characterise both avionics and automotive antennas.

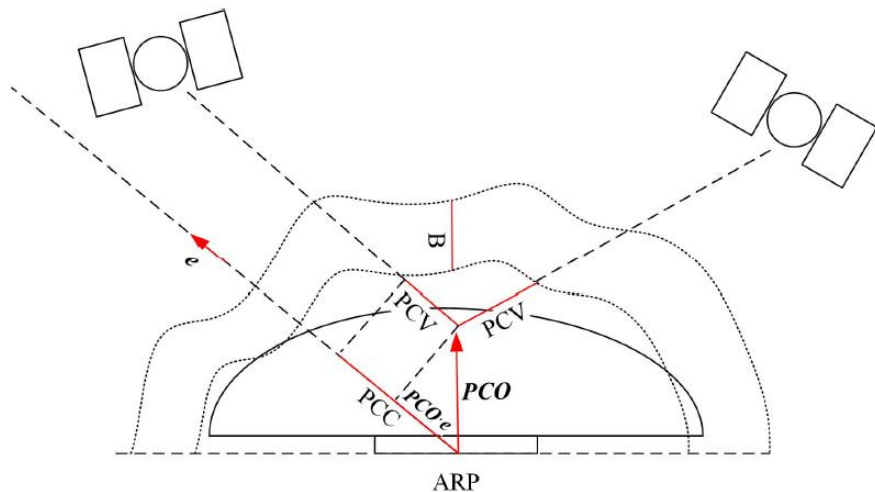


Figure 13. Antenna phase center correction model showing the PCO and PCV contributions to the observed phase variation [11]

The development of a dedicated post-processing tool is currently on-going and some preliminary results are hereafter provided. The PCO/PCV is computed applying standard PCC geometry in Figure 13 [11], hence the phase data distribution in azimuth and elevation is expressed as

$$PCC(\alpha, z) = -PCO \cdot e + PCV(\alpha, z)$$

Where e denotes the directional vector from antenna to satellite while α and z represent the azimuth and elevation angles respectively. Hence the superimposition of PCO projection along the line of sight and the PCV distribution. Some tests have been performed on a reference ZephyrType2 Antenna (IGS ANTEX id: TRM55971) with known PCO/PCV information. The objective is to crosscheck EMSL test bench measurement consistency comparing them with PCO information provided for the specific device and the PCV distribution retrieved from the International GNSS Service (IGS) ANTEX file igs14.atx file [12]. Considering the differences that can occur between different methodologies [11] an facilitate the comparison with the reference the following step have been considered [13]:

- Estimation of PCO by using least square adjustment of the raw phase measurements converted in millimetres
- Estimation of PCV from the correspondent phase residuals by fitting them by a spherical harmonic expansion [1] of order 6 and imposing PCV (0, azimuth)=0 , for any azimuth.

The computed PCO coordinates in mm are [0.2595; 0.4107, -1.3027]. The small values of the first two components confirm the expected alignment with the zenith direction. The offset in the vertical axis of -1.3 mm indicates that the PCO position of the antenna under test is very close to the focus or phase center of the anechoic chamber.

For the PCV, the three main results are provided in Figure 14 which show a very good matching between reconstructed and reference PCV distributions for one of the antennas under test, a Trimble Zephyr type 2 antenna in this case. A 3D representation of the phase center variation versus the azimuth and zenith angles is provided in Figure 15. Actually, the raw data and the reconstructed still exhibit a higher sensitivity to azimuth if compared with the reference. Further analysis and another antenna test will be performed in order to improve both measurement and data processing. However, the range of the values and, more important, the general pattern indicate a high stability and accuracy of the measurement system.

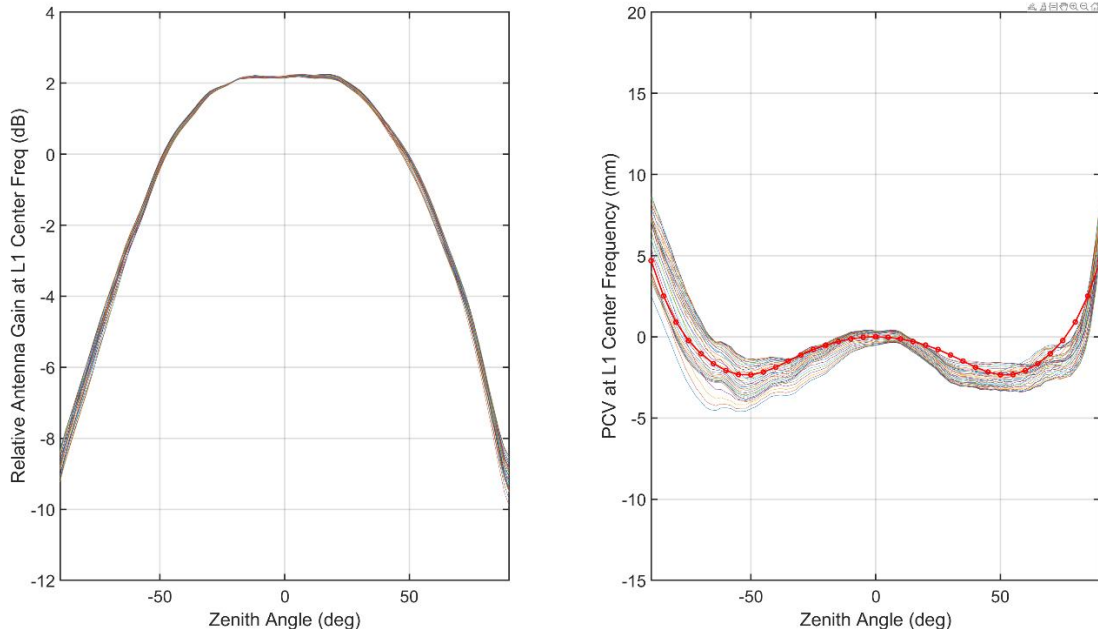


Figure 14. (left): 36 Vertical cuts of the relative antenna gain at steps of 5 deg in azimuth; (right) associated PCV vertical cuts and the NOAZM reference phase variation reported in the antex file IGS14.atx (in red) for the Trimble Zephyr type 2 under test.

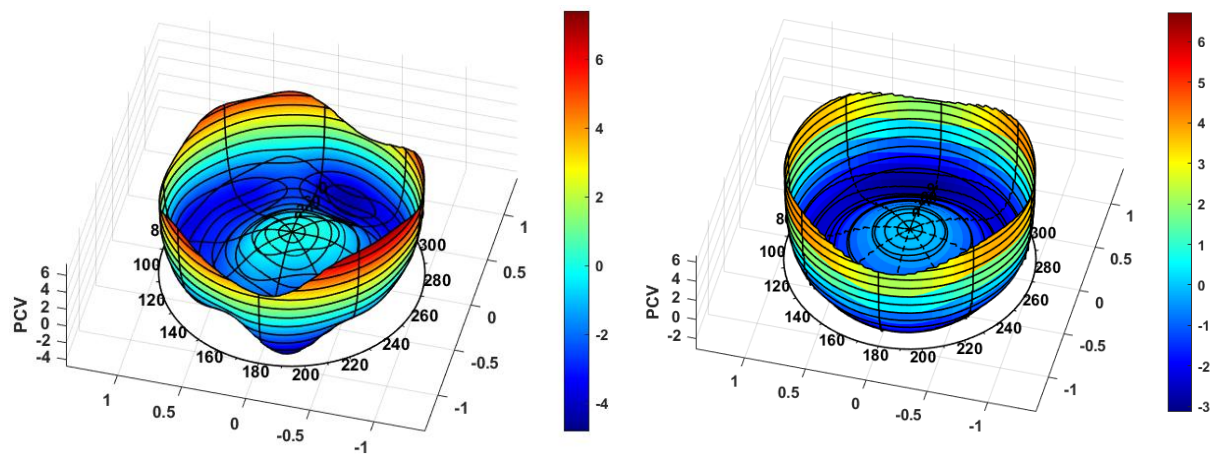


Figure 15. Reconstructed (left) and reference (right) PCV as a function of the azimuth and zenith angles.

3.2 Standardization and Conformance Testing

This section gives several examples of recent test campaigns where multiple GNSS receivers were assessed simultaneously with the aim to illustrate the testing capabilities currently available at the JRC. A description of the scope of the test campaign, the test scenarios, and the KPIs assessed is provided. In particular, four different applications are considered: timing, automotive, maritime and personal navigation. For these applications, specific examples are reported below.

The examples selected are:

- Conformance testing of the eCall devices, which was aimed at assessing the compliance of the available devices prior to the entry in force of the EU regulatory framework on the eCall.
- Performance assessment of SBAS-enabled maritime receivers. The goal of this campaign was to assess the conformity of SBAS devices to the requirements set in an existing IEC standard.
- Performance assessment of Galileo-enabled ship-borne GNSS receivers. The goal of this campaign was to assess the conformity of Galileo-enabled devices to the requirements set in an International Electrotechnical Committee (IEC) standard.
- Automotive tests for assessing the performance of Galileo HAS in urban scenario.
- Performance assessment of Android smartphones providing access to GNSS raw measurements.
- Galileo Timing Receiver standard definition support. In the context of support to the Galileo timing service, JRC is actively involved in the standard definition of Galileo timing receivers with CEN/CENELEC (European Committee for Standardization / Electrotechnical Standardization). Further details are described in Section 3.5.2.

3.2.1 Conformance testing of eCall devices

The emergency call (eCall) Commission Delegated Regulation (EU) 2017/79 is one of the first EU regulatory frameworks enforcing the adoption of Galileo and EGNOS in the road sector. The regulation establishes that all new passenger cars and light duty vehicles must be equipped with eCall; in Annex VI, the technical requirements for compatibility of eCall with EGNSS are reported. GSA launched the eCall testing campaign which was jointly designed and performed with JRC. The test campaign allowed both supporting manufacturers in reaching full compatibility with EGNSS signals and providing guidelines to the technical centre designated to grant EC type-approval of the vehicles. Fifteen devices were tested under static and dynamic scenarios. The tests were conducted using simulated signals characterised by different signal power levels and propagation conditions.

The JRC has set up a test-bed specifically designed to assess the performance of the eCALL devices with respect to the technical requirements for compatibility with the positioning services provided by Galileo and EGNOS systems. This test-bed is based on a GNSS simulator from Spirent Communication [8]. The GNSS simulator has been configured to generate the Open Service Signal of GPS L1, Galileo E1, and SBAS (Satellite-Based Augmentation System), in accordance with the specifications given in the eCALL Guidelines Report and with Galileo and EGNOS control documents.

The variety and the volume of data led to the generation of a unique dataset, which was useful to verify that the adoption of Galileo is quite mature, despite its early service provision stage, and provides a substantial contribution to reach the regulation objectives in the interest of EU citizens and in particular providing quality positioning information to enable a safer emergency service in European roads. At the same time, the campaign also allowed the manufacturers to identify margin for improvements in terms of capability to optimally acquire track and use EGNSS signals.

The main tasks performed during the eCall activity were:

- Definition and implementation of the test scenarios, according to Annex VI of the Commission Delegated Regulation 2017/79;
- Evaluation of a number of close to market eCall GNSS testing platforms to facilitate vendors' development, ensure consistency and share lessons learnt with manufacturers;
- Execution of the tests on each DUT;

- Test results analysis;

Preparation of the implementation guidelines document [14];

Generation of individual test report for both DUT manufacturers and test/simulator solutions, detailing the observed results and providing recommendations in view of compliance with the Annex VI of Commission Delegated Regulation 2017/79 [15];

Aggregation of the results and generation of an eCall Conformance Testing Campaign Overall Assessment Report [16], [17].

The DUT performance was assessed with respect to a selection of key performance indicators (KPIs), including usage of the SBAS corrections, positioning accuracy under static, dynamic and dynamic with shadow areas conditions, Cold Start Time-To-First-Fix (CSTTFF); re-acquisition time and receiver sensitivity in cold start mode. Details about the setup developed and the methodology for the tests are available in [1].

3.2.2 Performance Assessment of SBAS-enabled Maritime Receivers

The conformance testing of SBAS-enabled receivers is a key component for the standardization of user hardware equipment for Safety-of-Life applications. In this context, the IEC-61108-7 standard defines the minimum performance requirements for maritime receivers, using SBAS L1 signals to augment GPS L1, in order to be compliant with the IMO resolution A.1046 for navigation in ocean and coastal waters, as well as for harbour entrances/approaches, together with the methods for verifying equipment compliance.

In this context, a test-bed has been developed (see Figure 16), including the following features:

- A set of 16 GNSS scenarios specified in the standard have been implemented on a Spirent GSS9000 simulator platform, with the GPS L1 C/A and the EGNOS signals enabled, including also an Agilent PSG for the generation of radio-frequency interference.
- An inline low-noise amplifier (LNA of 25 dB gain) is used in between the GNSS simulator and the SBAS receiver under test. This is done to emulate the use of an active antenna, which is normally used in any ship equipped with an SBAS receiver.
- The performance of the DUTs is assessed by parsing and analysing the logs of the National Marine Electronics Association (NMEA) messages outputted by the receiver during the tests and also those from the GNSS simulator, which are taken as reference to estimate the accuracy of the PVT solution.
- All the tests were conducted in normal environmental conditions with temperature between +15 °C and + 30 °C and relative humidity between 20% and 75%.
- The test-bed includes a set of automated software tools to launch the test scenarios, collect and decode the receiver data and generate the corresponding performance figures.

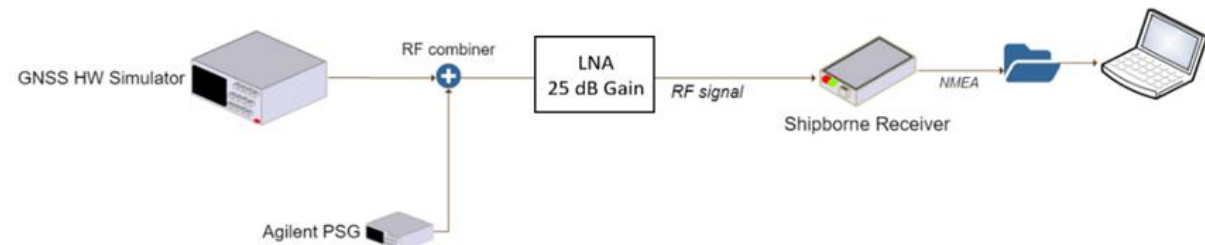


Figure 16. Test bed setup for compliance assessment of SBAS-enabled maritime receivers

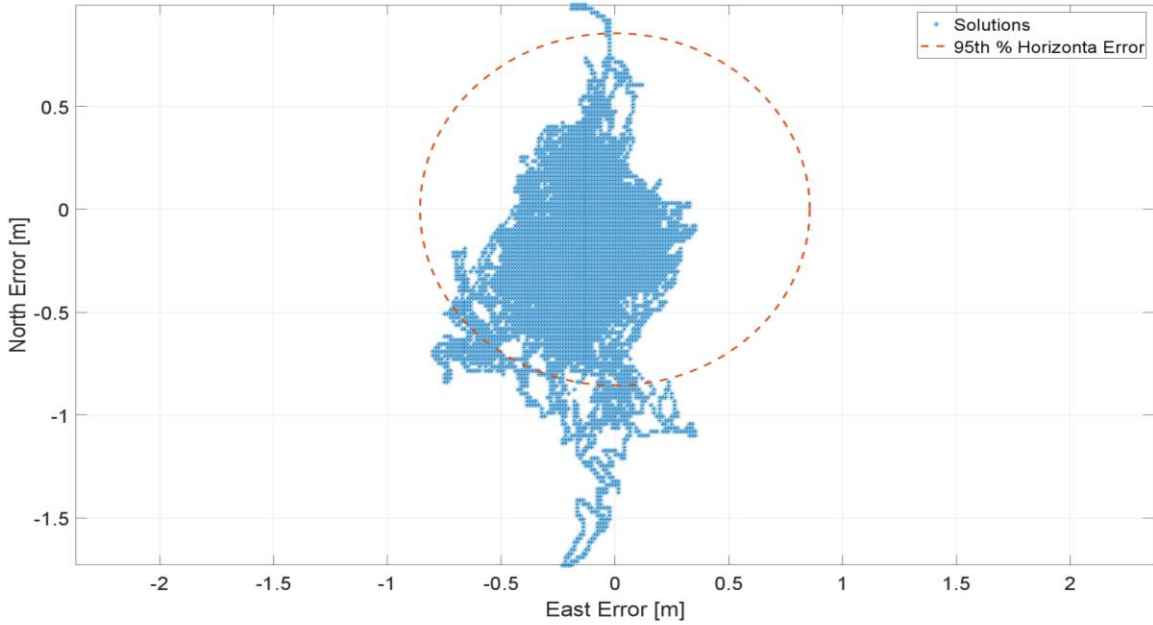


Figure 17. Example of EGNOS-based horizontal positioning performance for a maritime receiver

Furthermore, EGNOSv3 is being developed to support dual-frequency (L1+L5) multi-constellation (DFMC) GNSS (GPS+Galileo). The future testing of dual-frequency multi-frequency will be essential to facilitate the adoption of next generation of SBAS receivers. In order to facilitate the further update of IEC-61108-7 for DFMC, the test bed described above has been extended to support L1+L5/E1+E5a GPS+Galileo. The hardware setup is depicted in Figure 18. This configuration has been used to perform a tracking sensitivity analysis of SBAS receivers subject to various levels of pulsed or wide-band radio-frequency interference. Sample results are shown in Figure 19.

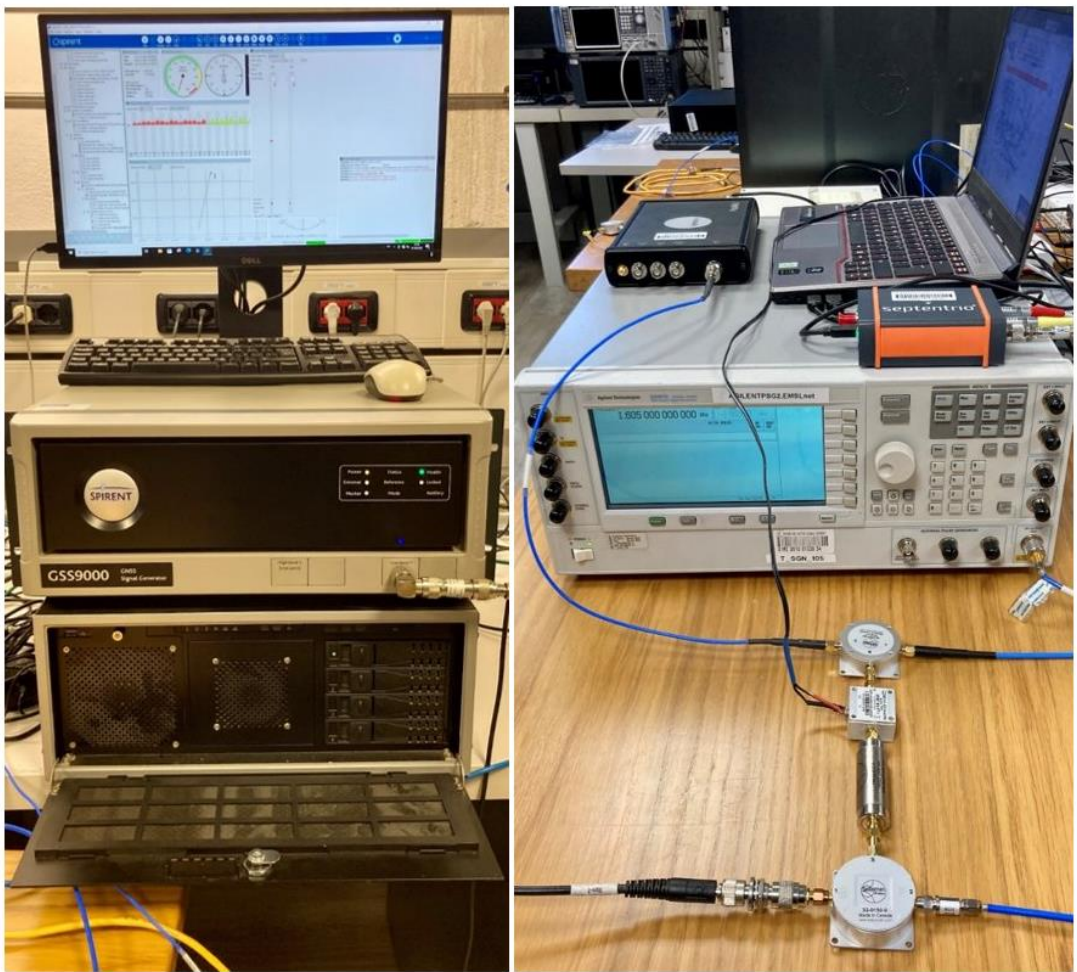


Figure 18. Test setup for performance testing of dual-frequency multi-constellation (GPS+Galileo) SBAS receivers

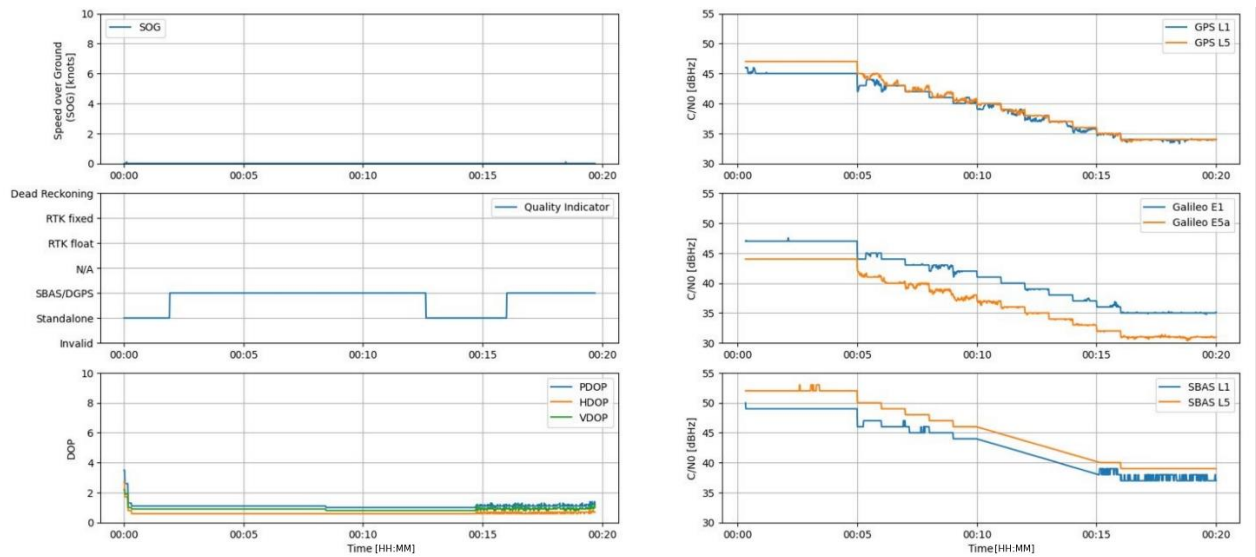


Figure 19. Tracking sensitivity analysis of dual-frequency multi-constellation SBAS receivers

3.2.3 Performance assessment of Galileo-enabled ship-borne GNSS receivers

GNSS receivers today have indisputably become the main source of Position Velocity and Time (PVT) information in the maritime domain. The International Maritime Organisation (IMO) has recently adopted performance standards for multi-system ship-borne receivers, which highlights the importance of integrating the new GNSS systems, with their space-based and terrestrial-based augmentations. In addition, IMO has recognised Galileo as part of the World Wide Radio Navigation System [18]. In order to assess the correctness of the implementation of Galileo, and secondly, to identify potential performance improvements and non-compliances to the requirements set for Galileo in the Maritime Standard IEC 61108-3 [19], a test campaign has been carried out by the JRC [20]. The main phases of the activity were:

- Analysis of the available standards for maritime GNSS receivers, including tests and procedures.
- Familiarisation with the DUTs, logging capacity and connectivity requirements.
- Set-up design and implementation, including calibration activities.
- Tests execution.
- Data analysis and report generation including best practice and suggestion for receiver manufacturers and testing centres.

The test campaign was based on a set of 24 Test Cases (TCs) which can be classified in the following main categories:

- Position accuracy: the DUTs position solutions were assessed in both static and dynamic conditions and compared with the thresholds set in the standard.
- Timing: Time-To-First-Fix (TTFF) was analysed in cold and warm conditions and re-acquisition capability after a power interruption.
- Sensitivity: position and timing requirements were analysed in different Galileo signal power conditions.
- NMEA availability was verified in low and high speed conditions.
- Course Over Ground (COG) and Speed Over Ground (SOG) were assessed in different dynamic conditions.
- Coherency between quality flags and absence of GNSS signal was evaluated.
- Interference: position accuracy and availability, TTFF and re-acquisition time were assessed during continuous-wave, narrow/wide and pulsed interference.
- Receiver Autonomous Integrity Monitoring (RAIM)/Fault Detection and Exclusion (FDE): the capability to detect and exclude faulty satellites under pseudorange anomalous events were analysed.

Following the recommendations of the IEC Standard, the DUTs were intended as the ensemble of GNSS receiver and its antenna and, consequently, tests were performed in radiated mode in the EMSL. The set-up used in this campaign was that described in Section 0. A photograph of the seven ship-borne receivers and their antennas positioned on top of the measurement tower of the EMSL is shown in Figure 20. The movable platform was placed in front of the measurement tower and was used to hold an RF signal generator and a transmit antenna with its tripod. This test equipment was used to generate the interference signals specified in the IEC Standard 61108-3.

The sled B of the EMSL was positioned at the zenith, with the LHCP probe antenna broadcasting the RF signals from the GNSS simulator located behind the dome. The distance between the probe antenna and the antennas of the DUTs was about 9.5 m. It is worth mentioning that during this campaign, as specified in the IEC standard 61108-3, all the test scenarios assessed are single frequency E1 Galileo-only.

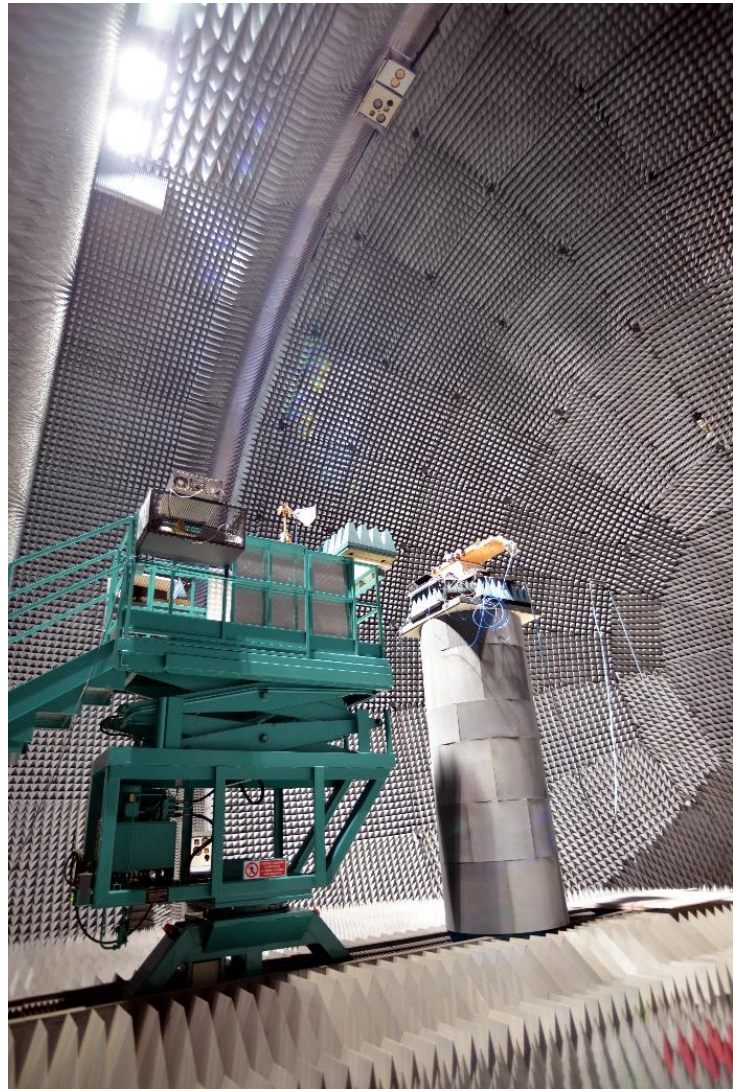


Figure 20. Photograph of the set-up used in the measurement campaign of the ship-borne receivers. The movable platform holds an RF signal generator and an antenna to generate RF interference signals.

The IEC Standard 61108-3 specifies GNSS signal power levels that would be measured with a 0 dBi antenna near the DUT. This means that the GNSS signal strengths have to be calibrated in advance. The power level of the GNSS simulator were adjusted such that the C/No measured with a reference GNSS receiver at the RF port of the front panel of the simulator were exactly the same as those measured with the same receiver and a 0 dBi RHCP antenna at the focus of the EMSL. In the radiated tests in the anechoic chamber, the high-power RF port of the GNSS simulator was used. The calibration of the power levels in the radiated tests was made as illustrated in Figure 21. The power loss of the programmable attenuator used in the radiated test was configured such that the observed C/No values measured with a reference receiver are the same as those in conducted mode using the calibrated RF output of the GNSS simulator. It must be noted that a 0 dBi RHCP antenna was not available and, instead, a standard gain horn of gain known was used. Further, an in-line low noise amplifier (LNA) of gain 25 dB was used both in the conducted and radiated tests. This was needed to raise the GNSS signal power levels and get them close with those that would be measured using an active GNSS antenna.

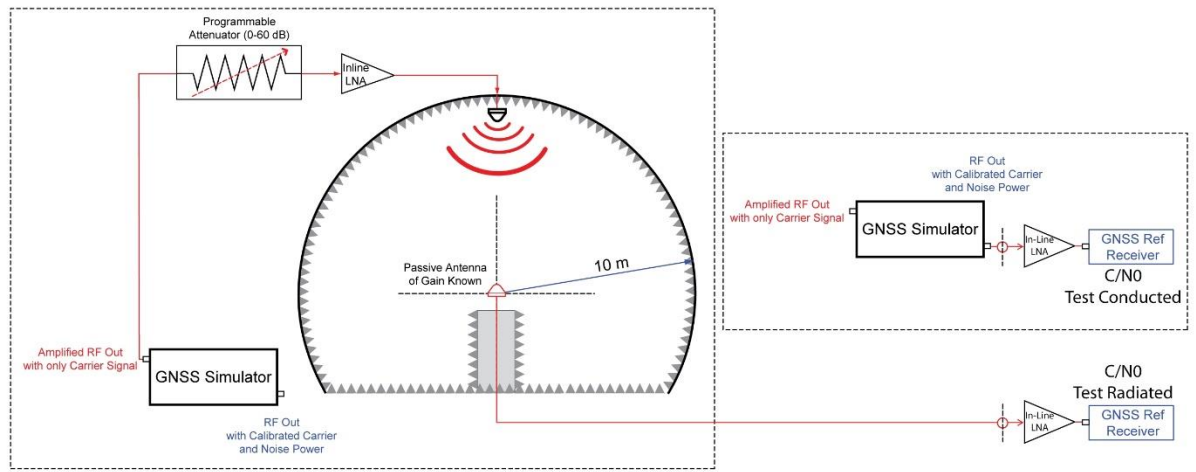


Figure 21. Sketch illustrating the calibration of the GNSS signal power levels in the radiated tests. Using the amplified RF output of the simulator and a programmable attenuator, C/No values observed with a reference receiver in the radiated tests (left) are fully aligned with those measured with the same receiver in conducted mode (right) using the calibrated RF output of the simulator.

The test scenarios with radio interference present were carried out using a programmable vector signal generator. This instrument can generate four classes of waveforms: continuous wave signals; frequency, phase and amplitude modulated signals; calibrated additive white Gaussian noise signals; and arbitrary digital waveforms with an instantaneous bandwidth up to 100 MHz. In order to verify that the power of the interference signal is compliant with the values reported in the standard, a calibration was performed. This calibration was made using a power meter and a reference horn antenna of known gain. This allowed to have signal power levels of the interference measured next to the antennas of the ship-borne receivers in line with the values specified in the standard. Two photographs with a close view of the set-up used with the programmable vector signal generator and a TX standard gain horn antenna on the movable platform of the EMSL are shown in Figure 22. The choice of having the interference signal generator and the TX antenna close to the measurement tower of the EMSL was made to limit the maximum power levels that had to be outputted by the signal generator. Having used a TX antenna at 10 m. distance would have required an RF high power amplifier able to output hundreds of Watts of RF power. This is due to the high propagation path losses from the TX antenna to the antenna of the ship-borne receivers under test.

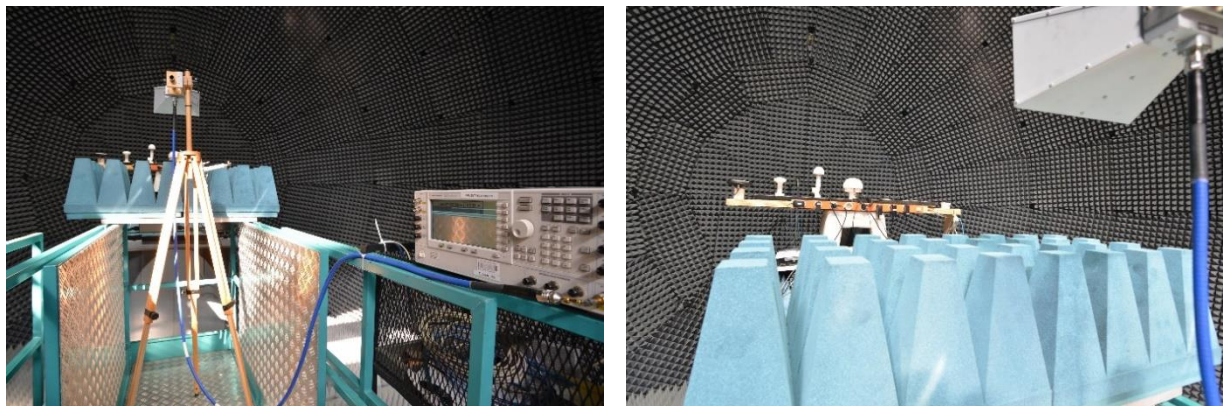


Figure 22. Two photographs with a close view of the set-up used with the programmable vector signal generator and a TX standard gain horn antenna on the movable platform of the EMSL.

An ad-hoc test suite was developed on a host laptop to automate the execution of the conformance tests specified in the standard. The suite was able to interface the DUTs via a virtual COM-USB RS232 and also over the network via a TCP socket. The control software was coded using PowerShell scripts that configured remotely the receivers and could also send specific commands (e.g., a configuration sentence or a cold start command). Moreover, the test suite interfaced and operated remotely the GNSS simulator. The execution of a

long series of test sessions logging the observation data from all the DUTs, going through the entire set of test scenarios, was possible. The latter is a very important point when comparing the performance of the DUTs under the presence of interference signals, as it guarantees that the test conditions for all devices are exactly the same.

Regarding the post-processing and analysis of the receiver logs, the NMEA format was used both for the logs of the receivers and the GNSS simulator. The NMEA log files were firstly parsed using an in-house software tool developed in C++. The datasets obtained were then formatted conveniently for a subsequent analysis using a suite of Matlab scripts, which was developed ad-hoc for this campaign.

For the sake of illustration, one example of the test scenarios that were assessed is given. Among the 24 test cases specified in the standard, there was a test to assess the RAIM/FDE capabilities of the DUTs. For this test case, an initial baseline static scenario had to be used. A second scenario introducing pseudorange ramps and satellite switch-off events, in accordance to the IEC standard specifications, was also created. This scenario starts with eight healthy satellites, after 25 minutes, a pseudorange ramp of one of the satellites was applied, with the pseudorange error gradually increasing up to 500 m. Right after, the error is kept constant for one minute, and then it is decreased down to 0 m. After the ramp, the satellite affected by the error is switched-off reducing the number of available satellites. In order to stress the RAIM/FDE algorithms implemented in the DUTs, this process is repeated with five satellites sequentially during the same test scenario. The pseudorange ramps together with the horizontal positioning errors observed by the DUTs are shown in Figure 23.

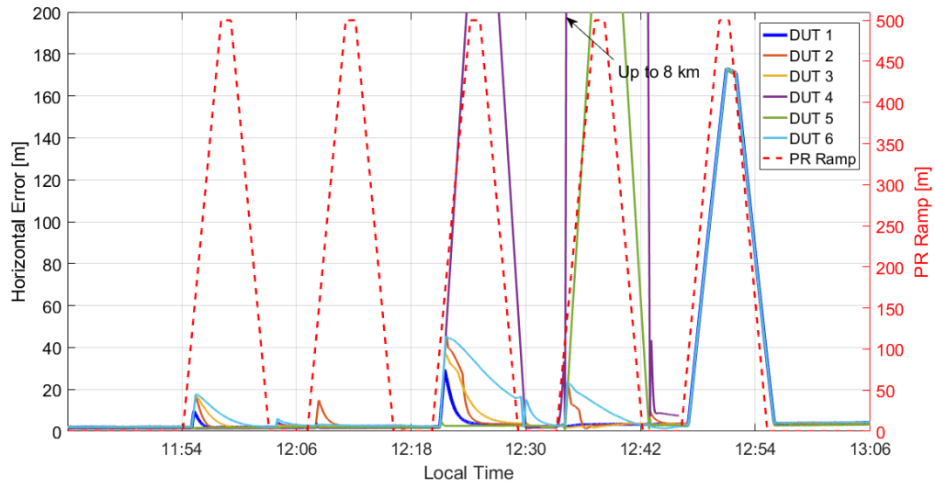


Figure 23. Pseudorange ramps and horizontal positioning error as a function of the time in the RAIM/FDE test case.

3.2.4 Assessment of Galileo HAS performance for vehicle in urban scenario

On 24 January 2023, the Galileo High Accuracy Service (HAS) was declared operational. Galileo HAS is a new service designed to enable positioning accuracy below 20 cm (with a confidence level of 95%) in the horizontal plane, and 40 cm (with a confidence level of 95%) in the vertical axis, after convergence, allowing users to benefit from centimeter-level or decimeter-level accuracy [21]. The demand for higher positioning accuracies is constantly growing, and Galileo HAS is a step towards meeting this demand, enabling users to benefit from high accuracy GNSS services for free, and opening up a whole new world of possibilities for applications such as autonomous vehicles, cadastre, construction, oil drilling, and many more. Galileo HAS is primarily addressed to the automotive user-segment, which is becoming a major user of high accuracy services. This section presents the outcomes of a test campaign performed at the European Commission's Joint Research Centre (JRC) in Ispra, Italy, aimed at evaluating the HAS performance on road vehicles in an urban scenario. The data collection was performed using different grades GNSS receivers including the HAS User Terminal (HAS UT) [22]. The test campaign aims to compare the performance of the HAS UT with respect to standard Precise Point Positioning (PPP) solutions with and without HAS corrections. The standard PPP algorithm exploits precise reference satellite orbit and clock products. Thanks to the available HAS corrections a different approach can be adopted: the broadcast ephemerides can be corrected with HAS corrections as

shown in [21]. The performance, in terms of positioning errors and solution availability, of the different configurations are assessed using the methodology described in Figure 24.

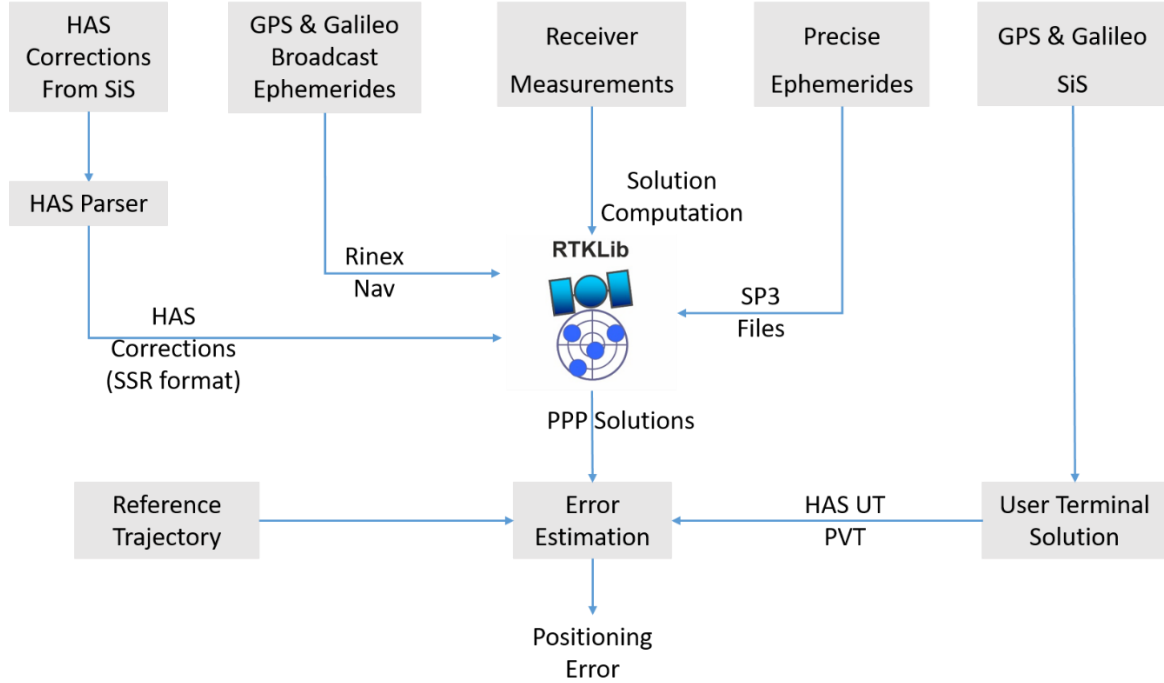


Figure 24. Working Flow of the processing scheme.

The PPP solutions are computed using RTKLlib (version 2.4.3), and the main inputs are:

- broadcast ephemerides for GPS and Galileo;
- GNSS observables (including code, carrier and Doppler shift measurements) collected by the receiver on board the van;
- Precise ephemerides in Standard Product 3 (SP3) format;

HAS corrections. In order to process the HAS corrections, Galileo navigation messages collected by a static receiver have been stored on a PC and then processed using HASlib software [23], [24].

The HAS UT solution is obtained directly as output of the UT receiver.

The following settings have been used to compute the PPP solution with RTKLlib software:

- Ambiguity Resolution (Float);
- Elevation Masking Angle of 10°;
- Tropospheric delay estimated;

C/No threshold is set to 20 dB-Hz (measurements with C/No lower than 20 dB-Hz are not used in the navigation solution computation).

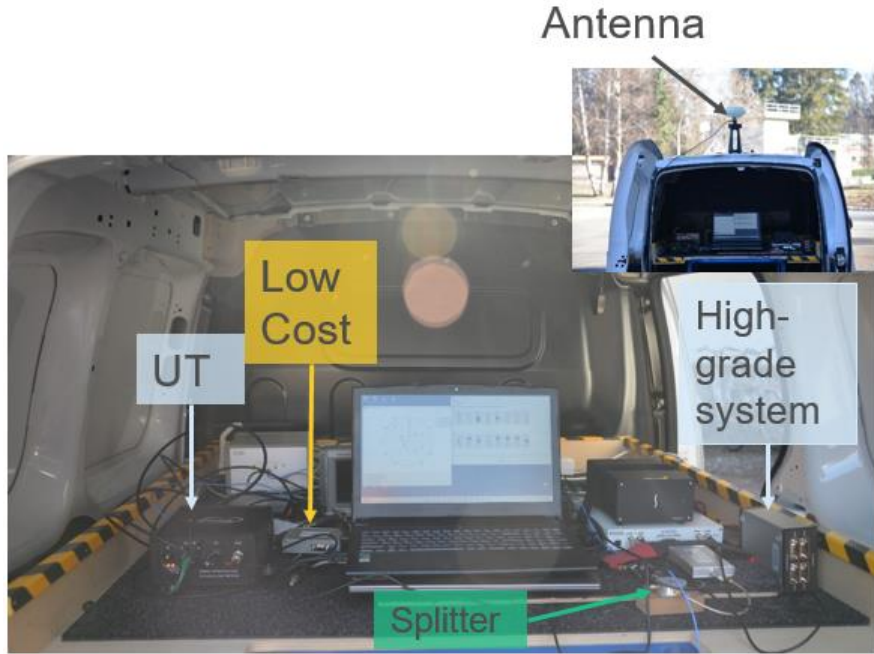


Figure 25. JRC van equipped for the kinematic test aimed at assessing the performance of a HAS-enabled user terminal.

Sample results related to the test campaign are reported below, the reference trajectory for the test has been computed using PPK post processing approach as described in Section 3.3.

In Figure 26 and Figure 27 the statistical parameters of the horizontal and vertical positioning errors are shown. In the upper boxes, the horizontal channel is considered while in the lower boxes the vertical channel is plotted. Specifically, Figure 26 shows the mean errors: the mean horizontal error of the UT is very close to the PPP SP3 solution. A mean error of about 46 cm has been observed for the UT solution while for the PPP with SP3 and the one using broadcast ephemerides and HAS corrections an increase of 1 cm has been noted. For the vertical case similar considerations can be made.

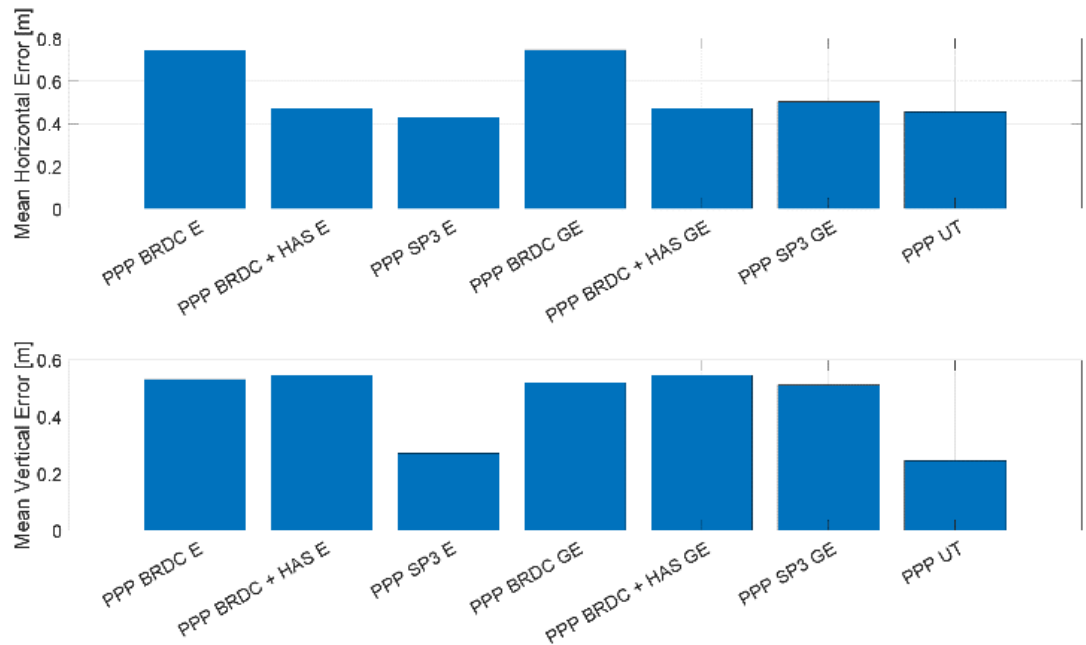


Figure 26. Mean horizontal (upper box) and vertical (bottom box) error.

In Figure 27, the standard deviation parameters are shown. In this case, the advantages of the UT solution are more clear. In particular, for the horizontal error a standard deviation of about 8 cm has been observed.

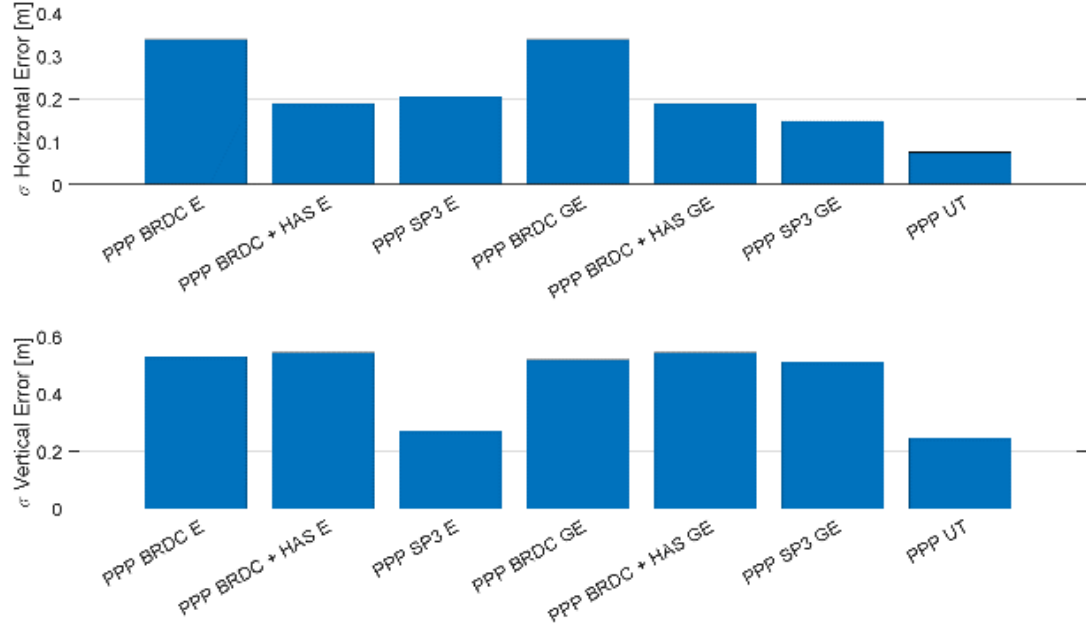


Figure 27. Standard deviation of the horizontal (upper box) and vertical (lower box) error.

For additional results, interested readers may refer to [25], [26].

3.2.5 Performance assessment of smartphones exposing raw measurements

Location-based services (LBSs) is the market segment of Galileo with the largest number of users [27]. At the end of 2019, the number of Galileo-enabled smartphones was estimated to have surpassed 1 billion devices [28]. The development of LBS is driven by different needs, depending on the application: mobility, productivity, safety, etc. To satisfy these needs, the key requirements for GNSS are the TTFF, the positioning accuracy and PVT availability. Galileo satellites will further improve signal availability, thus enhancing continuity of service for LBS in urban and challenging environments. By contributing to multi-constellation solutions, Galileo can satisfy the need for higher accuracy and fast TTFF of such demanding applications as personal tracking.

Noting the strategic importance of LBS and the need to monitor the adoption of Galileo in the new smartphones that are released on the market, the JRC in close coordination with the GSA, has carried out a number of testing campaigns conducted in the over the Air (OTA) mode in a shielded room using a GNSS simulator and a transmit antenna [29]. In addition to this, there have been H2020 projects aimed at promoting the adoption of Galileo and, more importantly, establish an EU-based, worldwide service to provide and/or enable location for LBSs and Machine-to-Machine (M2M) applications [30].

An interesting development that may enable higher accuracy for mass market devices is the new availability of raw measurements at the Operating System level, released in 2016 on smartphones running Android 7.0 (and higher) [31]. Until then raw measurements were exclusively accessible on high-end or professional GNSS receivers. This innovation was eagerly anticipated by the GNSS community and has triggered the development of numerous new LBS apps and services.

Future calls of R&D actions under the EGNSS Programmes are expected to target the development of new LBSs apps, services, or infrastructures. In the next sections, a description of two test campaigns, one with live Signal-in-Space (SIS) and a second one in the shielded room, is given to illustrate what are the testing capabilities available in this domain.

3.2.5.1 Smartphones testing using live signals in space

JRC has capabilities for performing tests campaign with the smartphones devices using the live SIS. Several tests have been conducted in different operational scenarios, from static open-sky to vehicular test in urban areas. For these tests the smartphones were placed inside a shielding box connected to a geodetic antenna placed on the rooftop of an office building (for static open-sky). A similar setup was used for the static test in signal degraded conditions, in this case the geodetic antenna was placed in the proximity of a building masking part of the sky and causing severe multipath. Additional details on these test setup are available in the previous version of this report [1]. In addition to static tests, vehicular and pedestrian tests were also designed and performed using specific setups. Examples of the set-up prepared are shown in Figure 28 for pedestrian and vehicular tests, respectively. The vehicular set-up exploited the shielding box as described above. Here, the main difference is the use of a professional receiver for generating the reference trajectory. A complete description of the setup and discussion of the results are available in [1].

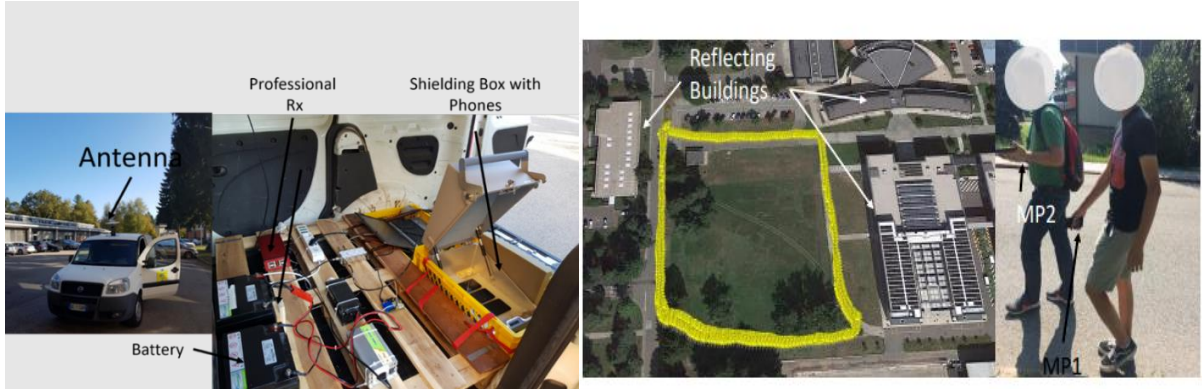


Figure 28. Setup developed for vehicular (left) and pedestrian (right) tests using smartphones.

3.2.5.2 Smartphone testing using a GNSS simulator

Emergency location services are an important element in the public safety and security policy toolbox. Timely and effective access to emergency services is a basic expectation of European citizens linked to the right of free movement and the European space of safety and security. EU Directive 2018/1972 [32] ensures access to emergency services through emergency communications to the Public Safety Answering Point (PSAP) with the goal to request and receive emergency relief from emergency services. Accurate caller location is a key enabler of access to emergency services supporting those services to quickly and effectively intervene. The Directive mandates the availability of both network-based and the more accurate handset derived caller location information provision to the most appropriate PSAP. The measures transposing and implementing the Directive (EU) 2018/1972 were adopted by all Member States by 21 December 2020. In this framework, smartphones have a key role in receiving and processing the electromagnetic signals, including GNSS and Wireless Local Area Network (WLAN) derived, on the basis of which the location of the caller should be estimated. The E112 Commission Delegated Regulation 2019/320 [33], aims to a more effective emergency communications by improving the accuracy of the caller location. This regulatory framework requires mobile devices manufacturers to support GNSS including at least Galileo. This requirement applies from March 2022 to all smartphones entering the EU market. The formal compliance to the requirements set is assessed by notified bodies through conformity assessment procedures. JRC has developed ad hoc recommendations and viable setup for this conformance test. A schematic representation of the setup is shown in Figure 29.

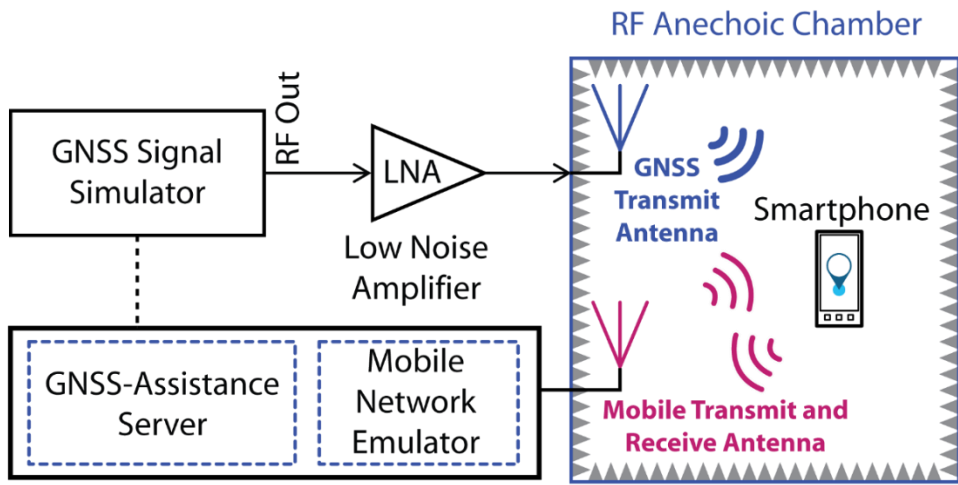


Figure 29. Sketch of the RF testing environment with the smartphone in an anechoic chamber.

In addition to the previous setup, the JRC laboratory is also able to test smartphone performance with simulated GNSS signals.

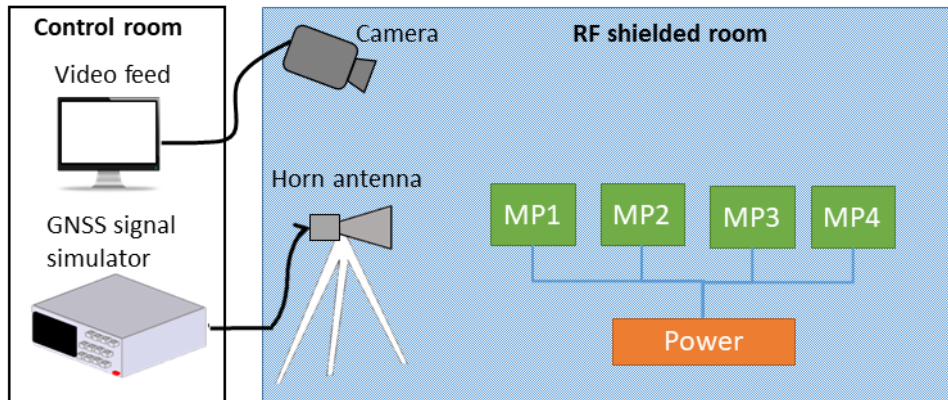


Figure 30. Schematic representation of the test set-up for smartphone testing using simulated GNSS signals.



Figure 31. Views of the actual set-up for smartphone testing using simulated GNSS signals, in the RF shielded room (left) and in the control room (right).

For this test, the devices were placed inside the RF shielded room, together with a standard gain horn antenna, as shown in Figure 31. The antenna radiates the GNSS signals generated by the simulator, located in the control room. Given the size of the room, a large number of devices can be tested simultaneously. The transmitted signal power can be calibrated using an approach similar to that used in the test campaign on the ship-borne receivers in the EMSL, presented in Section 3.2.3. A camera, installed in the shielded room, enables to remotely monitor the test. It can be used, for example, to control the correct logging of the data on the smartphone's screen. As for the live test, the collected data can then be analysed using the ad-hoc in-house software.

A suite of scenarios representative of diverse environments and dynamic conditions was created, and it is available for future testing campaigns. Testing using simulated GNSS signals enables to evaluate the performance of the smartphones under controlled conditions, which cannot be reproduced using live signals. For example, this set-up has been used to assess the performances of smartphones with Galileo only signals. In addition, the time of the scenario can be aligned with the current day of the testing to let the smartphones integrate live assisted-GNSS data.

3.3 Retrieval of Reference Trajectory Solutions

The estimation of reference solutions is of paramount importance to assess systems and algorithms performance. JRC has supported several H2020 and Fundamental Element projects in the estimation of benchmark solutions for testing activities.

The JRC laboratory is equipped with several high-grade systems suitable to provide reference solutions for different applications. Specifically, the JRC owns multiple high-end geodetic receivers and antennas, by different manufacturers, which can be used to set up Real Time Kinematic (RTK) reference stations, able to transmit RTK corrections for providing high accuracy solutions in real time, or to log reference data to be used for Post Processing Kinematic (PPK) purposes.

The JRC laboratory has also at disposal a high-grade platform combining GNSS and an Inertial Measurement Unit (IMU) especially suitable to provide reference solutions for dynamic tests also in the presence of short GNSS outages.

In addition, JRC experts can assist in estimating reference solution also in environments where the GNSS signal reception is challenging using the total station available in the JRC laboratory.

Finally, the JRC acquired vast experience in the estimation of reference solutions obtained by post-processing GNSS and, when available, also IMU data.

This section provides some sample test cases to showcase the above capabilities.

3.3.1 GNSS/IMU based reference solution: an agriculture case study

As illustrative case, in the following the support activity given in the frame of the Field Aware Navigation and Timing Authentication Sensor for Timing Infrastructure and Centimeter level positioning (FANTASTIC) Fundamental Element project is detailed [34].

One of the goals of the project was to develop high accuracy solutions for agriculture applications. Several dynamic tests were performed to assess the performance of the GNSS geodetic antennas and receivers developed during the project.

The JRC supported the testing activity by providing a Synchronous Position, Attitude and Navigation (SPAN) system by Novatel (*SPAN GNSS Inertial Navigation Systems*, 2021), used as benchmark during the dynamic tests¹. The system, shown in Figure 32, includes a high performing Micro Electro Mechanical System (MEMS) IMU to deliver high accuracy navigation solutions exploiting an integrated solution. SPAN-CPT tightly couples GNSS positioning and IMU gyro and accelerometer measurements. The system can be configured to receive RTK corrections reaching centimetre accuracy under nominal conditions. Moreover, the IMU allows to bridge temporary GNSS outages of up to 60 seconds in duration.



Figure 32. Novatel PwrPak7-E2, the reference navigation system available at the JRC.

¹ A previous version of the system (SPAN-CPT) was used in the frame of the FANTASTIC project.

During the project, dynamic tests were performed using a cart whose sketch is provided on the left side of Figure 33 [35]. The cart carried the receivers developed in the frame of the project, indicated with the label FANTASTIC, and other receivers and systems used for comparison purposes. The SPAN-CPT system has been placed on the top of the cart in proximity of the antenna to reduce the level arm between the GNSS antenna and the IMU. A picture of the real cart is provided in the right side of Figure 33 [36].

For the majority of these tests, the SPAN-CPT was configured to receive RTK corrections from a nearby reference station.

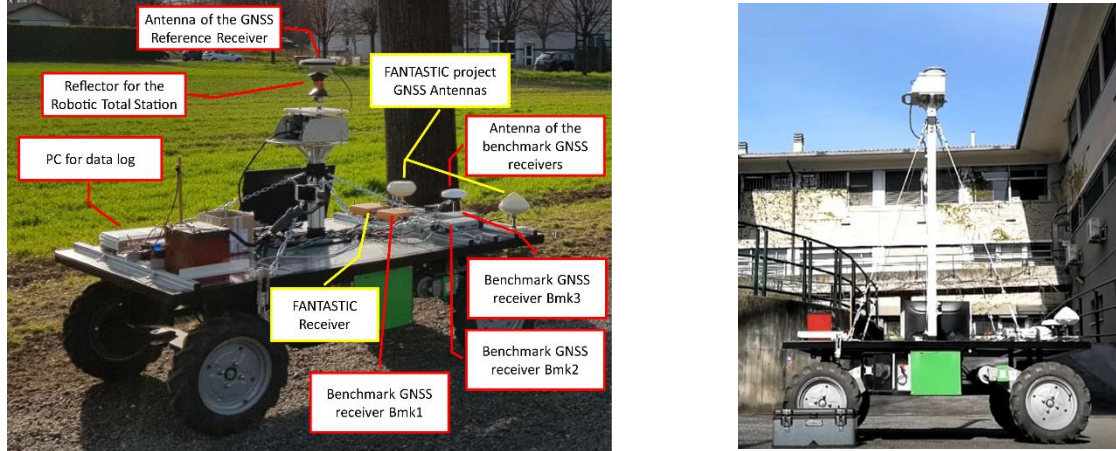


Figure 33. (Left side) Experimental set-up of the cart used for the dynamic test in the frame of the FANTASTIC project; (Right Side) Picture of the cart used for the dynamic tests carrying the SPAN-CPT system on the top (Extracted from FANTASTIC White Paper).

The data logged by the SPAN-CPT were also post-processed along with the base data, to obtain a PPK reference solution combining GNSS and IMU data through the Novatel Inertial Explorer software. This tool allows processing data from any receiver in PPK or in PPP mode, providing high accurate solutions suitable to be used as reference. The tool allows also post processing GNSS and IMU data system by giving the freedom to combine them in a tightly or loosely coupled mode.

In the frame of the FANTASTIC project, the JRC provided reference solutions for several dynamic tests. In Figure 34 the cart used for the dynamic tests is shown while performing a data collection in a vineyard. In Figure 35, the reference trajectory obtained by post processing SPAN-CPT data set in PPK mode and combining the GNSS and IMU data from the SPAN-CPT using a tightly coupled approach is provided.



Figure 34. Cart carrying the devices under test during a dynamic data collection in a vineyard [37].

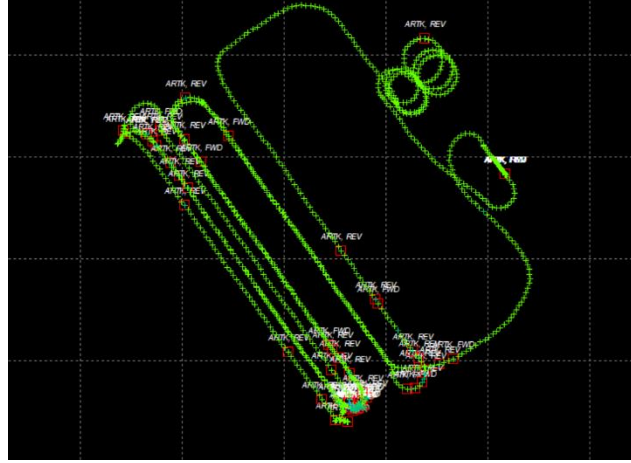


Figure 35. Reference trajectory obtained by post processing the SPAN-CPT and the reference station data.

The reference trajectory, is based on a fixed ambiguity solution for all the duration of the test, has been used by the consortium to assess the accuracy of all the DUTs, as shown from the plot in Figure 36. The latter reports the CDF of the horizontal position error, computed with respect to the SPAN-CPT reference solution, for the receiver developed in the frame of the project and all the other receivers used as benchmark.

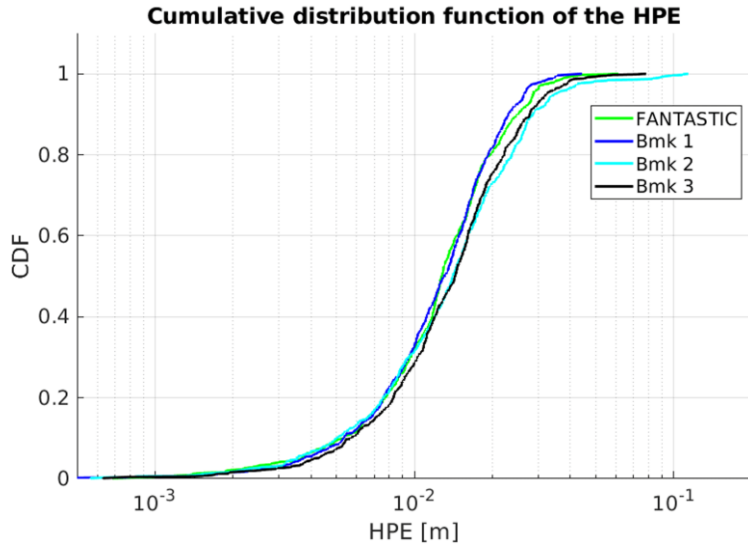


Figure 36. CDF of the horizontal position errors estimated for different devices under test and using the provided post-processed SPAN-CPT trajectory as reference [37].

3.3.2 GNSS based reference solution: a drone case study

The JRC supported the test activities performed in the frame of the Galileo-EGNOS as an Asset for UTM Safety and Security (GAUSS) H2020 Project [38].

The project had the objective to develop high performance positioning systems for drones. For this purpose, several flight tests were performed with different types of drones. The JRC assisted in setting up the reference station used to assess the GNSS solutions of the DUT carried on board of the drones.

In Figure 37 (left side), the RTK base station which was set-up at the ATLAS (Air Traffic Laboratory for Advanced Systems) facility is shown [39]. The tests were performed in Jaen, Spain in July 2020. A high grade GNSS reference receiver and antenna, provided by the JRC, logged 5Hz reference data during flight tests performed with different drones. The Tucan drone, one of the drones used in the testing activities, is shown in the right side of Figure 37.



Figure 37. (Left Side) High-end geodetic antenna placed under open sky at the ATLAS facility, connected to a high geodetic receiver to serve as reference station during flight tests with drones (Right Side) Tucan drone used in the frame of the GAUSS Project (images courtesy of the GAUSS project).

Reference trajectory solutions were also computed by the JRC in the frame of the GAUSS project. The data from the rover receivers on-board the drones and from the base station were post processed in PPK mode. JRC is able to provide PPK and also PPP solutions, for this purpose, a commercial software, Inertial Explorer, by Novatel is exploited. The software uses the RINEX files of the base and the rover to estimate the PPK solution. If the data from the base station are not available, the software can download the data from the nearest publicly available reference stations. Moreover, from the RINEX file of the rover, the software can also provide a post processed PPP solution after downloading clock and orbit corrections. Built-in ionospheric processing improves accuracies for dual-frequency users. Figure 38 shows a sample reference trajectory estimated for one of the test flights performed by the above drone.



Figure 38. Reference trajectory computed for one of the flight performed by the Tucan drone with Novatel Inertial Explorer.

For some of the test flights, the computed PPK reference trajectories were compared with the one obtained from a laser ranging system owned by the consortium. The consistency between both PPK and PPP solutions further validated the quality of the reference trajectory obtained. These reference trajectories were exploited by the consortium to assess the benefit of using Galileo and EGNOS to support drone operations (e.g. for navigation, detect and avoid, tracking etc.).

3.3.3 Total station based surveying

3.3.3.1 Static survey: a 5G case study

To determine reference solutions in GNSS challenging environments, a total station can be used. This device allows to determine the position of a target using angle and distance measurements. The absolute position of the target can be obtained integrating GNSS positioning information. This approach was adopted to support a 5G measurement campaign carried on the JRC Ispra campus. During the campaign, 5G measurements were performed with respect to a reference point, where the 5G transmitter was located. The measurements were taken in a challenging environment for 5G signals, due to the presence of nearby buildings and trees. Unfortunately, this type of environment is also very challenging for GNSS signals, and prevented the straightforward use of a standalone GNSS receivers to determine the location of the points of measurements. As a solution, the points were surveyed using a total station, as shown in Figure 39. The total station measures vertical and horizontal angles as well as of the slope distance from the instrument to a given point. To coordinate the measurements, the station was set over a known point and its orientation was fixed using an additional known point (back sight). These reference points were selected in open-sky areas and their coordinates were determined beforehand using GNSS data processed in PPK mode. Using these points to set up the total station and the back sight, it was then possible to coordinate the points of measurements, even under dense tree coverage as illustrated in Figure 40.



Figure 39. Surveying of the measurement points using a GNSS receiver (left) and the total station (right).



Figure 40. Survey results for the test carried out with the total station in the JRC Campus.

3.3.3.2 Robotic Tracking Station

A robotic total station or multi-station has the capacity to track a moving platform equipped with a reflector, as illustrated in Figure 41. The instrument is able to track the platform over a long distance (up to several km) and under a wide range of dynamics, as long as the line of sight between the reflector and the instrument is maintained. This approach was used by the JRC to compute the position of a drone flown in different environments around the campus. As for the static case, the instrument needs to be set-up over known coordinates in order to obtain the absolute position of the platform.



Figure 41. Tracking of a drone using a multi-station (left) and a reflector mounted on the drone (left)

3.3.4 Highly Degraded GNSS Environment – Test Drive in Milan

Galileo plays a key role for greener, smarter and safer transport and mobility applications. The new Galileo services [40], [41], Galileo High Accuracy Service (HAS) and Galileo Open Service Navigation Message Authentication (OSNMA), will have a direct and valuable impact on automotive scenario. Thanks to the HAS service, a positioning accuracy target of 20 cm in the horizontal plain in nominal conditions will be achievable and this will be instrumental for the use of applications requiring precise localisation, such as deployment of autonomous driving vehicles. OSNMA is included as a key element of the recent EU legislation on the Smart Tachographs, the new generation of on-board mandatory digital recorders of the professional drivers' activities (rest and driving hours). In addition to these two services, also Galileo INAV improvements will contribute to make the Galileo signals reception more robust under degraded environment.

Assessing the performance improvements stemming from the use of the new Galileo services represents an interesting research area at the JRC. A specific testing campaign aimed at collecting GNSS data in highly degraded environment, was carried out by JRC team. A van was equipped with state-of-the-art devices: a high-grade GNSS antenna was mounted on the roof and connected via a splitter to different GNSS receivers, a record-and-replay RF system and the reference navigation GNSS+INS system.

The dynamic tests were performed in the city center of Milan, where the presence of obstacles limits the satellites visibility and the vehicle speed is reduced. The whole path travelled in the Milan metropolitan area is shown in Figure 42, along with two examples of environments, that show a moderate to heavy urban scenario.



Figure 42. Dynamic test scenario in the Milan metropolitan area.

JRC has been working on the GNSS data collected during the campaign, including the estimation of the high-accurate reference trajectory and the preparation of a GNSS data library to be shared with interested players within GNSS community (see Section 4.5).

3.4 Galileo High Accuracy Service

Since January 24th 2023, EU's global navigation satellite system Galileo has reached a further milestone in the Galileo Services Roadmap: the High Accuracy Service (HAS) [42] becomes operational, offering unprecedented decimetre-level positioning accuracy, free of charge on a 24/7 basis over most parts of the globe in nominal conditions. This performance results is possible thank to the dissemination of the high accuracy PPP corrections in terms of satellites orbit, clock and code biases corrections. These corrections are applicable to the reference Galileo and GPS navigation messages and the ranging measurements of

- Galileo I/NAV navigation message and Galileo E1/E5a/E5b/E6 signals
- GPS LNAV navigation message and GPS L1/L2C signals.

Therefore, this new service will become fundamental for the use of applications requiring precise localisation, such as deployment of autonomous driving vehicles, safety road technology and drones. Other applications concern agriculture, rail, aviation, maritime, space, consumer solutions and geomatics. The high accuracy corrections are disseminated through two complementary channels: directly via the Galileo E6-B SiS, i.e. the HAS SIS [21], and through a terrestrial link, i.e. the Galileo HAS internet data distribution (IDD) [43], as shown in Figure 43 [44].

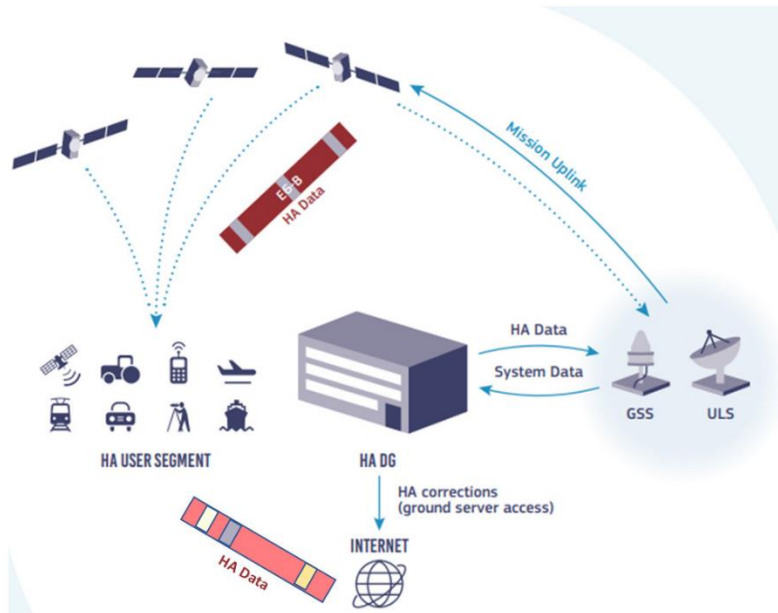


Figure 43. Galileo HAS data broadcasting scheme.

The JRC is contributing to the definition, testing and validation of HAS supporting DEFIS and EUSPA. The work included studies on the processing of the Galileo E6-B signal, carrying the HAS data, within Galileo receivers, technical support to the definition of Galileo Programme reference documents, as well as testing and validation activities of the HAS service [45]. The JRC assessed the ultimate performance of HAS under different conditions.

3.4.1 Reference HAS User Algorithm

JRC contributed to the definition of the HAS User Algorithm (UA) documentation, processing software (HAS UA SW JRC), test vector and monitoring/testing facility (i.e. HAS UA Testbed). The HAS UA document provides the detailed description of the algorithms for properly utilising the HAS corrections, from both SiS and terrestrial link, and estimating the filtered PVT solution. It also provides detailed description of how detecting cycle slips and measurement outliers, computing signal time of flight and implement the Extended Kalman Filter (EKF) for computing the position, velocity and time solutions. The HAS UA SW JRC provides a Matlab (and soon also Simulink and C) implementation of the algorithms described in the UA document. The test vector provides a

numerical example of expected solution for a UA implementation, with a full set of input data to be processed and the corresponding HAS UA SW output solution.

The monitoring and testing facility is realized through a testbed concept, the HAS UA Testbed, which is described in the following section.

3.4.2 HAS User Algorithm Testbed

JRC laboratory facility hosts the HAS UA Testbed in support to all the activities related to the testing and validation of the HAS service. This Testbed is composed of the following main equipment, as depicted in Figure 44:

- Zephyr Trimble antenna
- Novatel OEM7700 GNSS receiver
- Septentrio PolaRx5
- HAS server PC

Within the main block represented by HAS server PC, the following sub-equipment are fundamental in the necessary data generation for HAS service verification purpose:

- Novatel Application Suite, to extract GNSS measurements and ephemeris from the Novatel binary log into RINEX files;
- HAS SIS message decoder, to decode the HAS message from Galileo C/NAV and save it in a IGS State Space Representation (SSR) format;
- HAS ephemeris creator, to combine IGS broadcast ephemeris files with the SSR HAS corrections and create HAS ephemeris – SP3, CLK, BIA files;
- HAS ephemeris comparator, to compare the HAS ephemeris to IGS final ephemeris;
- HAS UA SW Spaceopal (SPO), to process Novatel data and HAS corrections with the HAS UT SW;
- HAS UA SW JRC, to process Novatel data and HAS corrections with the HAS UA;
- HAS positioning comparator, to compare the SPO and JRC solutions between them and w.r.t. the reference solution.
- Plot tools, to generate time series, CDF and infographic to show ephemeris and positioning performances.

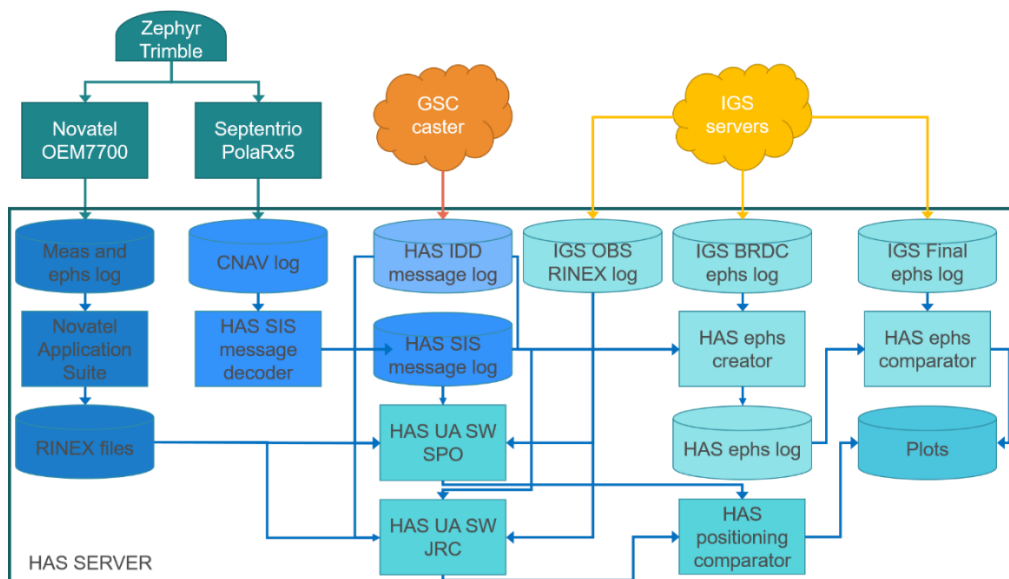


Figure 44. HAS UA Testbed currently deployed at JRC.

From above Figure 44, HAS UA test setup generates a set of files which include the different inputs that have been processed by the user algorithm in the UT,

- Observation RINEX file
- Navigation RINEX file
- OEM7 binary observation and navigation file
- SSR corrections files (SIS or IDD depending on the configuration):
- SSR binary file (RTCM3SSR formats)
- Decoded HAS corrections in ASCII (proprietary format text file)
- Output binary file with the positioning results.

In addition, HAS Server hosts two NTRIP casters to disseminate via internet the HAS SIS corrections obtained by the Septentrio PolaRx5 receiver and the HAS IDD corrections obtained by the official Galileo HAS caster at the European GNSS Service Centre (GSC).

3.4.3 Testing of HAS Performance

The HAS performance, in terms of product and solution accuracy, is evaluated in the HAS UA Testbed at HAS ephemeris level (i.e. the combination of the HAS corrections with the OS ephemeris) and at user PVT solution level (for the HAS test receivers in the lab and a few selected IGS stations). The HAS and OS ephemeris are compared with respect to the Multi-GNSS Experiment (MGEX) final products to obtain an indication of the HAS input quality (see Figure 45).

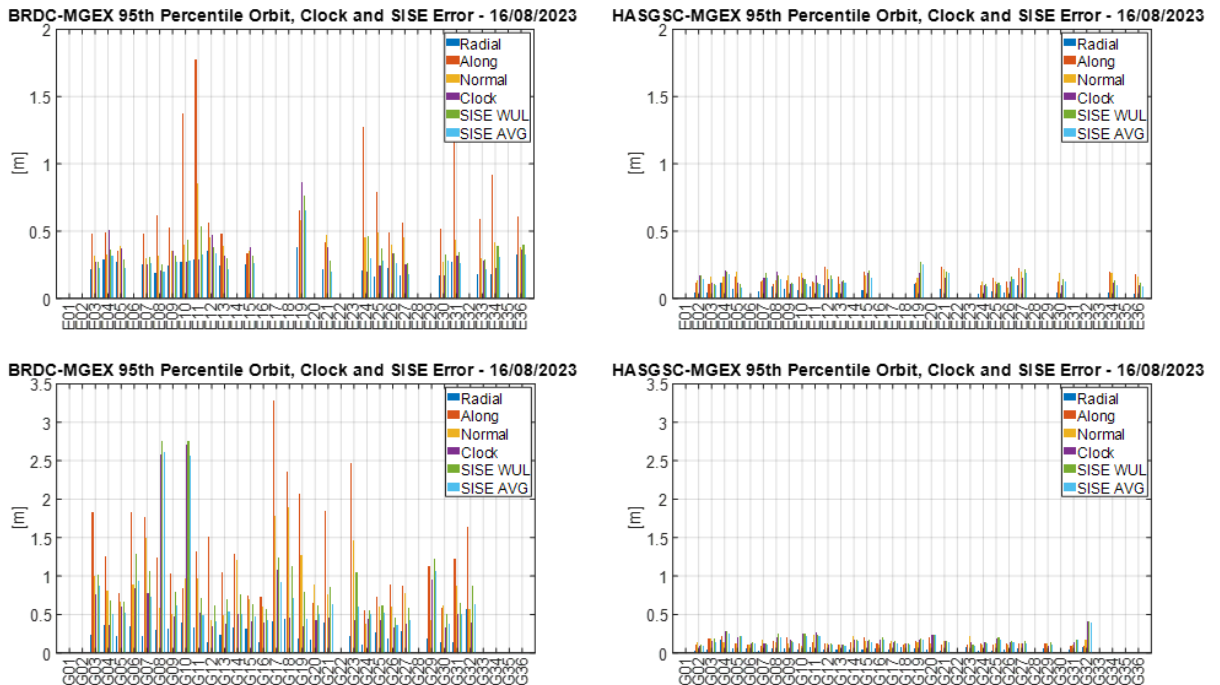


Figure 45. Comparison of Galileo (top) and GPS (bottom) SISE errors and components of Broadcast (left) and HAS (right) ephemeris w.r.t. IGS final products.

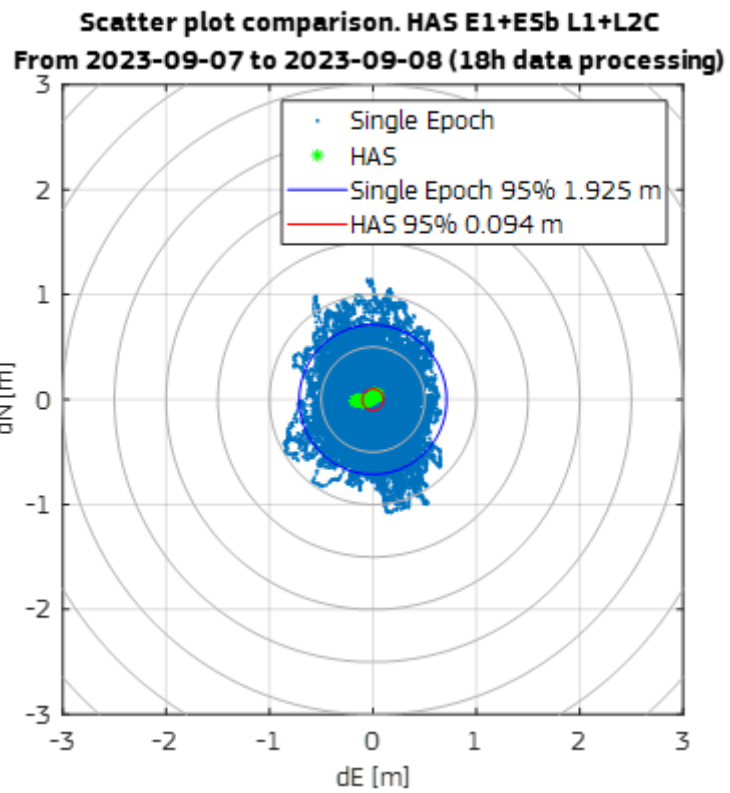


Figure 46. HAS solution for a static solution at JRC location with OS and HAS ephemeris.

3.5 Galileo Timing Service

GNSS Timing is used in a variety of critical infrastructures, like 4G/5G mobile networks, smart grids, and banking. Galileo Timing Service aims at providing a trustable and reliable global timing reference through the Galileo System Time (GST) and its traceability to UTC. The Galileo Timing Service will provide three different Service Levels targeting different GST and UTC accuracies. Furthermore, in case a service level cannot be guaranteed, Galileo will promptly notify the users within a maximum Time to Notification (TTN), expected to be below 30 minutes, via both Signal-in-Space and terrestrial means.

Information from the Galileo system on the Service Level and user notifications are contained in the Timing Service Message (TSM), which is one of the pillars the Galileo Timing Service relies on.

Another fundamental pillar is the Galileo Timing Receiver Standard, which ensures the information provided by Galileo is correctly processed and the receiver meets the minimum performance level required to support a specific Service Level.

A key element of the Galileo Timing Service is its traceability to UTC. The validation of the Galileo UTC timing solution requires a precise time reference to be used for comparison. At this scope, JRC is working on the integration of a UTC time scale in its laboratory, as described in the next section. Furthermore, since the UTC realization obtained using GNSS is subject to delays due to the receiving antenna and hardware, its solution shall be precisely time calibrated. To this aim, JRC is preparing the setup for an absolute calibration of the receiver and receiver chain. This activity will be described in a future issue of this document.

In addition, JRC is actively supporting the drafting and validation of the standard. This activity is conducted within the WG9 (Work Item JTC5) at CEN/CENELEC. JRC substantially contributed to the definition of the testing procedures and their validation through the execution of preliminary tests. Further details are presented in Section 3.5.2.

3.5.1 UTC Time Scale Transfer

The capabilities available at JRC for timing reference and UTC time scale transfer are described in [46], the JRC report that summarises the main results of the C-PNT test campaign, performed in the framework of a DEFIS call for tender (CFT), aiming to assess the performance of the C-PNT technologies delivering accurate and robust positioning and timing services.

JRC has provided the timing reference for all the experiments conducted. The test rig was organised as follows:

- UTC (IT) references JRC time reference, consisting of Septentrio PolaRx5 and SRS FS725 Rubidium oscillator. The GNSS signal was obtained from the antenna located on the buildings used for the Number of Agilent 3220A interval/frequency counters (TIC), monitoring the PUTs 1PPS against time reference;
- This setup can provide both 10 MHz and 1PPS input to DUTs;
- The platform Under Test (PUT).

The test rig was set up separately for each platform provider, with cable delays calibrated. Before each test, a known offset (200-500 ns) was set at the Septentrio PolaRx5 receiver. This was intended to avoid DUT 1PPS arriving before reference. This setup was run for at least 12h, to verify the timing test rig performance and stability, usually against Meinberg Lantime M300 or another Septentrio receiver (see Figure 47).



Figure 47. Calibration setup, with JRC time reference visible on top.

3.5.1.1 UTC(IT) Calibration

The setup was calibrated by the Istituto Nazionale di Ricerca Metrologica (INRiM), the Metrology Institute providing the official Italian UTC Time. The calibration provided GNSS-delivered time ‘sits traceability to UTC(IT) with nanosecond accuracy. This guarantees the reference to UTC(IT) at the 1PSS output from the JRC time reference.

Figure 48 shows the results of the INRiM calibration campaign, which lasted 46 days.

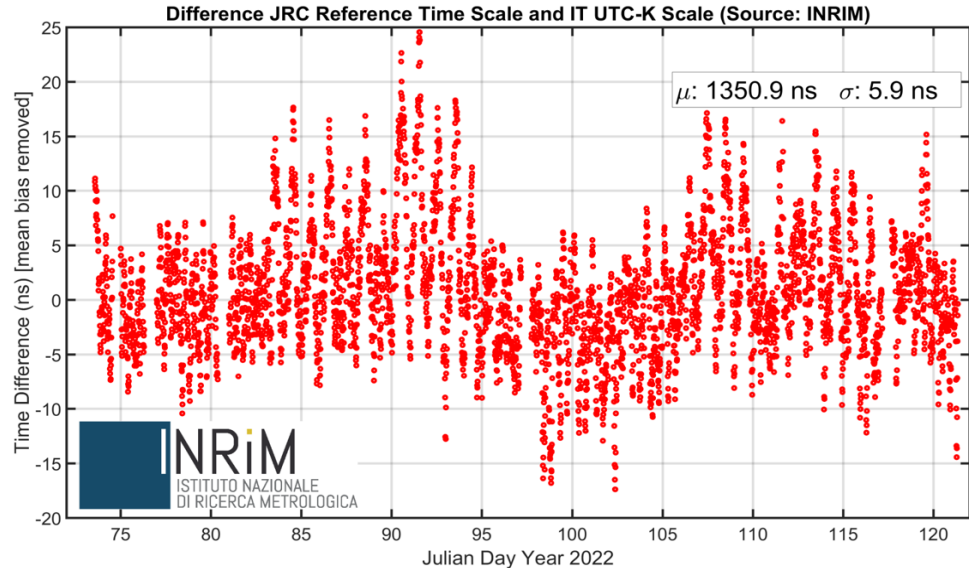


Figure 48. Results of INRiM 46 days calibration campaign.

3.5.2 Timing testing via Record & Replay

In order to support the future Galileo timing service, JRC is actively participating in the European Committee for Standardization (CEN) and the European Committee for Electrotechnical Standardization (CENELEC) Working Group 9 (CEN/CLC/JTC5/WG9) for the definition of the standard and associated compliance test scenarios for future Galileo timing receivers exploiting E1/E5b signals. The target users for such standard are all Galileo timing users, with particular focus on critical applications in infrastructure. The standard defines the minimum requirements as well as a set of tests to verify the receivers' functionality in terms of accuracy, availability, integrity and T-RAIM probability of missed detection. In this context, JRC plays an important role for supporting the standard definition as well as preparing the validation datasets for certified test laboratories.

Considering that the SIS conditions have a strong impact on the device under test performance, the tests results may vary considerably regardless of the receiver and depending on the RF signals captured by the antenna, how and where it was installed or what are the atmospheric conditions at the moment of the test. On the other hand, there is a clear need to have a controllable and reproducible test environment for testing timing devices. For this reason, a record & replay (R&R) approach has been proposed for the compliance testing of the Galileo timing standard.

The R&R approach requires a Software Defined Radio (SDR) equipment, or other equivalent hardware. While there are some plug and play solutions available in the market, the most advanced, flexible and configurable ones are designed for advanced users. In addition, for this type of tests not all the SDR hardware platforms are valid since at least two RF front ends are needed as two frequency bands need to be simultaneously processed. Moreover, at the record stage, various configuration parameters such as the bit depth, sampling frequency, duration of the recording represent a trade-off between the reliability of the recorded signal (mainly due to the quantization noise and sampling rate) and the hardware and storage limitations. JRC is playing an important role to test various R&R solutions to facilitate the tests that are being defined for the future Galileo timing receiver standard.

As an example, Figure 49 shows the equipment configuration for validating a record and replay approach for testing of Galileo timing receivers. The laboratory equipment used in this activity is shown in Figure 50, including all relevant hardware elements to perform tests of timing receivers, as well as to carry out absolute calibration of such receivers, in order to measure internal hardware delays for each GNSS signals, which is an important element in the definition of UTC with international metrology laboratories.

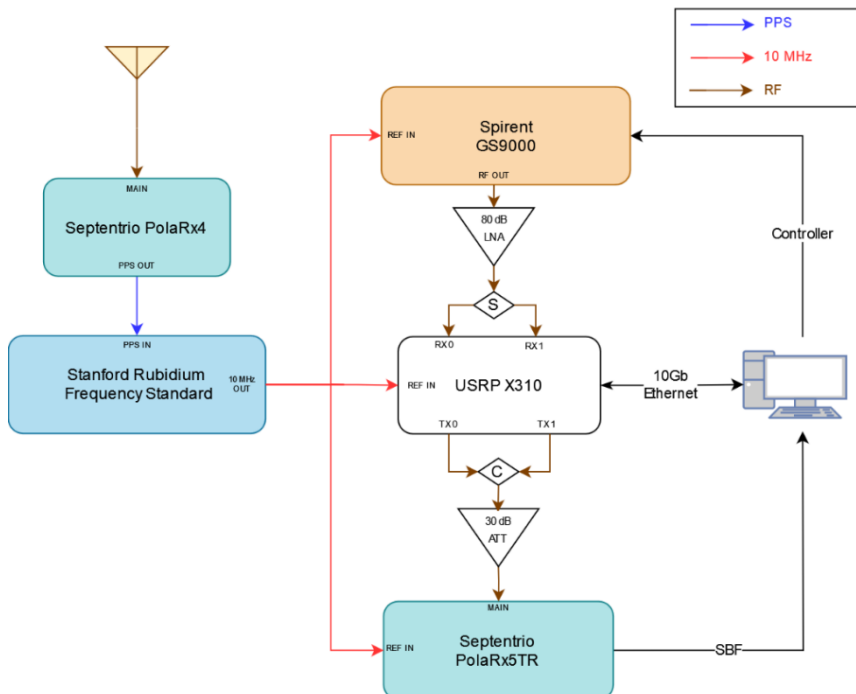


Figure 49. Record/replay setup for testing Galileo timing receivers

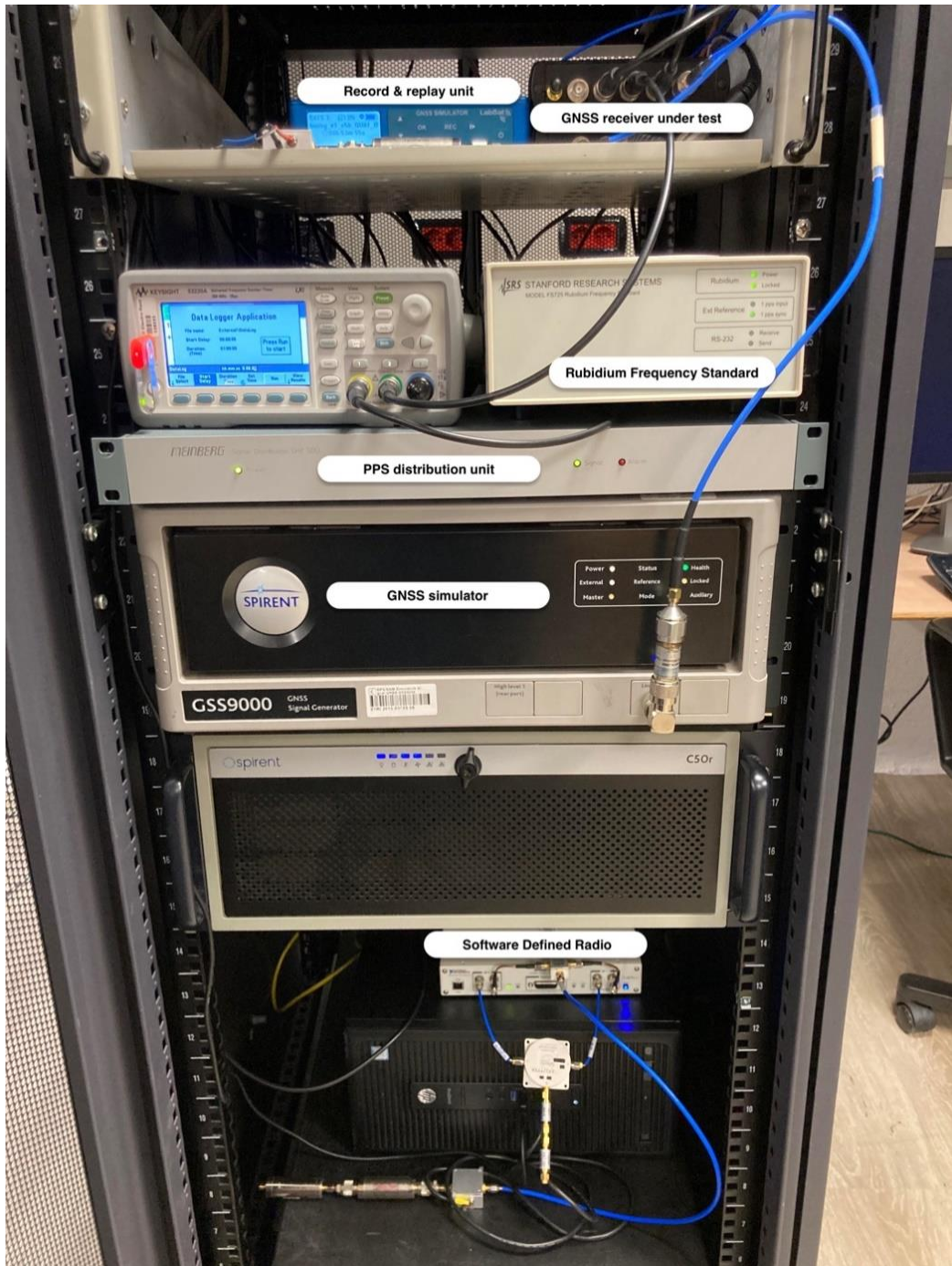


Figure 50. Timing test equipment in JRC laboratory.

3.6 Galileo OSNMA Service

The Galileo Open Service Navigation Message Authentication (OSNMA) is a new service that provides means to authenticate navigation data through information transmitted in the SIS, as part of the E1B I/NAV message [47], [48]. Starting in 2013, the definition and implementation of this new service at system level have been supported by a series of H2020 Mission And Services (MAS) R&D Actions and internal studies under the EU GNSS Programmes [49], [50], [51] and [52]. The GNSS laboratory of the JRC supported these projects, facilitating extensive testing and validation activities. In preparation of the foreseen entry-in-service of the OSNMA, the JRC also supported the adoption of the service by users, facilitating testing and demonstration activities of H2020, Horizon Europe and Galileo Fundamental Elements Projects with a focus on GNSS user-segments or use cases (e.g., smart tachograph, timing receivers, drones, maritime, etc.). Through these support activities, JRC has acquired a significant know-how on the OSNMA protocol, as well as several key testing assets, delivered by the supported projects or procured separately.

The following sections provide a description of the key assets and relevant testing capabilities that are available at the JRC to support OSNMA-related R&D actions under the EU GNSS Programmes.

3.6.1 Generation of the Galileo OSNMA data stream

3.6.1.1 *I/NAV data streams*

The E1B I/NAV data stream is continuously recorded by a receiver located in our laboratory. This data, as well as the OSNMA test vectors [53], can in turn be provided to a GNSS simulator in order to generate signals including OSNMA. This approach exploits the capacity of the simulator to accept user-defined I/NAV streams and can also be used with simulated OSNMA data. The RF signal generated in this way can also be recorded by an SDR system for future analysis or re-transmission.

3.6.1.2 *OSNMA record and replay*

JRC has the capability to record RF signal snapshots from the live signal covering various OSNMA configurations, both in static and dynamic conditions, including various environments for the dynamic samples (e.g. sub-urban, urban). These RF samples can then be replayed to the receiver under test using an SDR system.

The combination of real data and simulation capabilities represents a versatile solution to generate the most relevant aspects of the OSNMA protocol while covering as well specific conditions and corner cases.

3.6.2 Set-up for OSNMA testing

3.6.2.1 *OSNMA-enabled receivers*

To assess the performances of OSNMA enabled devices, a reference receiver is required, to act as a control. This is of particular importance for OSNMA, as the service is still in its early stages. The receiver used to this end is an OSNMA-enabled GNSS receiver from Septentrio [54].

3.6.2.2 *Test set-up*

The capabilities described in the previous sections can be fully exploited using the developed high flexible and modular testing set-up [55], described in Figure 51.

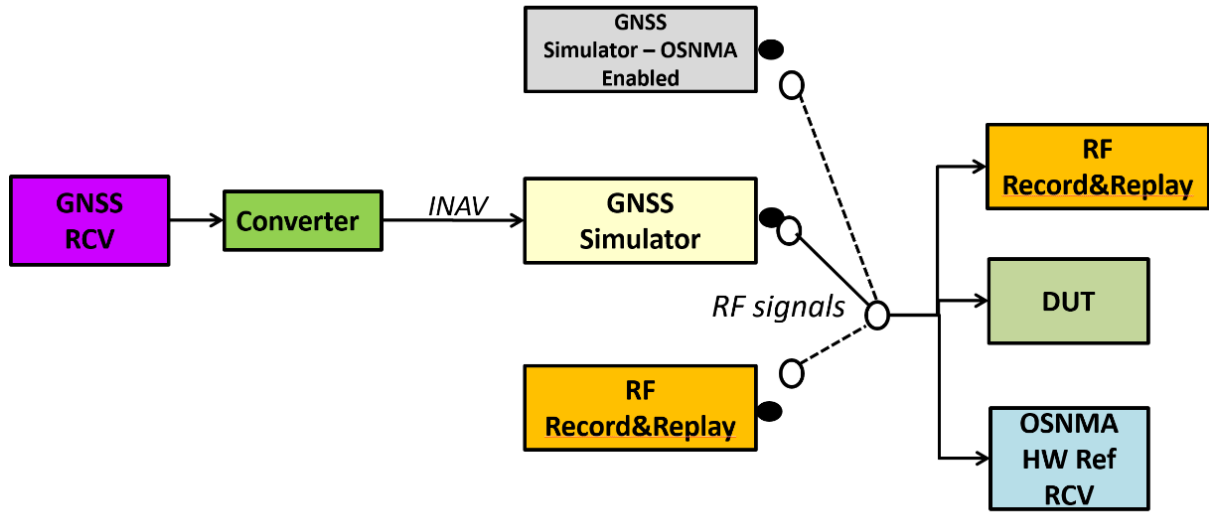


Figure 51. OSNMA testing capabilities.

In summary, the device under test can be assessed either:

- by replaying recorded RF samples;
- by using a GNSS simulator configured to use E1B I/NAV data containing OSNMA.
- by using a GNSS simulator with OSNMA generation capability enabled.

The performance assessment of the DUT can then be carried out using an OSNMA reference receiver as a baseline for comparison. Additional software tools developed at JRC can also be exploited to perform a detailed analysis of the behaviours observed (Section 3.6.3).

To support the adoption of OSNMA by the user community, thorough testing of OSNMA-enabled receivers is required. This testing shall cover two aspects:

- Ensure the correct implementation of the protocol through functional testing, aiming at verifying the cryptographic processing capabilities of the receiver, both during nominal operations and during renewal and revocation operations.
- Assess the performance of the receiver under different testing conditions (e.g. visibility, dynamic conditions). This assessment is carried out using traditional OS key performance indicators as well as specific OSNMA indicators, such as the authentication failure rate, time to first fix with authenticated data and OSNMA PVT accuracy.

In addition, robustness tests against specific attacks can also be carried out, as described in Section 3.13.

3.6.3 OSNMA Post Processing

The JRC has developed a post-processing software suite able to parse the Galileo I/NAV stream in its final format [48] and to analyse the relevant OSNMA-related information broadcast in the SIS, as illustrated in Figure 52. The analysis represents a useful mean to check the actual broadcasted OSNMA configuration and to complement the verification of the receiver's compliance to the OSNMA protocol.

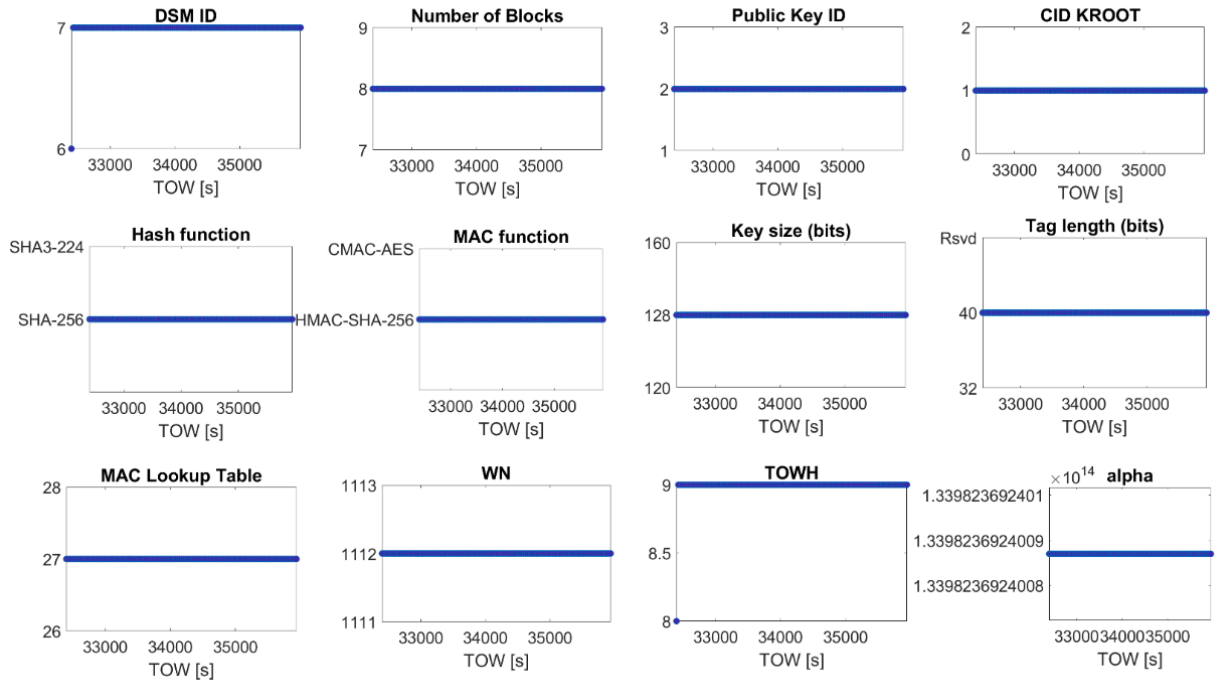


Figure 52. TESLA chain parameters retrieved from the JRC OSNMA parser

In addition, the software suite performs the different verifications mandated by the OSNMA protocol, which can be used for example to analyse the results of the robustness tests.

The JRC OSNMA parser has been used to quantify the benefits of different data retrieval strategies in terms of time to first fix with authenticated data and time between authentication, as published in [56], [55].

3.6.4 Examples of supported projects

3.6.4.1 BANSHEE

The BANSHEE project aimed to develop a hybrid technology combining Wi-Fi ranging and satellite navigation (GNSS) that allows an accurate seamless indoor-outdoor navigation. In order to increase the robustness of the solution, the OSNMA protocol was implemented.

Functional testing of the solutions was carried out by the consortium using the SIS and the OSNMA test vectors, while JRC supported with the execution of the robustness tests. These tests focused in particular on:

- Spoofing detection with simulated data (i.e. including incorrect OSNMA data that lead to verification failures).
- Spoofing detection with live synchronised counterfeit signal (mixing the live signal with a spoofed replica).
- Spoofing detection with a simulated meaconer (delayed of more than 30 seconds).

As a result of the project, a Galileo OSNMA library for embedded solutions was developed by the consortium [57], [58].

3.6.4.2 ASGARD

The ASGARD project aimed at designing, integrating, verifying and validating a shipborne dual-frequency multi-constellation receiver including Galileo OSNMA and IEC GNSS approval.

As part of the OSNMA functionality testing, several robustness tests were carried out with the support of JRC, in particular:

- Spoofing replicating the SIS without OSNMA information (field set to zero).
- Spoofing with OSNMA information replicated as in SIS (false ephemerides information).
- Spoofing of only some satellites in view (false ephemerides for one satellite only)
- Spoofing with OSNMA information replicated as in SIS keeping the same IODs (IODnav not updated despite having false ephemerides)

3.7 Galileo ACAS Service

The Commercial Authentication Service (CAS) is currently being developed by the European Commission (EC) to complement the Open Service (OS), providing an enhanced authentication function to the Galileo users and increase the location security [59]. It provides protection at the spreading code level by encrypting portions of the code chip sequences, thus allowing for a greater level of protection against malicious spoofing attacks [60]. Together with the OSNMA, it aims to offer a fully secure solution for authenticating the PVT. To achieve this without modifying the Galileo signal plan, an assisted mode, known as ACAS, has been proposed and is envisaged by 2024 [49]. In this scheme, some ancillary data from the E1-B signal will be used, allowing the receiver to decrypt the codes without the need of storing any secret key.

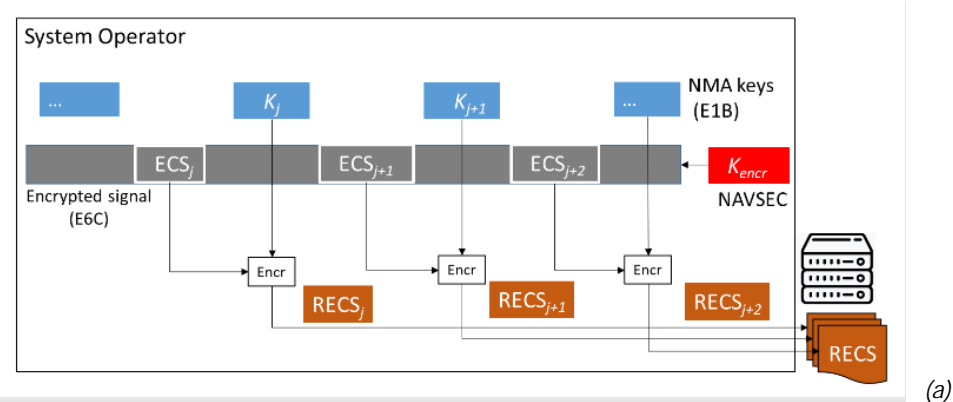
The Assisted Commercial Authentication Service (ACAS) scheme is intended for Galileo 1st Generation (G1G), with the purpose to facilitate the system implementation and maximize the receiver autonomy. It is applied to Galileo through the E1B OSNMA and the E6C pilot signal, currently open but soon to be encrypted.

For the sake of clarity, the working principle of the ACAS service is summarized hereafter, from the overviews given in [59] and [60].

At the system level, fragments of the encrypted E6-C keystream are re-encrypted using the Timed Efficient Stream Loss-tolerant Authentication (TESLA) key provided by the OSNMA protocol in the E1-B signal (Section 3.6), and published together with other useful information as files in GSC or any publicly accessible servers, at certain predefined instants and for a certain predefined duration. In detail, the GSC is required to publish the E6C Re-Encrypted Code Sequences (RECS) files and the authenticated satellite broadcast group delays (BGDs) between E1 and E6, as this information is not in the broadcast I/NAV message and therefore not authenticated by the OSNMA [60]. The main benefit of this approach is to allow the user receiver to operate in standalone mode for the duration of the pre-downloaded data (i.e., the RECSs files), and without the need of storing any secret key.

At the receiver level, the user downloads the RECSs, with their start and end times, for the desired autonomy period. At, or around, those times, the receiver records a signal snapshot that should contain the encrypted signal, then waits for the NMA key to be disclosed, decrypts the RECS to obtain the original Encrypted Code Sequence (ECS), and correlates a-posteriori the signal snapshot with the ECS. If the presence of the ECS is detected, under certain conditions and hypotheses the receiver can assume, with a high probability, that the signal is authentic. A key assumption is that the receiver has a loose synchronization time source, sufficient to prevent an adversary to replay the ECS after the NMA key is disclosed. This requirement is already in place for Galileo OSNMA.

The schematic of the ACAS concept is shown in Figure 53, at both the system and receiver level [59].



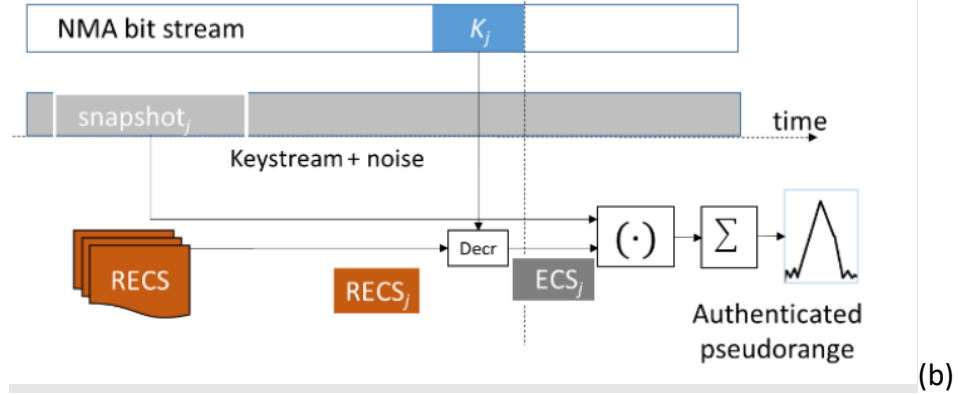


Figure 53. Schematic representation of the ACAS concept at the system (a) and receiver level (b).

3.7.1 Paula User Terminal

The Precise and Authentic User Location Analysis (PAULA) project, funded by the European Commission DG-DEFIS under contract DEFIS/2020/OP/0002, was launched in 2020 with the aim of evaluating and testing different techniques to improve the resilience and security of the overall system together with a high accuracy position solution.

The PAULA User Terminal (UT) was one of the main outcomes of the project. It is a high accuracy positioning user terminal which integrates the authentication information coming from the different authentication modules installed in the UT together with a High Accuracy Service (HAS) capable high accuracy positioning module. The main goal of the PAULA user terminal is to serve as a platform to test the integration of the different authentication modules with a HAS high accuracy solution.

In detail, the software modules of the UT are depicted in four main groups accessible through the GUI interface (Figure 54), i.e.:

- HAS-PVT module, that implements the precise positioning solution algorithms in the UT;
- OSNMA module, responsible for providing authenticated navigation message and OSNMA keys;
- ACAS module, for computing a position solution based on the authenticated range and OSNMA authenticated data
- Anti-Replay module, to provide protection against zero-delay Security Code Estimation-Replay (SCER) (for details about SCER see section 3.13.3.5).

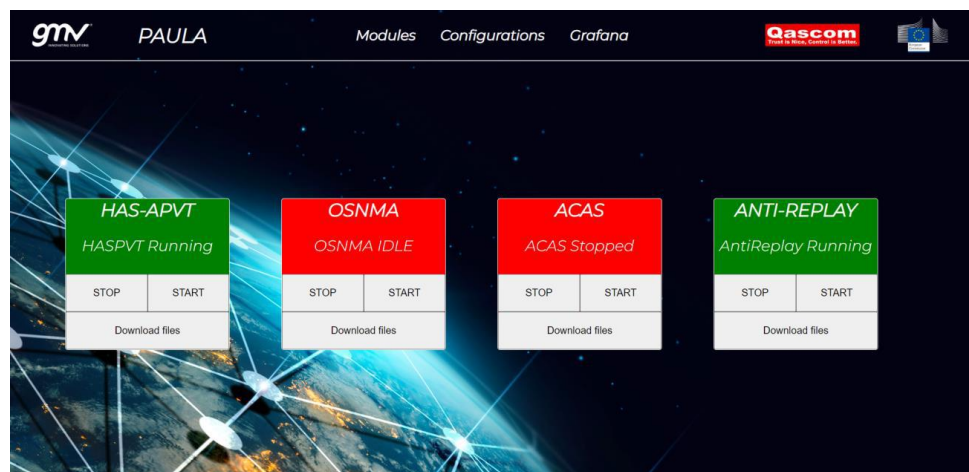


Figure 54. Paula UT modules options.

Focusing now on the ACAS module integrated in the PAULA UT, the ranges authentication is performed by means of a posteriori correlation of E6 signal samples by using E6 encrypted sequences provided by a server, which are in turn encrypted with an OSNMA key. The module will provide the acquisition status of the E6 signal, the verification of the E1 ranges and E6 PVT computation.

It is expected that the ACAS server provides encrypted sequences with a specific configuration, defining the rate and length of the recorded sequences; this configuration shall be known a priori and used to configure the Samples Recorder and the ACAS module. The ACAS module compares the E1 with the E6 observables and ranges and triggers an authentication alarms whenever inconsistencies (based on a configurable threshold) are detected.

As an ACAS server is not available, another project output was “ACAS TOOLS”, a set of software applications that generates sample “RECS/BGD” files in compliance with the ACAS specifications described above, with the purpose of supporting the validation of the PAULA ACAS module. It is worth mentioning that these tools are intended for software testing/debugging purposes and they have neither been validated to be used in an operational environment nor been validated for all the supported configurations.

3.8 Galileo I/NAV Improvements Testing Capability

From August 12, 2023, the gradual process of upgrading the operational Galileo Full Operational Capability (FOC) constellation satellites has been finalized and the improved I/NAV message is now freely accessible through the Galileo E1-B signal.

I/NAV improvements refer to the three new features added to the Galileo OS [41], freely available for all Galileo Open Service users. The improvements include:

- the Secondary Synchronization Patterns (SSP) at symbol level, to improve the capability of user receivers to reconstruct Galileo System Time using weak signals, without the need to demodulate the navigation message.
- the Reduced Clock and Ephemeris Data (RedCED), i.e., a compact set of satellite orbit and clock information with reduced accuracy, fit in a single word (namely Word Type 16) and is broadcast at a higher rate than the full accuracy CED. In return of a reduced accuracy in the position domain, the Time to First Fix (TTFF) is quicker and easier with respect to a legacy receiver.
- the FEC2 Reed-Solomon (RS) encoding of the CED, that provides improvements both in terms of Time-to-Data and data demodulation robustness.

EUSPA regularly publishes open calls for I/NAV improvements testing campaign inviting participants to express their interest in assessing the correctness of I/NAV improvements developments and solutions in their product.

The tests will be executed at the laboratories of the European Commission's Joint Research Centre in Ispra, Italy, and of the European Space Agency ESA/ESTEC in Noordwijk, The Netherlands. Each applicant will be assigned by EUSPA to any of the two laboratories depending on the specific conditions and availability.

The following sections provide a description of the relevant testing capabilities that are available at the JRC to support I/NAV improvements.

More detailed information can be found in [61].

3.8.1 Testing strategy

Two main categories of test cases have been identified and executed by JRC team:

- the first batch of tests are “functional” and is aimed at assessing the correct implementation of the protocol by means of simulated data properly manipulated in order to assess the receiver behaviour under specific conditions. These tests are carried out in simulation and in Galileo-only mode. Under this typology the following test cases are identified:
 - RedCED-only PVT: the test aims at verifying that the receiver is able to provide a PVT solution by using only reduced ephemeris.
 - RedCED age of data: the test aims at verifying that the receiver uses Reduced CED no longer than 10 minutes starting from its reference time.
 - FEC2 RS Erasure Correction - Only ParityWords: the test aims at verifying that the receiver is able to exploit FEC2 Erasure correction capability.
 - FEC2 RS Error&Erasure Correction: the test aims at verifying that the receiver is able to exploit FEC2 Error&Erasure correction capability.
 - SSP implementation: the test aims at verifying that the receiver is able to exploit the SSP synchronization pattern.
- the second batch of tests comprises “nominal” E1 OS INAV data including I/NAV improvements and is intended to assess the performance of the receiver when processing INAV improvements. Either fully simulated or live signals conditions can be used. Static/open sky and dynamic/urban scenarios are used to assess relevant KPIs including position accuracy, TTFF and availability.

3.8.2 Test Conditions

In order to prepare the test set-up more efficiently, the manufacturers having formally shown their interest to EUSPA, will be asked to fill a questionnaire: the selected questions are meant to provide details both on the current receiver capabilities in terms of I/NAV improvements implementations and on other technical aspects useful for a better understanding of the test set-up configurations to be put in place.

In addition to the questionnaire, each participant will be asked to provide, at least, the following items:

- The GNSS receiver to be tested.
- DUT user manual with detailed information about RF and communication interfaces.
- SW tool (e.g. receiver settings, output converter, etc.).
- Power supply and cables.

Moreover, a list of minimum expected receiver capabilities includes:

- Receive a cold start command thanks to which the receiver is forced to clean all previous PVT and GNSS data (e.g. ephemeris, almanacs) information.
- Log (at least) Global Positioning System Fixed Data (GGA), GNSS DOP and Active Satellites (GSA) and GNSS Satellites in View (GSV) sentences NMEA version higher than 4.10.
- Capability to provide PVT solution in Galileo-only mode.

Additional features that would make the test execution completer and more efficient are:

1. Proprietary output message containing the decoded RedCED.
2. Proprietary message describing whether the PVT solution has been evaluated by means of RedCED or CED information.
3. Capability to set the internal receiver time realisation in order to align it with the simulated time. This capability is needed for the SSP test.

3.9 ARAIM User Algorithm Implementation

The Advanced Receiver Autonomous Integrity Monitoring (ARAIM) is the evolution of the RAIM algorithm to accommodate a dual-frequency multi-constellation solution, at the cost of higher computational load.

Since 2004 The European Union (EU) and the United States (US) have established a cooperation between Europe's Galileo system and GPS to promote cooperation on the design and development of the next generation of civil satellite-based navigation and timing systems though a Working Group C (WG-C) [62].

The WG-C worked on the definition of a reference ARAIM implementation meeting the H-ARAIM/FDE requirements defined in the DFMC SBAS MOPS (ED-259). A reference ARAIM implementation based on [63] is described in the “ARAIM reference Airborne Description Document v4.2” (ARAIM ADD v4.2) developed within the WG-C [64]. The ARAIM ADD provides a description of the algorithms, optimisation strategies and guidelines.

As part of the ARAIM standards development, a Validation Task Force was created by WG-C. Six different groups coded the ARAIM ADD’s reference algorithm in their Global Navigation Satellite System (GNSS) availability simulation tools, including ARTEX (ARaim demonstrator for Testing and EXperimentation) by the Joint Research Centre (JRC) of the European Commission, GPAT by MITRE, MAAST by Stanford University, Pegasus by EUROCONTROL, SVS by GMV, and ATAA by Virginia Tech. This effort was aimed at finding a common understanding of the ADD and at ensuring that the availability simulation tools consistently predict identical levels of performance.

The JRC’s ARTEX implementation has been fully validated using a set of effective algorithm verification and comparison mechanisms designed by the Validation Task force. More details about the validation of the tools involved in the validation Task Force are given in [65].

The following pictures show the flowchart of the processing logic, including exclusion, implemented in the ARTEX tool.

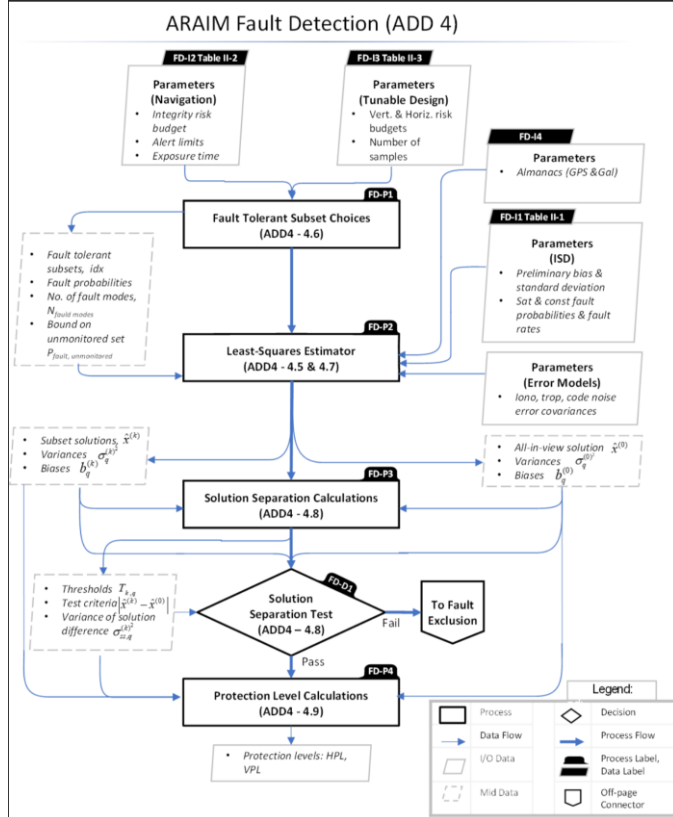


Figure 55. Fault Detection Flowchart (figure taken from [65])

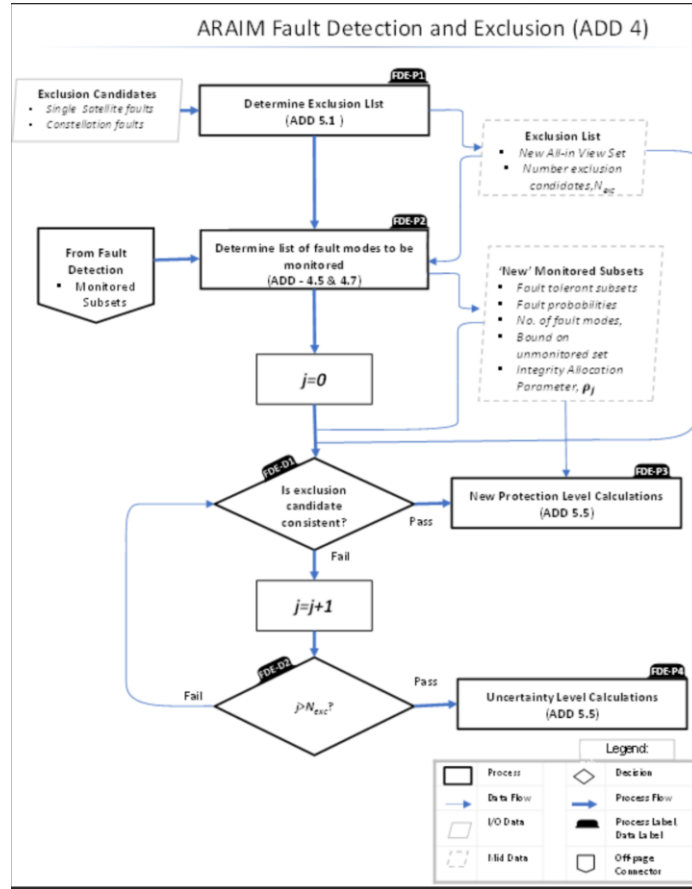


Figure 56. Fault Detection and Exclusion Flowchart (figure taken from [65])

The ARTEX tool is developed in MatLab. It is fully flexible and implements all the optimisation strategies suggested in [64]. It also allows the user to enable or disable specific features and optimisation. The tool can be also set to output the protection levels of a timing solution, namely T-ARAIM.

The following picture shows an exemplary output of the ARTEX tool.

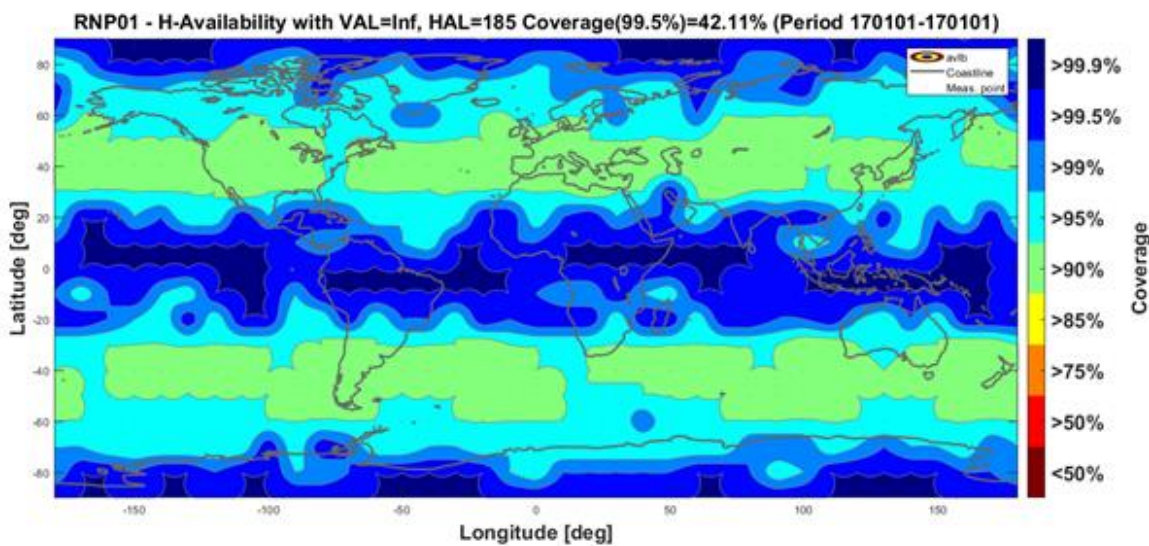


Figure 57. Horizontal Protection Level Coverage @99.5% of RNP 0.1

3.10 Galileo for Space Applications

GNSS system, originally designed to support Positioning, Navigation, and Timing (PNT) services to terrestrial user, is becoming a fundamental backbone of current and upcoming space applications. In this direction since 2018, within the International Committee on GNSS (ICG) Working Group B (WG-B), the United Nations Office for Outer Space Affairs (UNOOSA) published “The Interoperable Global Navigation Satellite Systems Space Service Volume” to drive the GNSS SSV concept definition and included the availability and performance of GNSS signals at high altitude (the region of space extending from 3,000 km to 36,000 km altitude above the Earth’s surface) as the primary SSV service indicators [66] (see Figure 58). Nowadays this concept has been extended also for the lunar navigation and communication missions thanks to preliminary studies which can confirm the feasibility of the navigation to the Moon with the implementation of dedicated high-sensitivity techniques at GNSS Spaceborne Receiver (RX) level plus other instruments [67].

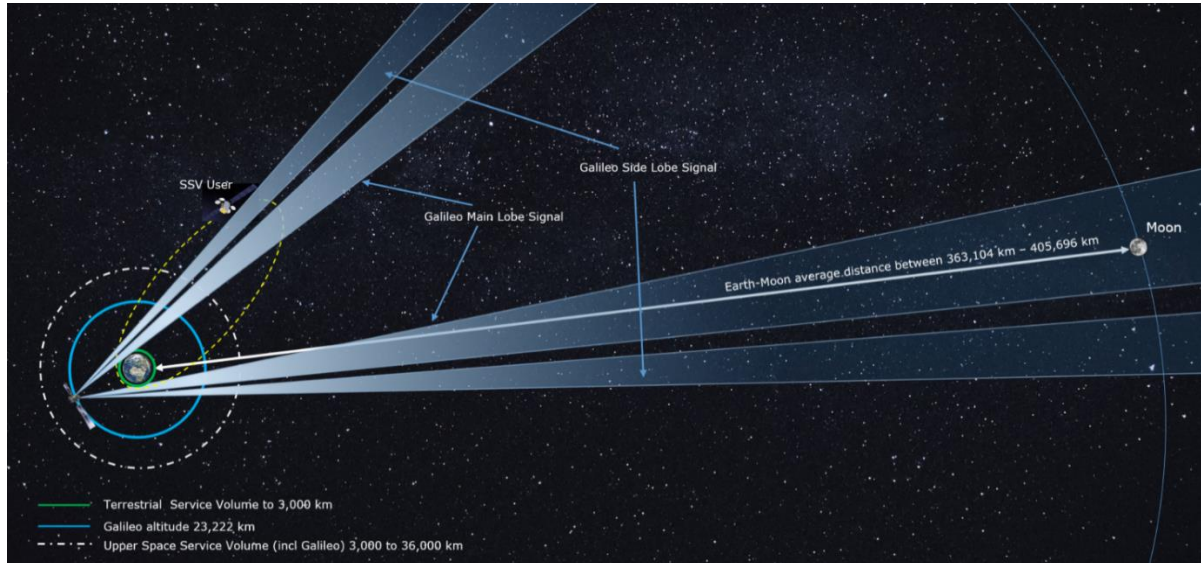


Figure 58. Space Service Volume and beyond.

In this context the JRC laboratory facility has recently developed a testing environment, the Integrated SSV Test Bench (JRC-ISSVTB) that integrate several hardware and software components supporting the development and testing of a GNSS Spaceborne receiver through a complete realistic simulation environment to confirm the achievable performance in SSV and beyond.

The following subsections provides further details about:

- the description of the JRC-ISSVTB testing environment with focus on the main building blocks characterizing a space mission simulation and HIL test.
- a summary of the possible JRC-ISSVTB configurations supporting the GNSS Spaceborne Rx verification in the SSV
- the Precise real-time On-board Orbit Determination (P2OD) verification capability, GASPER project experiment

Therefore JRC space laboratory capability allows also a GNSS Spaceborne Rx prototype development for current and future mission demonstration (e.g. navigation for LEO-PNT application [68] and lunar missions) and to gather data and support further system activities.

3.10.1 An Integrated SSV Test Bench

The JRC-ISSVTB implementation has been realized thank to the state-of-the-art GNSS simulators that are currently capable to generate Galileo E1/E5/E6, GPS L1/L2/L5 and Satellite Based Augmentation System (SBAS) [8]. Its flexible hardware-in-the-loop (HIL) approach is realized by the integration on the following main components as depicted in Figure 59.

- Input Data Interface, provides the SSV scenario specification and constraints characterisation. It is defined through three main blocks: the Spaceborne Rx mission specification, the GNSS Constellation data and the Space Environment definition. The first input data block includes the dataset suitable for the speciation of the GNSS Spaceborne Rx implementation. The second block involves the constellation data suitable for the orbit dynamic reconstruction, i.e. the almanac data, the broadcasted ephemeris. The latter block includes all the dataset concerning the Space Environment definition, for example the Earth Orientation Parameters (EOP).
- SSV Mission Simulator (SSV-MS) supports the high fidelity spacecraft orbit and attitude dynamic simulation through validated mission engineering simulation software. The satellite trajectory can be generated starting from several input data such as orbital elements, keplerian parameters, SP3 and Two Line Element (TLE) files. The mission attitude dynamic profile is generated starting from the nominal spacecraft attitude (i.e. Earth pointing) and adjusting it through body maneuvers (e.g. yaw, pitch and roll sequences).

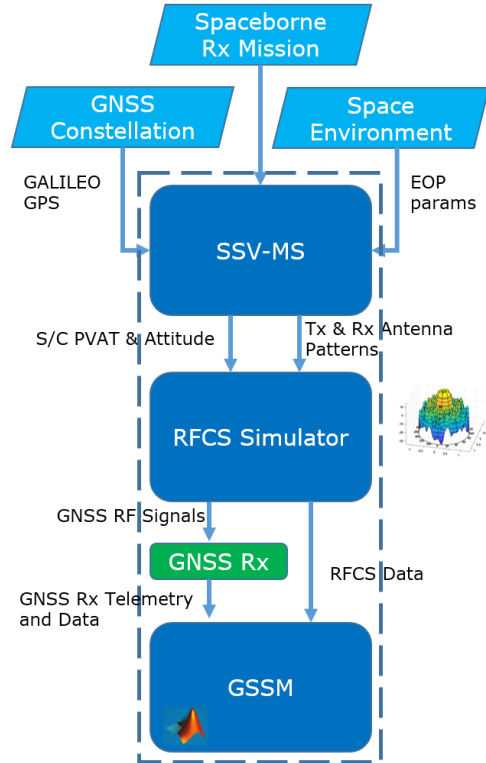


Figure 59. JRC-ISSVTB Block Diagram.

- RFCS (Radio Frequency Constellation Simulator) HW simulator for generate the Galileo constellation observables (pseudorange, Doppler and phase measurements) and the correspondent triple frequency RF signals (E1, E5, E6). A full calibration campaign has been performed in order to align the Galileo constellation and the signal in space propagation parameters to the reference system performances. The last released Galileo 3D EIRP model [69] has been considered and integrated into the RFCS simulator aligning signal transmission power, transmitting antenna pattern distribution and hardware implementation losses in order to cope with Galileo ICDs [41].
- GNSS Scenario Simulation Module (GSSM), a developed post-processing tool with the aim to perform feasibility and sensitivity analysis according to predefined thresholds and tuning parameters. The analysis includes the received signal power, the carrier to noise ratio (C/No), the Doppler shift and the expected receiver measurement accuracy relying on systematic and hardware errors (e.g. tracking loops). The signal and ephemeris availability, the Geometric Dilution of Precision (GDOP) and the standard positioning errors are derived as well
- Target GNSS Spaceborne Receiver, a GNSS Commercial Off The Shelf (COTS) receiver used as a permanent and reference receiver for the RFCS out signals acquisition via RF cables and navigation performance verification.

The EMSL facility presence (Section 0) close to a dedicated room behind the dome, in which the IRC- ISSVTB is located, provides a unique opportunity to perform End-to-End (E2E) SSV test campaign with a GNSS navigation system composed by a GNSS Spaceborne receiver plus its receiver antenna. A sketch of the configuration of the laboratory when the GNSS simulator is used as the signal source to characterise a GNSS antenna, and a photograph of the GNSS simulation rack are shown in Figure 8.

3.10.1.1 User Mission Definition

Through the SSV-MS module the desired SSV user mission trajectory and system design can be generated or integrated within the JRC-ISSVTB. The mission trajectory can be defined and integrated with respect to

- different reference frames, for example Earth Centred Earth Fixed (ECEF) or Earth Centred Inertial (ECI)
- a customized attitude dynamic profile as maneuver sequences generation, for example yaw-pitch-roll body rotation, sun-pointing rotation
- a dedicated user receiver antenna(s) specification and position(s)

The SSV user mission profile can be simulated in relation of the possible space mission summarized hereafter:

- Low Earth Orbit (LEO) / Medium Earth Orbit (MEO) / Geosynchronous Orbit (GEO)
- Rendezvous
- Formation Flying
- Attitude Determination
- Transfer Orbit
- High Eccentric Orbit (HEO)
- Launchers
- Radio Occultation
- Reflectometry / Scatterometry
- Moon Transfer Orbit (MTO) / Moon Orbit

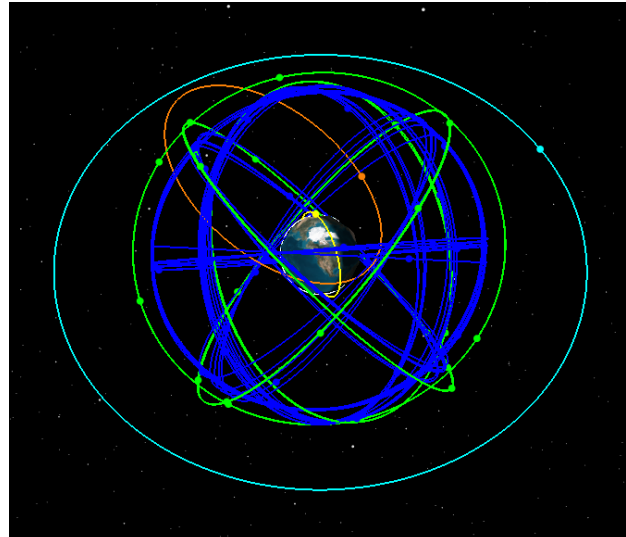


Figure 60. SSV user mission profile example

In Figure 60 an example of possible SSV user mission profiles are depicted: LEO mission (in yellow), HEO mission (in orange) and GEO mission (in cyan) plus the Galileo and GPS constellations (in green and blue respectively). The compatibility with such a wide range of space mission and orbit regime simulations is achieved thank to the JRC-ISSVTB flexible capability about the complete multi-constellation, multi-frequency, multi-antenna and multiple spacecraft scenarios implementation. In particular concerning the high orbit compatibility further simulation configuration details are described in Section 3.10.1.3 while Section 3.10.1.4 provides details about the multi spacecraft simulation capability.

3.10.1.2 RF Calibration

The RFCS Signal Power Calibration represents the core of the JRC-ISSVTB implementation. In fact, this procedure aims to “calibrate” and properly “adjust” the GNSS Navigation Signals levels of a RFCS Simulator to guarantee the minimum signal level requirement as per the applicable SIS ICDs [41], [70], [71]. The calibration accounts both simulation configuration and RF setup parts: the first includes all the atmospheric losses and signals power parameters definition (e.g. frequency offset, signals offset, power sharing) while the

latter involves the HW losses (e.g. RF Cable, LNA) between RFCS RF output port and the RX antenna port or LNA input.

Therefore, the outcome of the calibration procedure is represented by a set of configuration parameters. One of the key elements in the signal power calibration for the functional feasibility and performance assessment of a DUT is linked to the Transmitter (TX) antenna pattern implementation, indeed in Section 3.10.1.3 the antenna pattern implementation is introduced.

In Figure 61 the general test set-up considered for this calibration is composed by:

- RFCS Simulator
- RF harness (e.g. cables, LNA)
- Spectrum Analyser
- Network Analyser

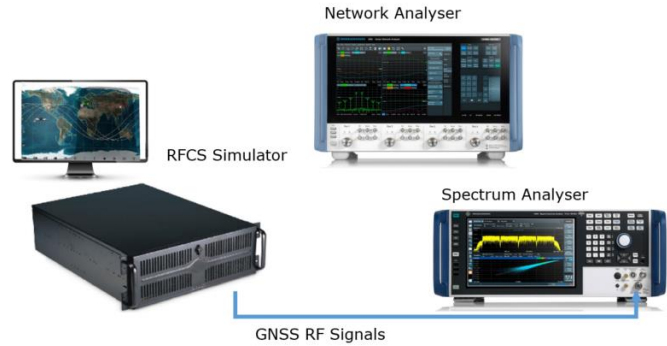


Figure 61. RFCS Signal Calibration Setup.

3.10.1.3 Antenna Patterns Implementation

A key role in the SSV user navigation capability and performance is played by the correctness and knowledge of the antenna patterns implementation between the TX and RX. At constellation side, the transmitted antenna pattern implementation aligned as much as possible to the recent results in literature [69], [72] provides a significant contribution to the constellation signals availability in the different SSV zones. In particular at higher altitude and beyond GEO the usage of the side-lobes became essential for the user navigation functionality [73]. On the opposite end, at the SSV user perspective, the antenna pattern is strictly linked to the mission specification, i.e. the spacecraft trajectory and dynamic, with the aim to maximise the GNSS signal availability and continuity. The RX antenna pattern types can be mainly summarized in two categories: the low-gain (LG) patch antenna and high-gain antenna (HGA) as depicted in Figure 62.

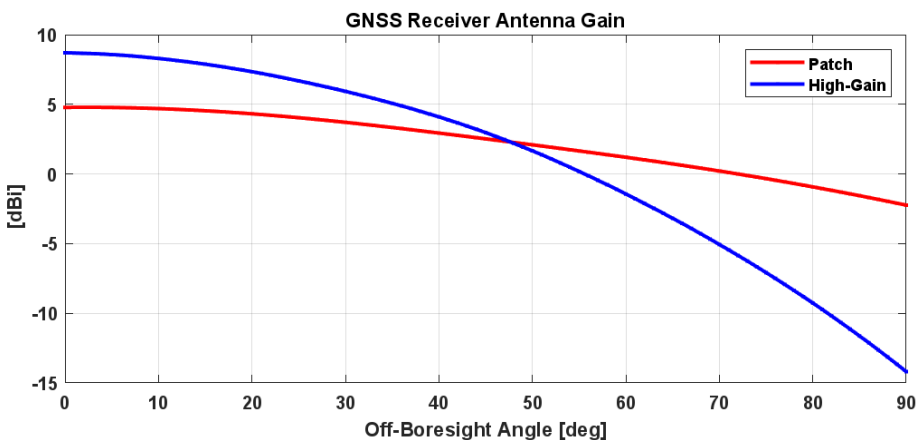


Figure 62. GNSS Receiver Low-Gain (Patch) and High-Gain profiles example

Concerning the TX antenna pattern integration, the several GPS blocks have been integrated starting from the already published information [74] and latest results [72]. A remarkable added value in the JRC-ISSVTB is demonstrated by the integration of the new Galileo Antenna been introduced in last ICG-WB in October 2023 [75], see Figure 63.

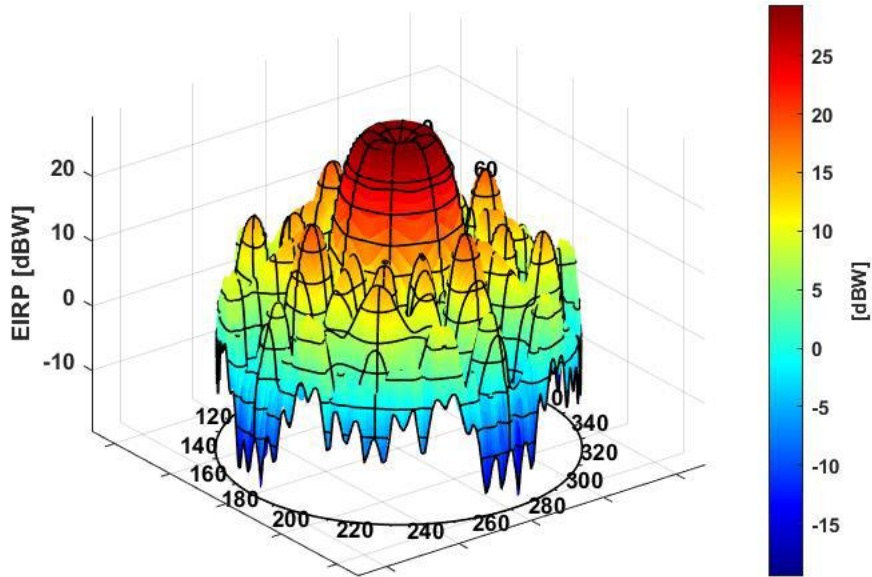


Figure 63. EIRP of Galileo E1-BC [69], [75].

Therefore, the antenna patterns are expected to greatly facilitate the analysis of GPS performance for GEO, HEO and lunar communication applications.

Both the TX and RX antenna patterns implementation can be defined with respect to:

- the desired gain profile in elevation and azimuth for the antenna amplitude response purpose
- the carrier phase response for the implementation of the satellite body and wind tip distortions
- the vehicle's Centre of Gravity (CoG)

3.10.1.4 Reference GNSS COTS Receiver

A relevant HW component within the JRC-ISSVBT implementation is represented by the integration of a GNSS COTS receiver used as reference receiver for all the aspects concerning the functional and performance SSV user testing verification capability. The JRC laboratory facility is currently equipped with two Septentrio mosaic-x5 development kit boards configured with a firmware version with disabled NATO limits. Therefore, this configuration allow to perform any kind of research and testing campaign in the SSV context. In addition, the possibility to integrate the two board within the JRC-ISSVTB enables the ful implementation of the mission application listed in Section 3.10.1.1.

Thanks to an high number of available channels, these receivers support [76]

- the multi-constellation and multi-frequency tracking, e.g. Galileo E1, E5a, E5b, E5 AltBoc and E6, GPS L1C/A, L1PY, L2C, L2P, L5
- OSNMA service
- 5 constellation RTK
- Tracking performance (C/No threshold) : Tracking 20 dB-Hz and Acquisition 33 dB-Hz

In Figure 64 an example of setup configuration with the two receivers is shown.

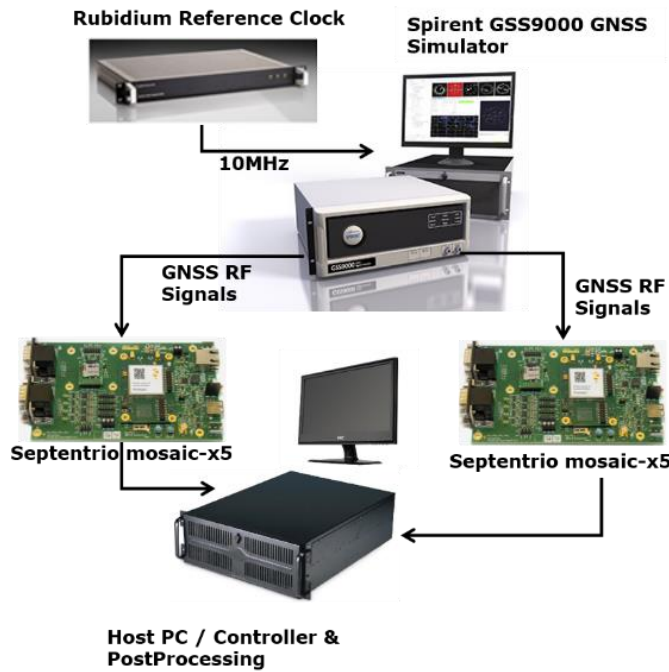


Figure 64. Multiple GNSS Receivers testing hardware-in-the-loop

3.10.2 JRC-ISSVTB Configuration

The JRC-ISSVTB supports a multitude of simulation scenarios characterized by different conditions targeted on the desired testing verification scope or research activity in the SSV and beyond regions. For example, each test case can be characterized by a different configuration of the SSV user altitude, the constellation and frequency usage, the single or multiple target service or performances, etc.

A sample of possible scenarios type and configuration can be summarized in the following Table 3.

Table 3. JRC-ISSVTB Scenario Configuration Overview.

FUNCTIONAL & PERFORMANCE TEST CONTROL SHEET		
#	NAME	OVERVIEW
1	Navigation Processing and Raw Measurements	Navigation and Raw Measurements error performance in SSV and beyond
2	Navigation Processing with GNSS Rx Antenna	Navigation Performance with GNSS Receiver antenna integrated in EMSL anechoic chamber
3	P2OD Navigation Functionality	P2OD capability
4	Timing and PPS Test	Timing performance evaluation
5	Galileo Services Functionality in Space	Galileo Services functional verification and performance in Space

The goal of the above test scenario cases is summarized below:

- Consolidation of the SSV PNT user requirements for high SSV altitudes and orbit transfer phases (e.g. a Geostationary Transfer Orbit (GTO) or MTO)
- to support a dedicated system study on the use of GALILEO or multi-constellation GNSS signal in the SSV, and beyond, missions complementing previous studies, confirming feasibility, assessing achievable performance and verifying the Galileo legacy and new services impact

- to support the performance demonstration of P2OD techniques using a GNSS receiver
- to support sensitivity assessment of the critical assumptions in terms of GNSS system performance (e.g. antenna lobe gains) and necessary high-sensitive GNSS receivers/antenna

The possible set of test cases are fully configured and described by JRC staff in a configuration and control system with the aim to provide a consistent control check of the scenario main parameters configuration with the related test KPIs and results.

3.10.3 GNSS Spaceborne Receiver Testing Capability

The new HIL-aided SSV characterization is used to provide to the next generation SSV user a complete and updated picture of the following design drivers SSV KPIs variation with respect to space vehicle trajectory, attitude, different platforms, and mission requirements such as:

- the availability and exploitation of single and multiple frequency (E1/E5/E6) measurements in SSV scenarios
- the RX sensitivity contribution, i.e. improved acquisition and tracking thresholds.
- the navigation performance and related raw measurements analyses
- the effect of the full Galileo 3D antenna pattern, coping with the general antenna gain variation trends in elevation and azimuth with the focus on the combination of the Galileo main-lobe and side-lobe signals
- the GNSS receiver antenna type, i.e. the low-gain (LG) patch antenna and high-gain antenna (HGA) , as well as the single or dual Galileo Receiver antenna configuration

The analysis includes the received signal power, the carrier to noise ratio (C/No), the Doppler shift and the expected receiver measurement accuracy relying on systematic and hardware errors (e.g. tracking loops). The signal and ephemeris availability, the Geometric Dilution of Precision (GDOP) and the standard positioning errors are derived as well.

The following figures provide an overview of the RX testing capability results in terms of: GNSS visibility, pseudo-ranges, carrier phases and navigation solution performance. It should be noticed that the following results have been derived through a RFCS scenario with a SSV user in LEO and reduced errors in the measurements generation.

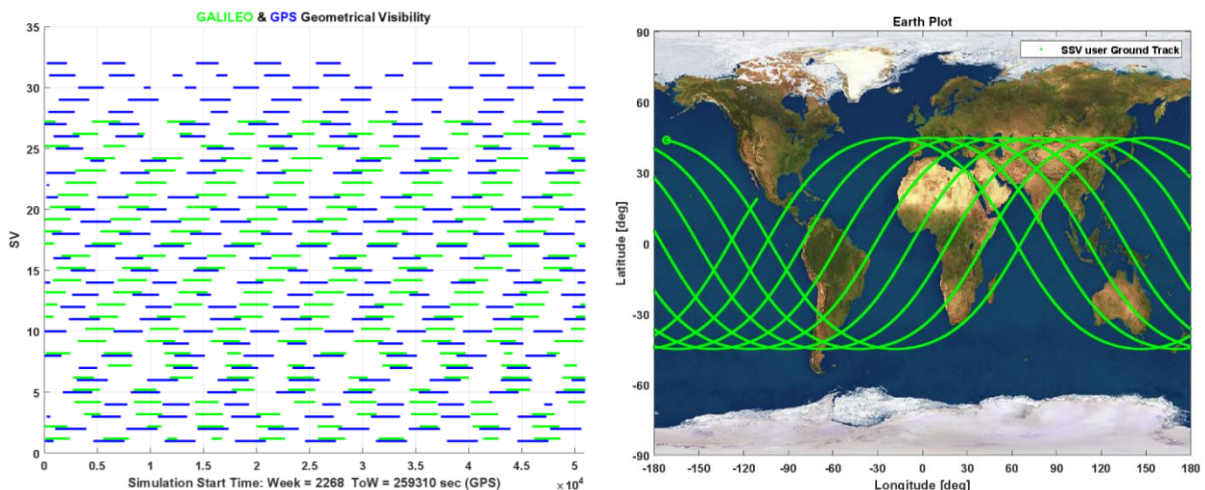


Figure 65. Galileo and GPS Visibility (left) and SSV user ground track (right)

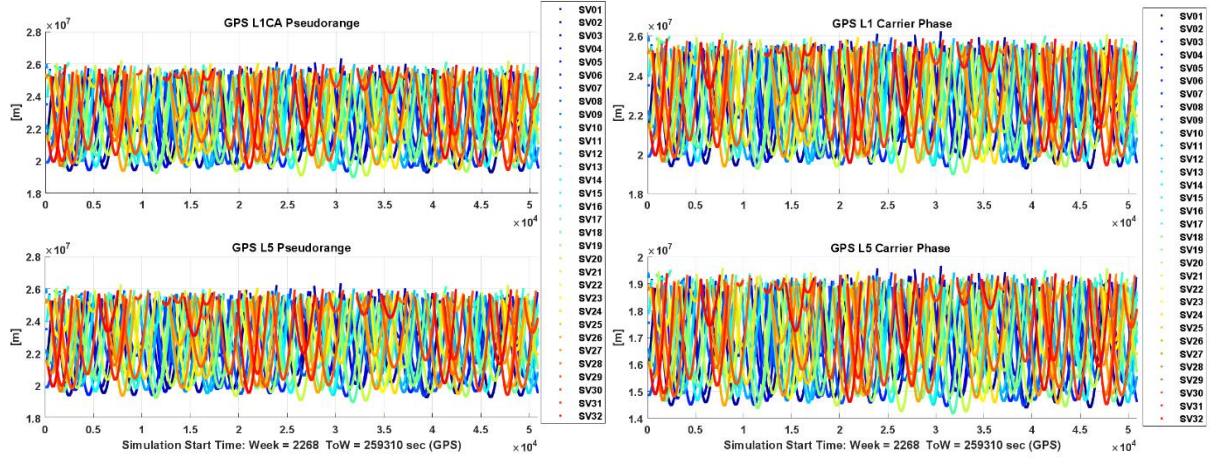


Figure 66. GPS L1C/A and L5 Pseudoranges (left) and Carrier Phases (right)

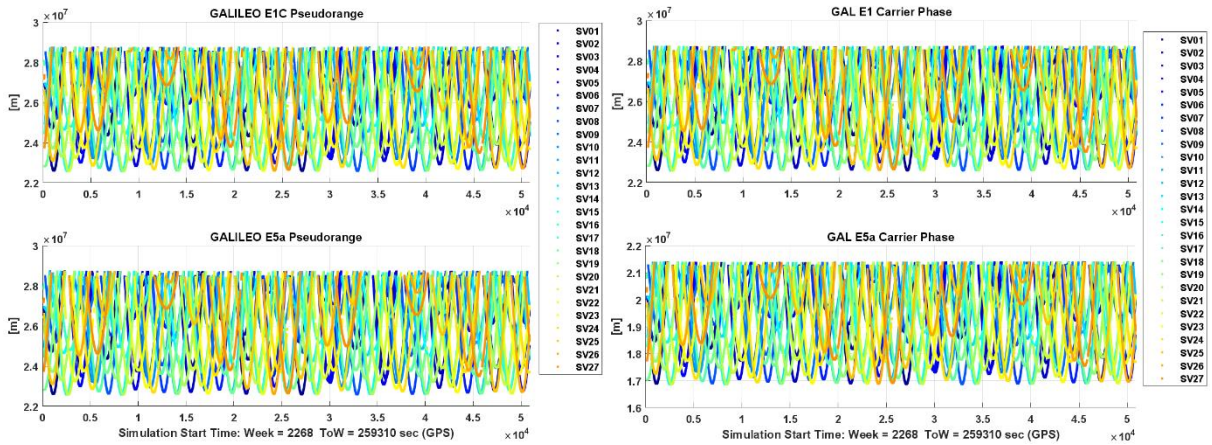


Figure 67. Galileo E1C and E5a Pseudoranges (left) and Carrier Phases (right)

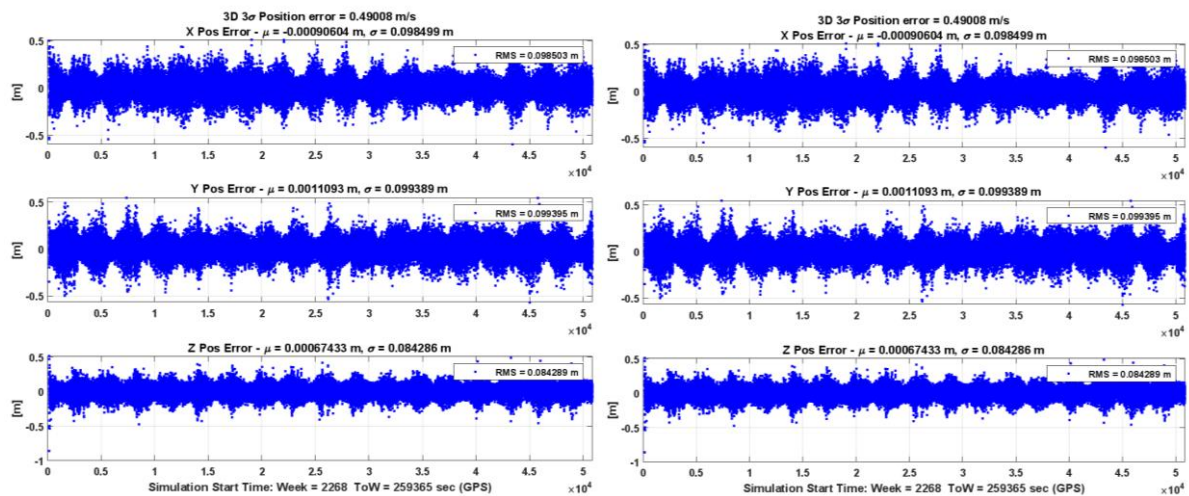


Figure 68. Navigation Solution Performance, ECEF position error (left) and ECEF velocity error (right)

3.10.4 GASPER P2OD Test Setup

In the frame of Space Service activities, the JRC Laboratory facility and staff are technically supporting DEFIS in the implementation of the GALileo SPace ReceivER for Horizon 2020 IOD/IOV Mission (GASPER) under In-Orbit Demonstration and Validation (IOD/IOV) [77]. The IOD/IOV service plays a key role in the space R&D activities with the aim to demonstrate in space innovative technologies and operational concepts for scientific, public, or commercial purposes. The main objective of GASPER experiment is to implement a low cost/new space Galileo-enabled receiver to be embarked on the IOD/IOV carrier in order to fulfil the following objectives:

- to validate the performance requirements for the Galileo 2nd generation space service
- to demonstrate techniques for real-time on-board precise orbit determination in space (such as P2OD). The objective is to perform a demonstration of such techniques using a GNSS receiver, exploiting Galileo signals and services and in particular the Galileo HAS in the E6 band. The demonstration is intended to be limited to the P2OD techniques and would not involve the avionics of the platform.

In this context the JRC Laboratory facility and technical staff support GASPER project at testing and research level through the usage of its

- GNSS RFCS Simulators and SSV scenario simulation for
 - SSV navigation performance verification
 - P2OD performance assessment
 - Galileo HAS performance verification
- SDR devices to record and playback IF samples at frequency sampling up to 120MSamples/second with bit depth from 1 to 8 bits.
- shielded TEMPEST room to conduct radiated and jamming tests in a safe manner.
- EMSL anechoic chamber for the GASPER GNSS Receiver antenna characterization in terms of PCO and PCV variation (Section 3.1.5).

In the following Figure 69 an example of the GASPER E2E test setup with the GNSS Receiver antenna in the EMSL anechoic chamber.

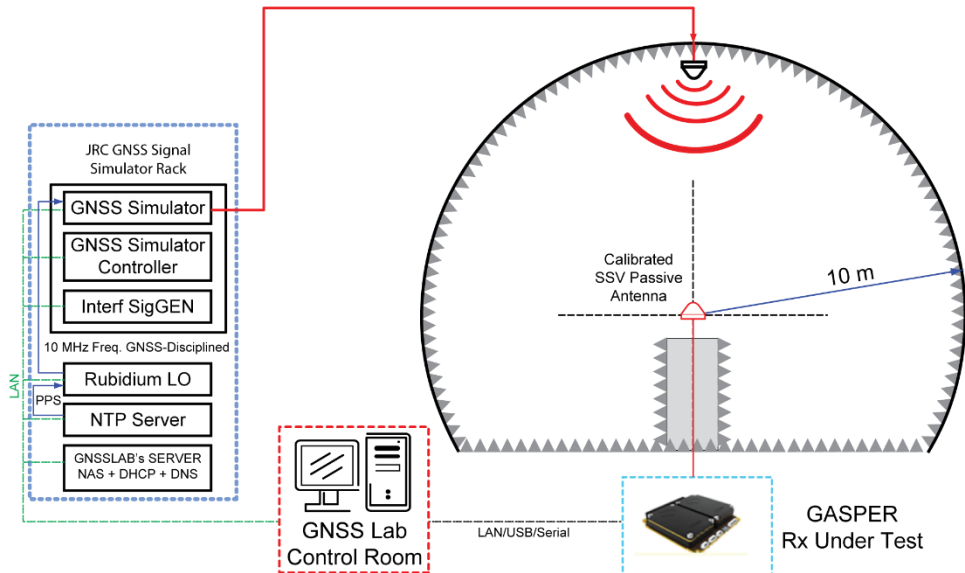


Figure 69. GASPER configuration for EtE test with the GNSS receiver antenna

3.11 Complementary Position, Navigation and Timing (C-PNT)

Today, many EU critical infrastructures, such as energy supply networks, transport infrastructures, telecommunications, and financial networks, have a strong reliance on Global Satellite Navigation Systems (GNSS). In fact, GNSS services are the backbone of Positioning, Navigation and Timing (PNT) services and its central role is bound to increase in the future with the advent of a new wave of services and business-like car-sharing, smart logistics, autonomous vehicles-ships-aircrafts, geo-localising applications, precision agriculture and others. Since these infrastructures have become primary users of PNT services, the availability of additional resilience to mitigate the impact of a potential disruption of GNSS should be a priority.

The European Radio Navigation Plan (ERNP) [78] considers the future of EU PNT as an ecosystem, underpinned by GNSS, and consisting of multiple independent systems, sharing the same time and position reference frame. Within this concept, the non-GNSS components would be best referred to as Complementary (Continuous) PNT (C-PNT), given their objective to provide resilience, extend PNT to specific environments that cannot be served by GNSS, and act as limited spatial and temporal backup supporting existing infrastructure. This concept supersedes previously reported activity on backup/alternative PNT (A-PNT) as fully independent system was identified as not optimal for the proposed ecosystem.

Section 3.11.1 hereafter gives a first overview of the JRC testing capabilities for C-PNT demonstrations, while Sections 3.11.2 and 3.11.3 enter into the details of the positioning and timing reference, respectively. They mainly refer to [46], the JRC report that summarises the main results of the C-PNT test campaign, performed in the framework of a call for tender (CFT) launched by the DG DEFIS in December 2020. More in details, it was a performance assessment campaign on a total of seven state-of-the-art C-PNT demonstration platforms, conducted with the scientific and technical lead of JRC. The main scope of the tender was to assess the performance of the C-PNT technology demonstrators capable of delivering accurate and robust positioning, and/or timing services, independently from GNSS.

3.11.1 JRC Ispra site as C-PNT Demonstrator (Living Labs)

The JRC Ispra Site was the main host of the 2021-22 C-PNT demo exercise. It covers over 170 ha with over 100 buildings, one to five-floor high, and 36 km of roads, consisting of forest, semi-urban, urban and rural areas with varied topography, including woodlands. This and the presence of the dedicated EMSL lab, makes it ideal for the Alternative PNT testing campaign in varied conditions.

For the timing and position testing (both outdoor and indoor), the following facilities and installations were made:

- A separate infrastructure and network access arrangements were organised for each platform demonstration and testing;
- Installation of transmitting equipment around the campus;
- Installation of dedicated equipment indoors;
- Timing Laboratory setup;
- Temporary License Granted by IT Spectrum Regulator (Ministero dello Sviluppo Economico, MISE) with the endorsement from the licensed users (Railway and mobile operator) to transit within the 921.8845 – 927.0000 MHz, which allowed for up to 2 h several days of activation of the radio beacons.

3.11.2 C-PNT Demonstration – Precise Time Transfer

As detailed in Section 3.5.1, JRC provided the timing reference for all the experiments conducted in the framework of the C-PNT tests campaign. This section describes a couple of examples, to demonstrate the JRC timing capabilities. For more detail information please refer to [46].

WR technology is described in Section 3.5.1. The Optical Positioning, Navigation and Timing (OPNT), a Dutch enterprise working on telecommunication networks, demonstrated both the time and frequency transfer over

fibre utilizing the White Rabbit protocol and also over a radio link with signalling in accordance with the Long-term Evolution (LTE) standard.

Prior to these tests and due to the difficult logistics to ship a Caesium Standard clock to be used as a time source, it was agreed to use a time source provided by the JRC. This time source was generated with a PPS and 10 MHz reference from a high-end Rubidium standard disciplined with multi-frequency multi-constellation GNSS receiver. It was calibrated with traceability to an UTC(k) realization of the Italian Metrology Institute INRIM (see Section 3.5.1).

A specific test has been conducted with the scope to measure the time and phase offset between two nodes, separated by a two spools of 50 km fibre each, with a repeater in between. The results are shown in Figure 70, as recorded at one of the node and measured over approx. 72 hours. The measured time stability is 57 ps peak-to-peak with 8.3 ps of standard deviation.

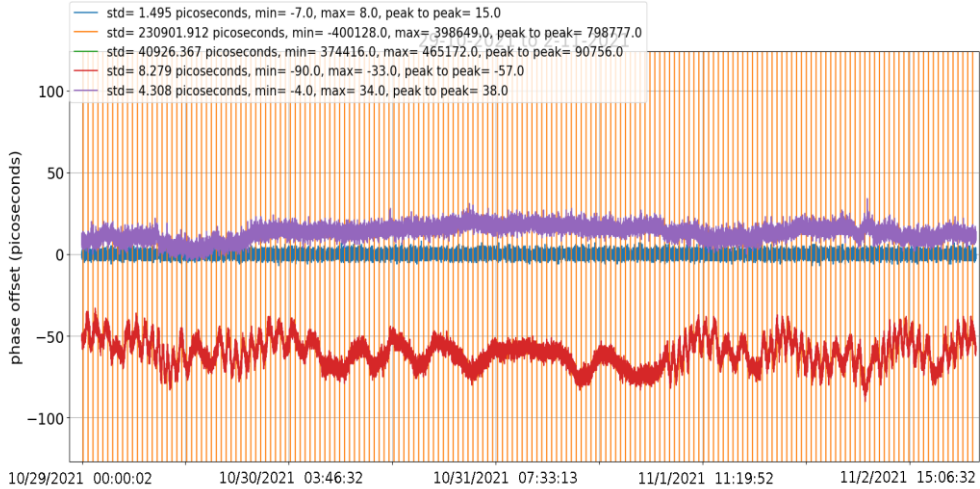


Figure 70. Results of the link frequency stability test [46]

As a further example, the tests campaign involved also Satelles STL, a US based enterprise that provides customers around the globe with a PNT service using low Earth orbit (LEO) satellites. The constellation signal provides both time and position information and its time reference is synchronised to UTC. To verify the accuracy of the time provision and distribution a roof-mounted antenna was installed on the roof of the JRC lab (Figure 71). In addition, a further atomic clock was used to monitor the JRC time source against UTC.



Figure 71. Satelles antenna on the roof of the building 72C in the Campus of JRC Ispra.

Figure 72 shows the results of 101 days of data collection in red, and difference between the two JRC reference clocks in blue. Apart from occasional spikes, the data collection results are stable and follow a normal distribution, with mean of 0.4 ns and standard deviation of 132 ns. The maximum observed peaks were -817 ns and 681 ns.

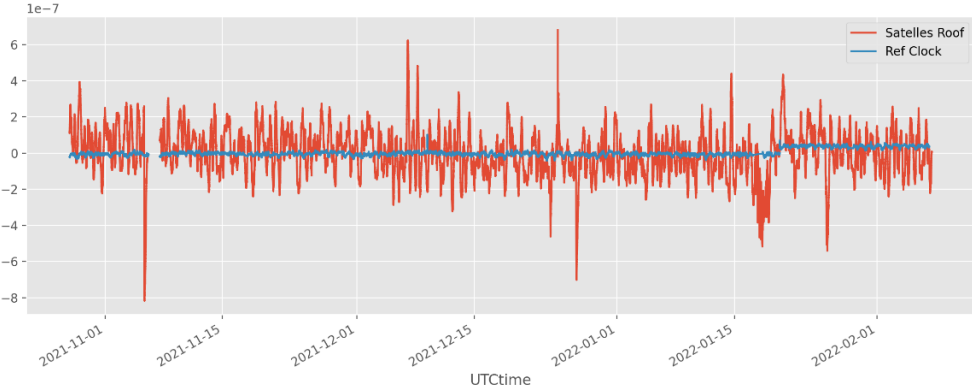


Figure 72. Results of 101 day of time generation and OTA test on the Satelles platform.

3.11.3 C-PNT Demonstration – Indoor and Outdoor Positioning

A grid of permanent points, in the European Terrestrial Reference Frame (ETRF), were established using GNSS RTK around the campus to support any outdoor trials, as shown in Figure 73 and indoors building 48 and 102 for the indoor trials.

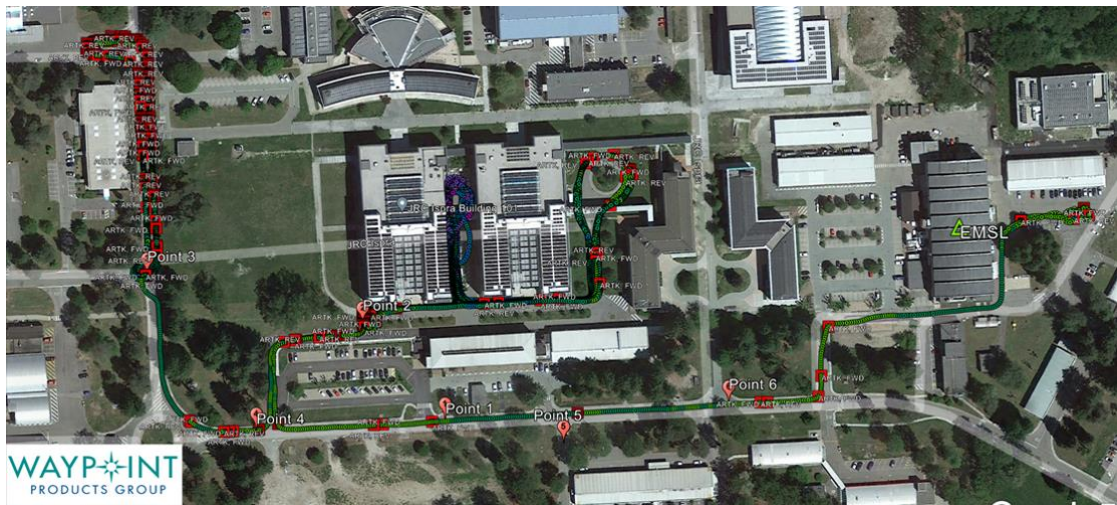


Figure 73. Example of referenced permanent points at the JRC site for kinematic tests.

Specific approaches were taken to both establish the absolute height of each building level and fix internal coordinates, consistent with the ETRF, as described in [46].

A dedicated moving platform, based on the trolley was set up for the kinematic experiments, with two variants: outdoor and indoor. In both cases, the platform consisted of a trusting system, the power supply, a data logger (laptop) and the DUT (see Figure 74).

For the outdoor trials, the trusting system consisted of a Spirent AsteRx-U and Novatel SPAN CPT, connected to a high-raised GNSS antenna, while for the indoor trials, a survey 360 degrees prism is used. An example below show the prisms mounted on top of the Locata's Orb antenna (device under test), with known offset.

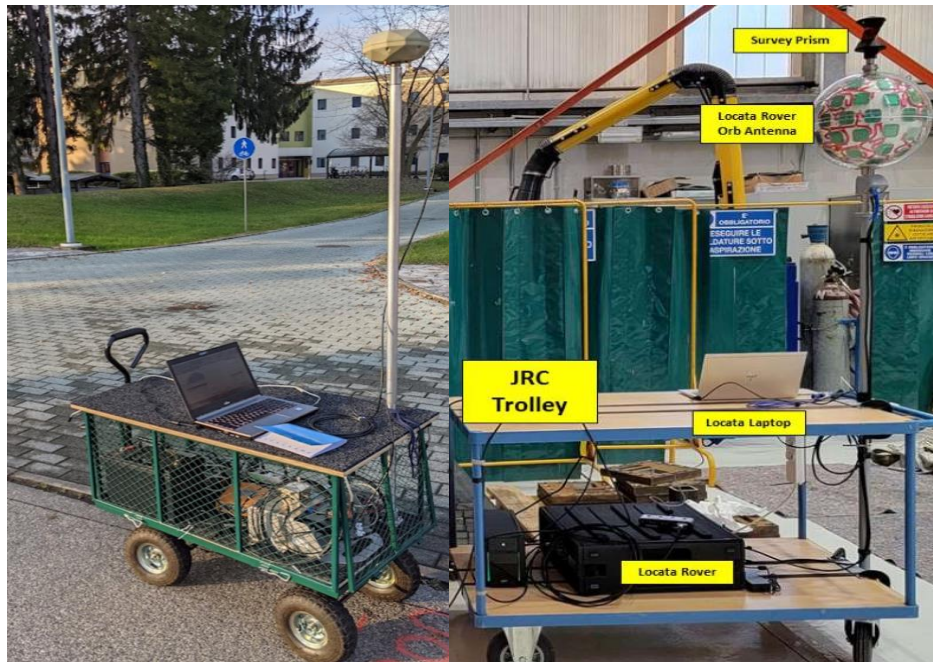


Figure 74. Outdoor (left hand side) and indoor (right hand side) experimental set up.

3.12 GNSS Signal Record & Replay Testing

This section gives a description of the testing capabilities regarding the record and playback of the GNSS signals, outlining the specific functionalities and the test equipment that can be made available to the project consortia coming to the JRC.

In recent years, GNSS record and playback systems have become a standard piece of test equipment in many laboratories due to their flexibility, compactness, and affordability. These devices allow to record GNSS signals for a time that is just limited by the available storage capacity. These recorded scenarios can be played by the same device or by other GNSS playback devices, provided an inter-changeable data format was used. The latter is a very important point as it allows the sharing of pre-recorded reference datasets with interested users.

The record and replay systems available at the JRC are based on a variety of platforms and are optimized for specific user requirements, as described in the next two subsections.

3.12.1 SDR (Software Defined Radio) Record & Replay System

The JRC utilizes a variety of Universal Software Radio Peripheral (USRP) devices to cater to diverse research and experimentation needs. These USRPs encompass a range of capabilities, empowering researchers to delve into various aspects of wireless communication and signal processing. The following USRPs are employed at the JRC:

National Instruments NI-USRP 2944r, NI-USRP 2943r [79];

Ettus Research USRP X300, USRP X310, USRP N310, USRP X410 [80].

Here is a comparison of the six USRP devices in terms of number of transceivers (Rx-Tx), bandwidth, and frequency range:

Table 4. NI and Ettus Research USRP devices list.

Device	Transceivers Nr.	Bandwidth	Frequency Range
NI-USRP 2944r	2	160 MHz	10 MHz to 6 GHz
NI-USRP 2943r	2	120 MHz	1.2 GHz to 6 GHz
Ettus USRP X300	2	120 MHz	1.2 GHz to 6 GHz
Ettus USRP X310	2	160 MHz	10 MHz to 6 GHz
Ettus USRP N310	4	80 MHz	10 MHz to 6 GHz
Ettus USRP X410	4	400 MHz	1 MHz to 7.2 GHz

3.12.1.1 Record & Playback Software

The JRC's dedicated record & playback software continues to support both the Gigabit Ethernet Interface (GBE) and PCIe x4 interfaces, ensuring seamless data acquisition and manipulation across all USRP devices. These software tools are specifically designed for the USRP platform and integrates seamlessly with both the GNU Radio and LabVIEW environments. It provides a user-friendly interface for managing recorded data, enabling researchers to perform various signal processing operations, including filtering, power spectrum and histogram visualization, post-processing and analysis.

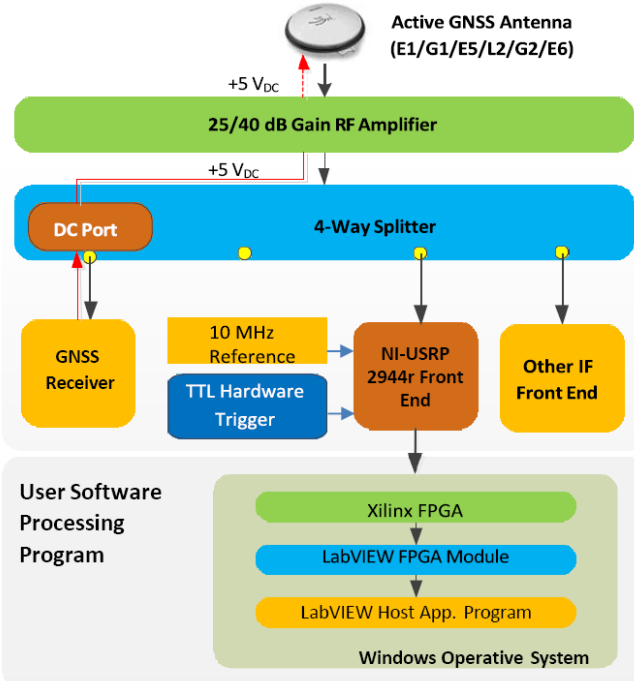


Figure 75: Block diagram of the JRC recording system for GNSS signals

Figure 75 depicts a simplified diagram of the communication flow between a NI-USRP 2944r device and a Windows host computer using the PCIe Gen3 x4 interface. The USRP captures RF signals, digitizes them, and sends the data simultaneously over the communication interface to the host computer. The host computer processes the data using software-defined radio techniques and sends control signals to the USRP for configuration and synchronization. The host computer can also record the processed data and replay it back to the USRP for further analysis or experimentation.

Figure 76 shows an interesting implementation for a mobile setup with USRP devices. By using a PCIe-to-Thunderbolt 3 adapter, the JRC has successfully integrated the USRP devices with portable laptops, enabling researchers to carry out RF streaming applications on the go. This setup is particularly beneficial for field testing and experimentation in outdoor or remote locations where access to desktop computers may be limited.

The Thunderbolt 3 interface offers high-speed data transfer capabilities, allowing for continuous record and playback of IF data streams at up to 100 MSamples/sec. This is crucial for real-time RF processing and analysis, enabling researchers to capture, analyse, and manipulate RF signals in real-time.

The mobile setup with USRP devices and Thunderbolt 3 connectivity demonstrates the flexibility and adaptability of SDR technology. By leveraging portable laptops and high-speed interfaces, researchers can now conduct wireless communication experiments and collect real-world data even in mobile or remote environments.

Here are some of the key benefits of using a mobile setup with USRP devices and Thunderbolt 3 connectivity:

1. **Portability:** researchers can perform RF experiments and collect data on the go, eliminating the need to be tethered to a desktop computer;
2. **Real-time processing:** high-speed data transfer enables real-time signal acquisition, analysis, and manipulation, facilitating rapid prototyping and evaluation of new ideas;
3. **Flexibility:** researchers can adapt their experiments to various locations and environments without compromising data acquisition and analysis capabilities.

Overall, the mobile setup with USRP devices and Thunderbolt 3 connectivity represents a significant advancement in wireless communication research. It enables researchers to conduct field trials, collect real-world data, and develop innovative solutions in a more flexible and portable manner.



Figure 76. Illustrative photographs capturing the interior and exterior of the JRC's van, showcasing the record and replay system employed in OSNMA test drives. These images depict the laptop, the NI-USRP 2944r device, the rubidium clock, and the PCI-to-Thunderbolt 3 adapter, highlighting their integration within the van's setup.

3.12.1.2 Reconfigurable Bit Depth

The JRC's record and replay system for USRP devices offers remarkable adaptability in data handling. It allows for the recording and playback of RF signals at a programmable bit depth, ranging from 1 to 16 bits, enabling researchers to balance data compression and signal fidelity. This flexibility is particularly beneficial in GNSS testing, where the GNSS receiver correlators permits the use of lower bit depths without sacrificing signal integrity. For Windows-based applications, the JRC has implemented bit reduction techniques directly within the USRP's internal FPGA, leveraging its specialized hardware capabilities for efficient signal processing. This results in faster processing speeds and reduced computational load on the host computer. However, for GNU Radio/Linux environments, the bit reduction techniques are implemented in the host computer's software, leading to slightly slower performance compared to the Windows-based implementation. The system design the balance between efficiency and flexibility, where the Windows-based approach prioritizes speed while the GNU Radio/Linux approach preserves the versatility of the open-source platform.

In summary, the reconfigurable bit depth feature of the JRC's record and replay system demonstrates the system's ability to cater to diverse requirements and optimize performance based on the specific application. The FPGA-based implementation for Windows applications offers superior speed, while the software-based implementation for GNU Radio/Linux environment maintains flexibility and open-source compatibility. This flexibility empowers researchers to tailor the system to their specific needs and optimize performance for their chosen platform.

3.12.1.3 GNSS Repeater with Adaptive Time Delay

The JRC's record and replay system for USRP devices boasts an innovative feature: the ability to function as a GNSS repeater with a variable time delay that can be adjusted in real-time. This unique functionality extends the system's capabilities beyond mere signal playback, enabling it to simulate the behaviour of various communication environments and assess the performance of GNSS receivers under dynamic conditions. The adjustable time delay feature allows researchers to introduce artificial delays ranging from 5 milliseconds to a maximum of approximately 60 seconds. This range covers a wide spectrum of delay scenarios, enabling researchers to evaluate the receiver's ability to cope with varying signal propagation times and potential synchronization issues.

The real-time adjustment of the time delay empowers researchers to dynamically simulate different signal propagation environments, mimicking the effects of atmospheric delays, multipath propagation, and various

signal processing delays. This flexibility allows for a comprehensive assessment of the receiver's performance under diverse conditions, ensuring its robustness and reliability in real-world deployments.

The implementation of the variable time delay functionality within the record and replay system demonstrates the JRC's commitment to providing researchers with versatile tools for analyzing and evaluating GNSS technology. This feature is particularly valuable for assessing the performance of OSNMA-enabled receivers, which rely on loose time synchronization to ensure accurate positioning and timing information.

Figure 77 provides a block diagram illustrating the functionality of the variable time-delay mechanism in the JRC's record and replay system. It clearly depicts the ability to introduce time delays at different stages of the signal processing pipeline, allowing researchers to simulate various propagation conditions and assess the receiver's resilience.

In summary, the GNSS repeater with adaptive time delay functionality further enhances the capabilities of the JRC's record and replay system, making it an invaluable tool for GNSS research and development. This feature enables researchers to simulate realistic signal propagation environments, evaluate OSNMA-enabled test receiver performance under dynamic conditions, and ensure the robustness of GNSS technology for various applications:

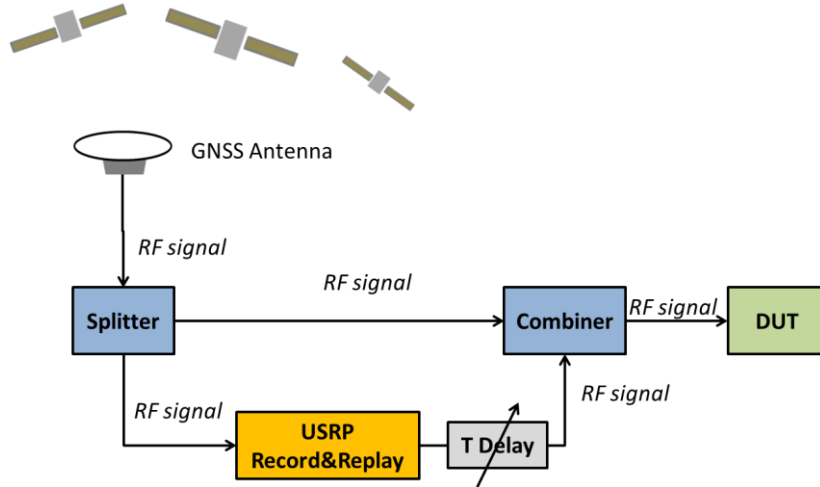


Figure 77. Detailed diagram depicting the record and replay system's configuration as a GNSS repeater with an adaptable time delay

3.12.2 LabSat-3 platform

The LabSat-3 is a portable, stand-alone software-defined receiver that provides a complete GNSS testing and experimentation platform [81]. It is designed for researchers, engineers, and students who need to conduct GNSS testing and analysis in various environments. The LabSat-3 is small, lightweight, and easy to use, making it ideal for field trials, remote sites, and even moving vehicles.

Key features of the LabSat-3 (Figure 78) include:

1. Portable and standalone operation;
2. Record and replay of GNSS signals;
3. Simulate GNSS signals;
4. Analyse GNSS signals;
5. Supported GNSS bands:
 - a. GPS: L1 / L2 / L5.
 - b. GLONASS: L1 / L2 / L3.
 - c. BeiDou: B1 / B2 / B3.

- d. QZSS: L1 / L2 / L5 / L6.
- e. Galileo: E1 / E5a / E5b / E6.
- f. NavIC: L5 & S-band.
- g. SBAS: WAAS, EGNOS, GAGAN, MSAS, SDCM.

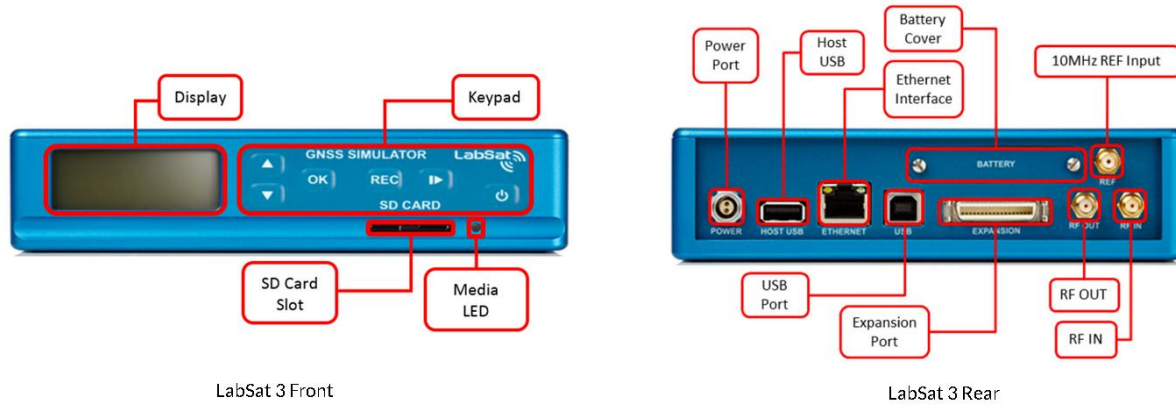


Figure 78. LabSat-3 front and rear panels components.

LabSat-3 has been designed to be portable and simple to use allowing virtually anyone to gather field test signals without in depth training. Recording GNSS signals is as simple as positioning the antenna and pressing one button. The sunlight-readable graphic display gives instant feedback of record status and can show live histogram data to verify satellites in view during recording. Back at the Lab, recorded signals can be replayed at the push of a button for repeatable, reliable testing.

The availability of the LabSat-3 device within the JRC testing capability portfolio allows to

- complements its existing USRP-based record and replay system, further expanding its capabilities in addressing a wide range of GNSS-related research challenges
- overcome of the portability and ease of use limitations of the aforementioned USRP-based systems
- provide user-friendly and cost-effective alternative for conducting GNSS testing and experimentation

3.13 Laboratory testing with RFI and spoofing signals

It is well known that radio frequency interference (RFI) poses a serious threat to GNSS [82], [83] and [84]. This is particularly true in case of liability critical and safety critical applications: in the former, the PVT information is directly related to legal and economic aspects while in the latter any malfunction of GNSS could have severe impacts on human life.

Noting the severe impact that RFI may have on the GNSS receiver performance, a stream of the R&D actions under the EU GNSS Programmes has addressed the need to develop technologies to monitor and detect GNSS jammers, particularly those used in cars or trucks [2],[85]. Additional R&D actions have been aimed at strengthening the robustness of the receivers using antenna systems with an enhanced resilience against jamming and spoofing in the road and maritime transport domains [86], [87] , [88] and [89].

In this section, a description of the key assets and relevant testing capabilities related to the assessment of the impact of the jamming and spoofing threats on GNSS receiver performance. Two recent testing campaigns conducted at the JRC are presented as illustrative examples.

3.13.1 Testing of GNSS receivers with RFI signals

One of the first testing campaigns with interference signals at the JRC was in radiated mode in the EMSL. This test campaign was conducted back in 2012, and was aimed at assessing the coexistence of a terrestrial mobile network in the USA (i.e., LightSquared). This terrestrial mobile network was subject of a compatibility study because it was proposed to be allocated in a band adjacent to GPS L1/GAL E1 [90], [91]. In this testing campaign, three Galileo-enabled COTS receivers were used and a quantitative assessment of the impact of the coexistence with this terrestrial network (i.e., with the LTE signals broadcast from nearby base stations) could be made. The metric used in that case was the loss of C/No observed in relation to a baseline scenario with no signals from the terrestrial network present in the adjacent bands.

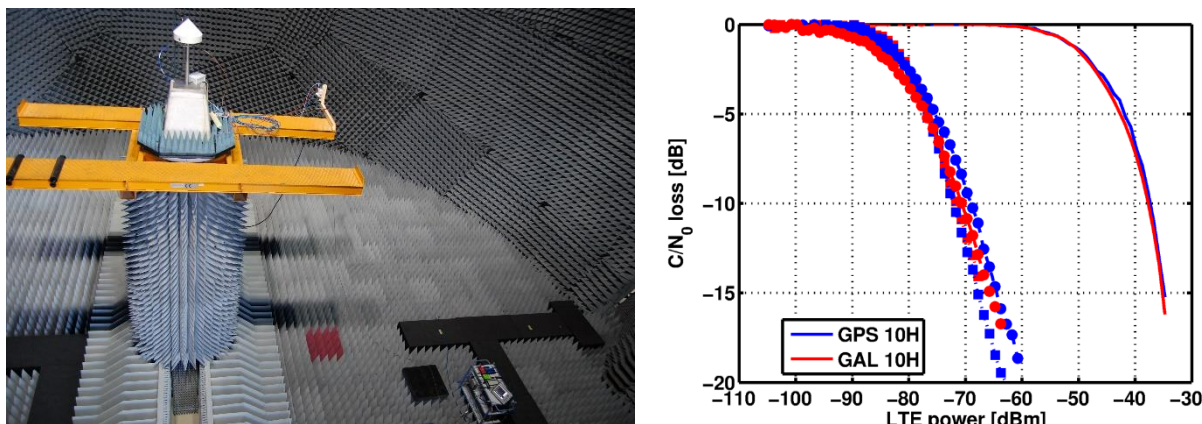


Figure 79. Photograph of the setup used in the EMSL for the compatibility assessment with LightSquared (left). Observed loss of C/No versus power of the LTE signals with the three receivers tested and one of the proposed band allocations (right).

An important testing capability to highlight here is that the laboratory at the JRC is equipped with state-of-the-art programmable RF vector signal generators. With these instruments, it is possible to generate a wide range of signal waveforms, signal modulations and pulsing schemes that might be needed in an interference or coexistence study. As an example, in the coexistence testing with LightSquared, a 3GPP FDD LTE waveform emulating the downlink from a LightSquared base station had to be generated and its power level ramped up in a controlled manner during the tests. Prior to these tests, a calibration of the power levels of both the GNSS simulator and the vector signal generator had to be completed. The former calibration was made following a test procedure equivalent to that used in the testing of the ship-borne GNSS receivers presented in Section 3.2.2 in [1]. In this type of tests, the location where the radiated power levels are calibrated must be in the vicinity of the antenna of the receiver under test.

The test campaign reported in Section 3.2.2 in [1] included multiple radiated tests with RFI signals present and therefore, it is worth giving a more detailed description here. These tests were specified in the Maritime Standard IEC 61108-3 [19, p. 61108], which identifies specific performance requirements in terms of position accuracy and re-acquisition capability under narrow-band and wide-band interference, respectively.

As an example, one of the radiated tests with narrow-band interference required the generation of a pulsed continuous wave centred at 1575.42 MHz, a duty cycle of 10%, a pulse duration of 1 ms, and a peak carrier power of -20 dBm in the vicinity of the GNSS antenna. This pulsed RFI waveform was measured with a real time spectrum analyser inside the anechoic chamber, next to the measurement tower of the EMSL. A snapshot of this measurement is depicted in Figure 80, where the RFI signal power versus time, the power spectrum, and a spectrogram are shown.

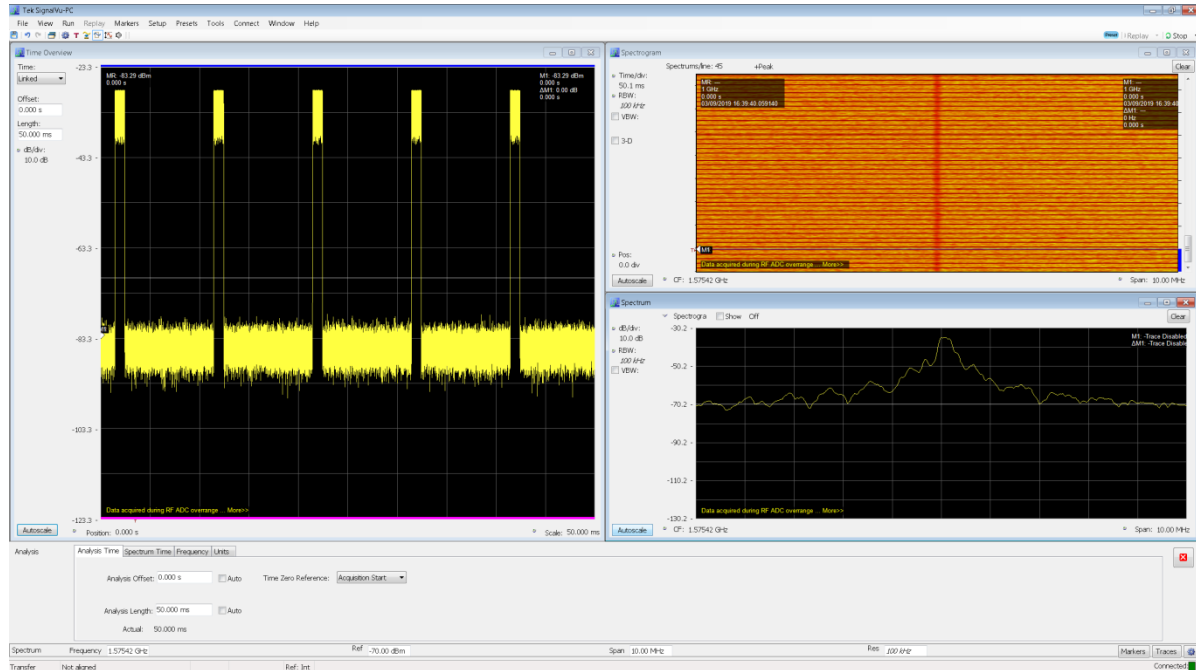


Figure 80. Snapshot of the real time spectrum analyser showing the narrow-band pulse interference signal, its power spectrum, power versus time, and power spectrogram.

The radiated tests with the wide-band interference in the standard were specified with a calibrated additive white Gaussian noise (AWGN) signal with instantaneous bandwidth of 1 MHz, centre frequency of 1575.42 MHz, and RMS power of -101 dBm in the vicinity of the GNSS antenna. In this test, the interference signal was not active permanently and had to be switched on and off following the timeline shown in Figure 81.

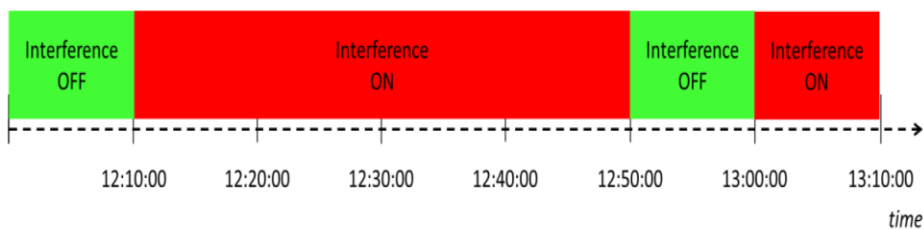


Figure 81. Timeline showing the time intervals where the wide-band interference signal was present.

The snapshot of the real time spectrum analyser got during the radiated test with the wide-band interference is depicted in Figure 82. As in the previous example, the power versus time, power spectrum and a spectrogram are shown.

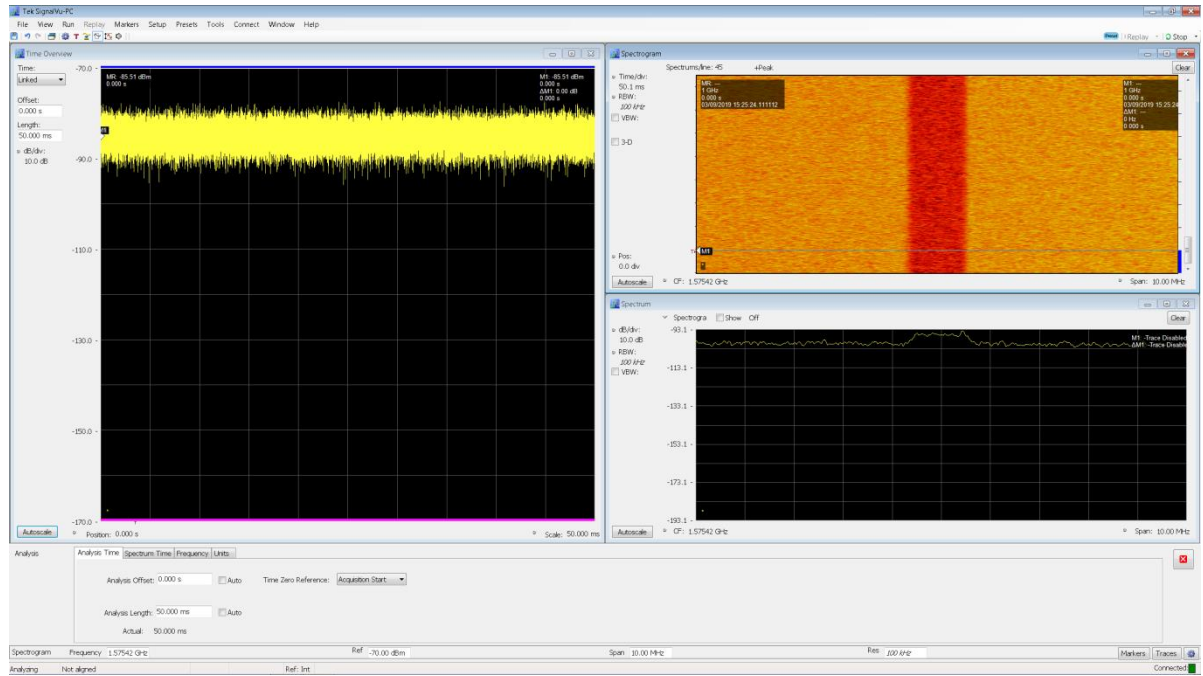


Figure 82. Snapshot of the real time spectrum analyser showing the wide-band AWGN signal, its power spectrum, power versus time, and power spectrogram.

A recent test campaign completed at the JRC was aimed at establishing a battery of automotive test scenarios generated with a GNSS simulator, with representative jamming and spoofing threats present [92]. This campaign was conducted to support the implementation of an EU regulatory framework for the Smart Tachograph (ST) [93], [94], which happens to be the first one mandating the adoption of the new OSNMA authentication service of Galileo.

For the jamming test scenarios, three RFI waveforms were selected based on what was observed during the extensive field monitoring made in the frame of the H2020 STRIKE3 Project [85]. Figure 83, Figure 84, and Figure 85 show the spectrograms and power spectral density of the three RFI waveforms selected for the ST test battery. These interference waveforms were programmed in Matlab and uploaded to the vector signal generator used in the test campaign.

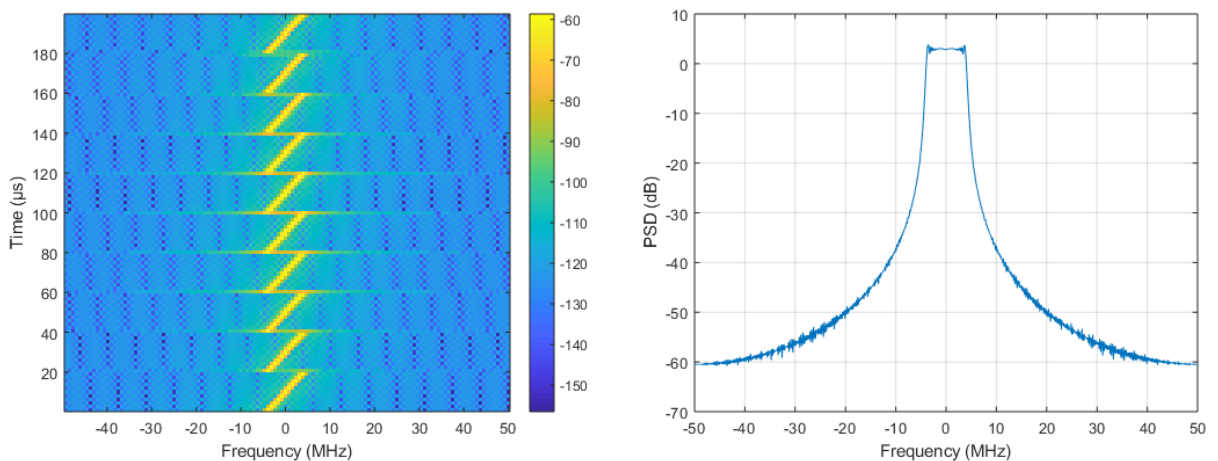


Figure 83. Spectrogram and power spectral density of a narrow-band sawtooth FM waveform, with a bandwidth of 10 MHz and a sweep time of 20 usec.

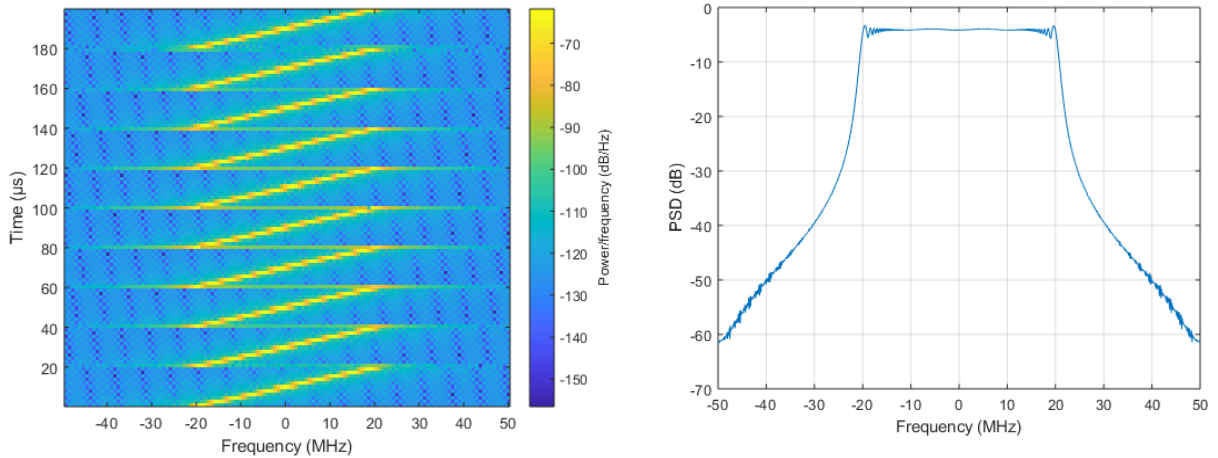


Figure 84. Spectrogram and power spectral density of a wide-band sawtooth FM waveform, with a bandwidth of 40 MHz and a sweep time of 20 usec.

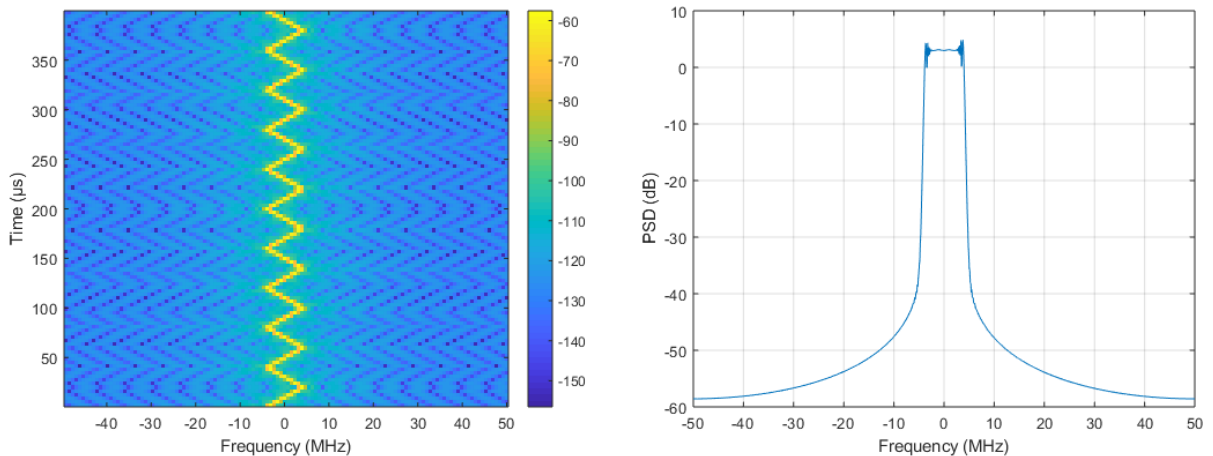


Figure 85. Spectrogram and power spectral density of a narrow-band triangular FM waveform, with a bandwidth of 10 MHz and a sweep time of 20 usec.

3.13.2 Testing of GNSS receivers with spoofing signals

Considering the high interest of the GNSS community in assessing the impacts and the effectiveness of detection/mitigation strategies versus GNSS attacks, JRC has extended its portfolio of testing capabilities to cover a wide range of attacks from the simplest meaconer up to more advanced synchronized attacks.

The two GNSS simulator commercial solutions available at the JRC Lab, namely the Spirent GSS9000 [8] and the Safran/Skydel GSG-8 [95] have been equipped with their ad-hoc software options to support advanced spoofing generation.

JRC can support both live synchronized and fully simulated spoofing scenarios.

- In the live synchronized set-up, a reference GNSS receiver is responsible for the processing of the live GNSS signal and passes the PPS, 10 MHz and the live satellite ephemeris (i.e. RINEX nav data file) to the simulator that can generate a counterfeit signal highly synchronized and satellite visibility-wise similar to the genuine signal. Typically, the counterfeit signal is configured to have a certain power advance and to move the actual target trajectory with respect to the genuine signal power and position respectively.
- In the simulated spoofing set-up, the design and the generation of the genuine and counterfeit signals are under full control. The simulators offer the possibility to configure several parameters including (not exhaustive list):

- Spoof location/trajectory
- Spoof power advance
- Spoof ON/OFF time windows
- Counterfeit generated position/trajectory
- Counterfeit satellites/constellation

3.13.3 JRC GNSS simulated attacks library

It is worth noting that several spoofing classifications, terminology and interpretations are available in literature and in the GNSS community. For this reason, JRC has drafted a technical report describing the design and details of a representative set of RFI attacks prepared with the GNSS simulator.

The document and the related simulated scenarios have been used in supporting the CERTIFLIGHT project [96]. This Horizon Europe project aims at proposing a new U-space service for the legal certification of flight tracks generated by UAAs and aircrafts flights, through the introduction of a new disruptive EGNSS-IoT digital system. The JRC attacks library has been used to trainee the developed AI detection and classification algorithms.

In the following sections, the simulated scenarios are presented. It is worth mentioning that this subset of representative scenarios will be regularly complemented with additional and/or modified variants test scenarios.

3.13.3.1 *Nominal Scenario*

This scenario describes the reference scenario without attacks. A dynamic scenario is selected and well represents typical dynamic conditions experienced by ground automotive vehicles and low-speed quadcopters drones.

Here following the main characteristics:

- Starting Date: 4th August 2023
- Duration: 30 minutes
- GNSS constellations: GPS L1/L5 and Galileo E1/E5
- OSNMA: valid
- Trajectory: rectangular shape, see Figure 86.
- Speed Profile: Static for the first minute and then moving anti-clockwise with different speeds and acceleration/deceleration profiles after/before each curve (see Figure 87).
- Heading profile, see Figure 88
- Altitude: constant 300 meters.
- GPS Satellites: 6, 12, 22, 24, 25, 32
- Galileo Satellites: 4, 9, 13, 21, 26, 31

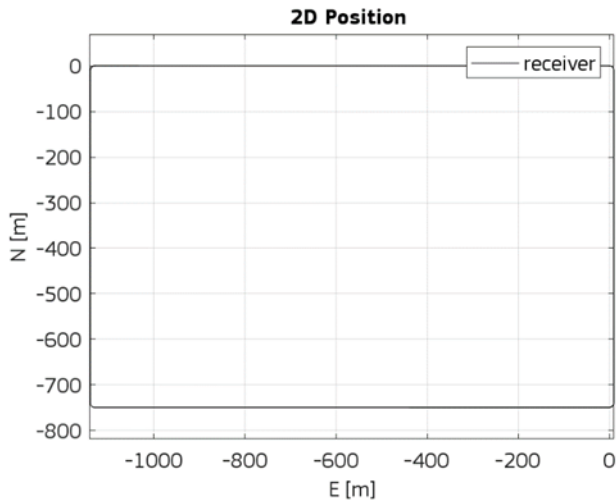


Figure 86. 2D nominal-genuine trajectory with a rectangular shape.

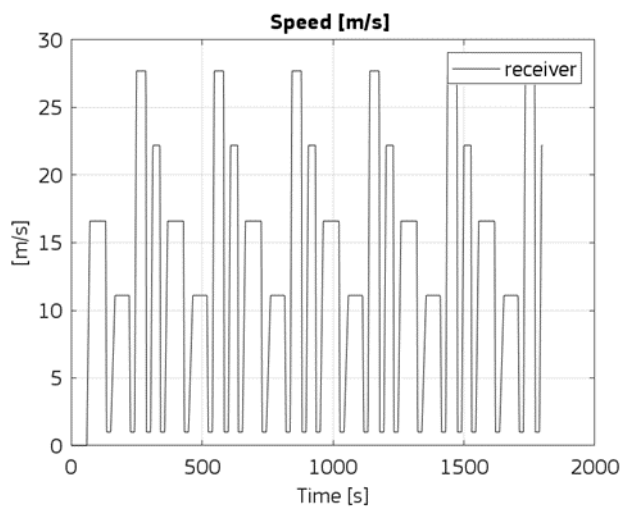


Figure 87. Nominal-genuine Speed profile versus time.

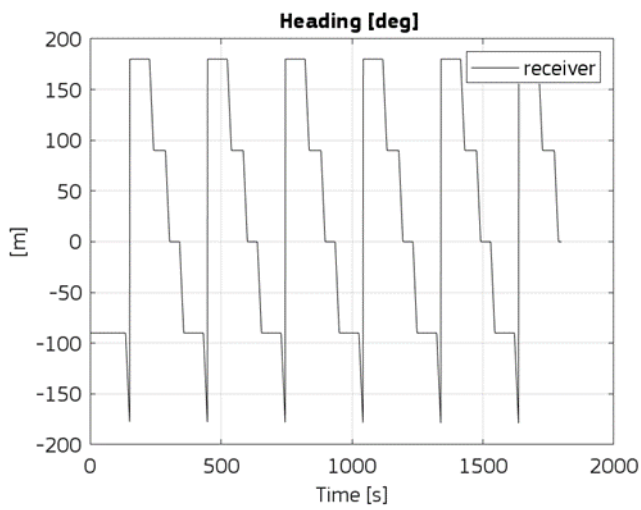


Figure 88. Nominal-genuine heading versus time.

3.13.3.2 Meaconer

The objective of this type of attack is to simulate the re-transmission of the GNSS signal. The meaconer receives the GNSS signal and applies a time delay before re-transmitting it. In case the meaconer is successful, the target receiver will see the meaconer's position with a time delay resulting in the sum of two contributions: one is the processing delay applied by the meaconer and the second derives from the travelling time between the meaconer and target receiver locations.

3.13.3.2.1 Meaconer_01 (100 ms processing delay)

This scenario simulates a static meaconer re-broadcasting the same RF bandwidth as that simulated in the nominal scenario.

Here following the main characteristics of the meaconer:

- Jamming phase: no
- On/Off: OFF [0:5minutes], ON after 5 minutes
- Constellation/Signals affected: all as nominal
- Meaconer Height: 200 m
- Relative 3D Positions:

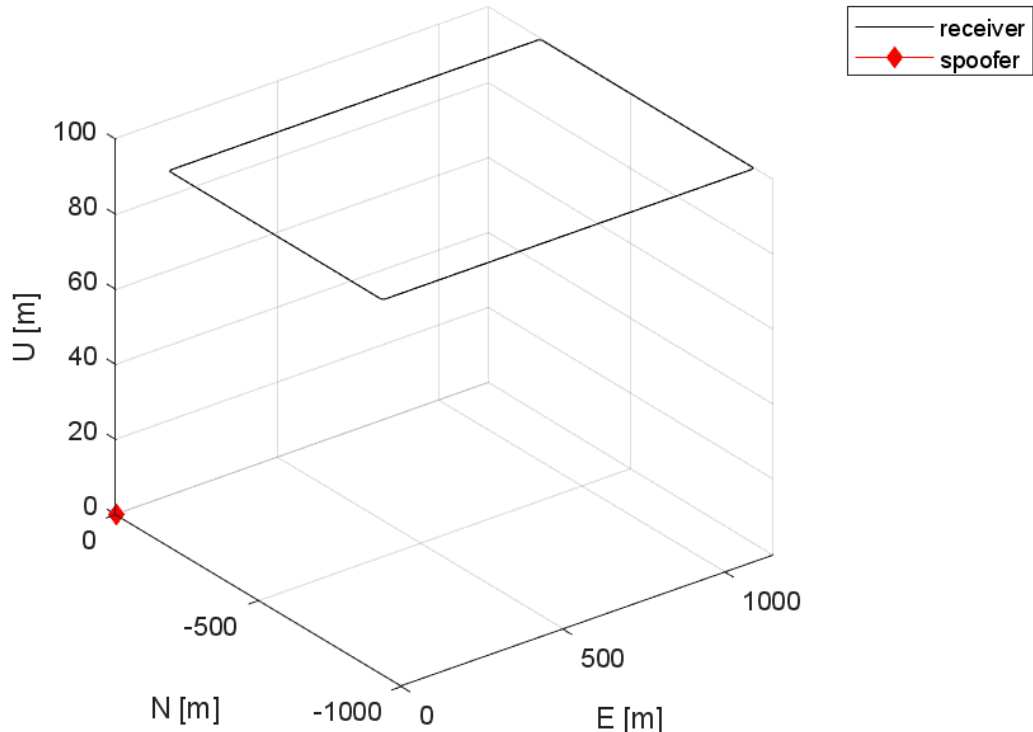


Figure 89. 3D genuine trajectory and meaconer location

- Simulated Satellite power levels as received by the target receiver taking into account the path loss due to relative distance. It can be noted that the meaconer is active after 300 seconds. By the comparison of the following figures with those related to the genuine signals, a power advance in the range of [-2:+12] dB is clearly noticeable.

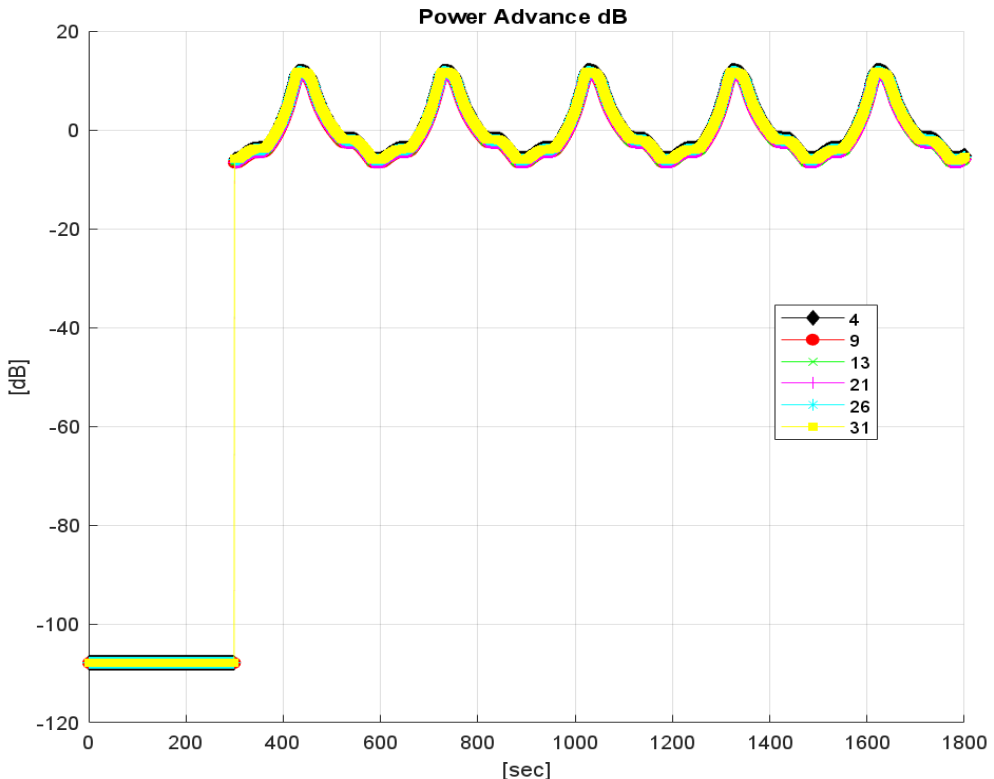


Figure 90. Galileo spoofed signals power advance versus time on Galileo Satellites: 4, 9, 13, 21, 26, 31.

- Meaconer Delay: 100 ms.

3.13.3.2.2 Meaconer_02 (100 ns processing delay)

As scenario Meaconer_01 with the only difference residing in the simulated processing delay corresponding to 100 ns.

3.13.3.3 Synchronized RFCS-like Spoofing

The objective of this type of attack is to mimic the scenario in which a GNSS signal simulator is capable of generating a counterfeit signal aligned in time with the genuine signal (< 100 ns of synchronization error) but not aligned in the measurement and position domains.

For instance, this scenario reflects the attacks carried out by GNSS simulator capable of getting the PPS and Rinex navigation information from a genuine receiver, and transmitting a signal aligned in time with the live signal and containing similar information in terms of satellite visibility.

It is assumed that the attacker can only roughly estimate the real position of the target receiver.

3.13.3.3.1 Synchronized_RFCS_Spoofing_01

Here following the main characteristic:

- Jamming phase: between 5 to 7 minutes simulated by switching all the simulated signals off.
- On/Off: ON after 7 minutes
- Constellation/Signals affected: all as nominal
- Spoofed OSNMA info: not valid

- Spoof Height: 200 m
- 2D plot describing genuine trajectory, spoofer position and counterfeit trajectory.

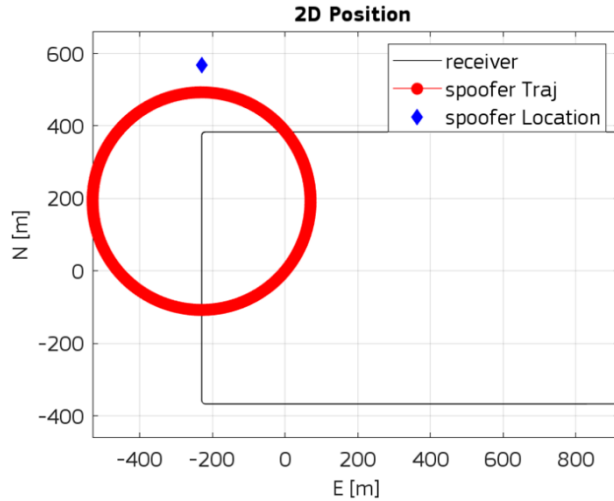


Figure 91. Genuine trajectory, spoofer location and counterfeit trajectory.

- Speed profiles (genuine and counterfeit)

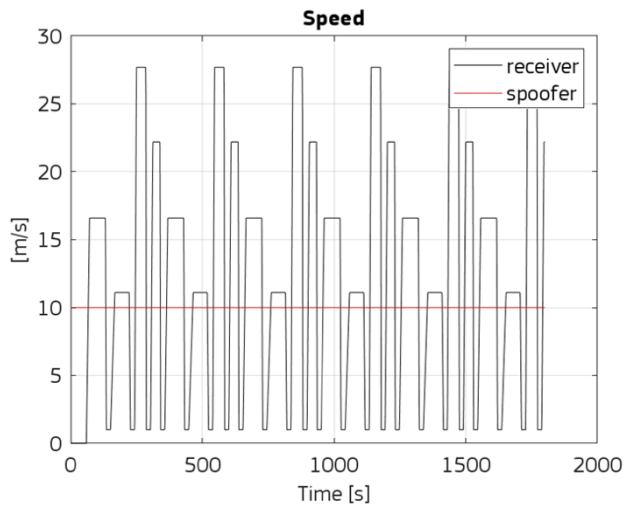


Figure 92. Genuine and counterfeit speed profiles.

- The spoofer power levels, as received by the target receiver taking into account the path loss due to relative distance, is almost always about +12 dB.

3.13.3.4 Advanced Spoofer

The objective of this type of attack is to mimic the scenario in which a signal generator is capable of generating a counterfeit signal both aligned in time and in position domains with the genuine signal. Being capable of transmit the counterfeit signal aligned within the genuine correlation peak region, the spoofer starts transmitting at low power and then increments it gradually. In the first phase, the counterfeit trajectory corresponds to the nominal one and once the spoofer achieves a certain power advance, it starts simulating different trajectory.

It is worth noticing that the same spoofing scenario can be used to emulate two different attack conditions that lead to the same overall effects.

- a. The spoofing device is located at the same location of the target receiver (e.g. a spoofing device placed on the truck dashboard in with a vehicle OBU with GNSS receiver is located).
- b. The spoofing device is distant from the target receiver but it is capable of properly estimating the target receiver location and compensating for the travel time and the power levels resulting from the relative distance.

3.13.3.4.1 Advanced_Spoofing_01

Here following the main characteristic:

- Jamming phase: no
- On/Off: ON after 5 minutes
- Constellation/Signals affected: all as nominal
- Spoofed OSNMA info: not valid
- Spoofing Height: 300 m
- 2D plot describing the genuine and counterfeit trajectories. It is worth noticing that the spoofing location is simulated with relative distance to target receiver equal to 0 meter. After 12 minutes, the counterfeit trajectory starts diverging (straight direction)

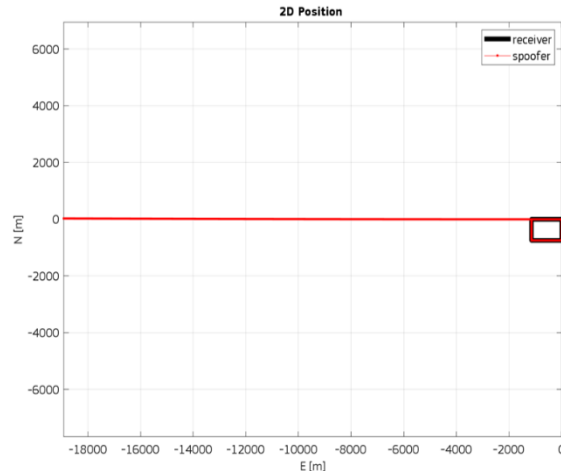


Figure 93. Genuine and counterfeit trajectories.

- Speed profiles (genuine and counterfeit)

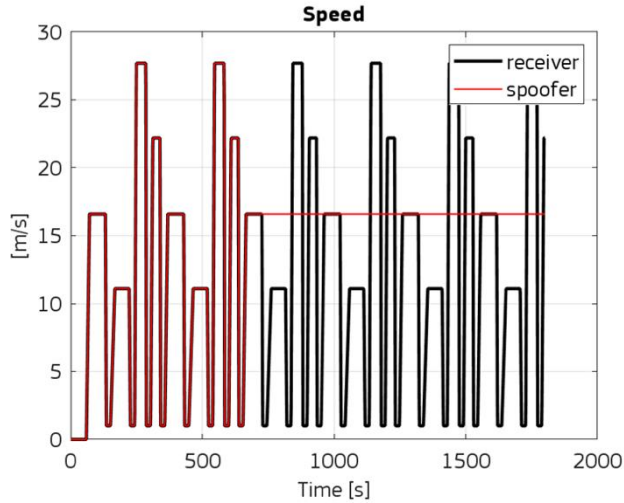


Figure 94. Genuine and counterfeit speed profiles

- The spoofers signals power levels as received by the target receiver. It can be noted that the spoofers increments the power level gradually reaching a final power advance of about 12 dB.

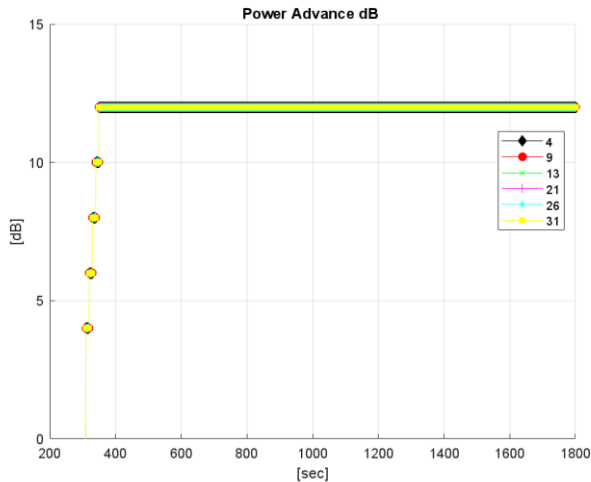


Figure 95. Galileo spoofer signals power advance

3.13.3.5 Security Code Estimation and Replay

The objective of this type of attack is to mimic a SCER attack. By definition a Security Code Estimation and Replay (SCER) attack allows greater flexibility than a meaconing attack in manipulating the target receiver's PVT solution. In a SCER attack, a spoofers receives and tracks individual authentic signals and attempts to estimate the values of each signal's security code on-the-fly. It then reconstitutes a consistent ensemble of GNSS signals, with the security code estimates taking the place of the authentic security codes, and transmits the ensemble toward the target receiver [83].

3.13.3.5.1 SCER_01 (nonzero delay)

In a nonzero-delay SCER attack, the spoofers rebroadcasts a counterfeit signal that arrives at the defender's RF front end with a delay $d > 0$ relative to the authentic signal. This d value is the result of the sum of the signal travelling time (from the spoofers location to the target receiver) and the SCER processing time.

It is assumed that the attacker can only roughly estimate the real position of the target receiver.

Here following the main characteristics:

- Jamming phase: between 5 to 7 minutes simulated by switching all the simulated signals off.
- On/Off: ON after 7 minutes
- Constellation/Signals affected: all as nominal
- Spoofed OSNMA info: valid
- 2D plot describing genuine trajectory, spooper position and counterfeit trajectory: as Syncronized_RFCS_Spoofers_01
- Speed profiles (genuine and counterfeit): as Syncronized_RFCS_Spoofers_01
- Simulated Satellite power levels as received by the target receiver taking into account the path loss due to relative distance: as Syncronized_RFCS_Spoofers_01
- SCER Delay: the spooper takes 100 μ s to carry out an error-free estimation of the genuine symbols transmitted.

3.14 Testing at JRC Campus

3.14.1 JRC Ispra Campus Description

The JRC Ispra Campus provides an ideal ground for on-site testing campaigns as it offers:

- Smart city infrastructure including smart grids, smart homes and smart mobility;
- Varied topography urban, semi-urban, rural and woodland areas.
- Ability to deploy specific testing scenarios.

In the specific case of the Ispra Site, the JRC offers living labs test environment spread over the 170 ha campus that includes:

- Over 100 buildings, one to five-floor structures and 36 km of roads. Site is utilised by 2,250 staff daily. It has independent logistical services necessary to run a small town, including energy generation and water provision. This enables smart city testing with interconnected infrastructures and interlinked facilities for smart grids, smart homes, smart mobility and advanced communication testing. Additionally, this infrastructure, modelled on smart city/campus concept, embeds sensors and devices that take constant readings of variables such as traffic flow, energy consumption, air quality and similar. The campus composition is shown in Figure 96.



Figure 96. Satellite high-resolution image of the campus of JRC Ispra Site (source: Google Earth).

- Urban, flat semi-urban, rural and woodland areas with varied topography, allowing for the varied testing campaigns, as shown in Figure 97.

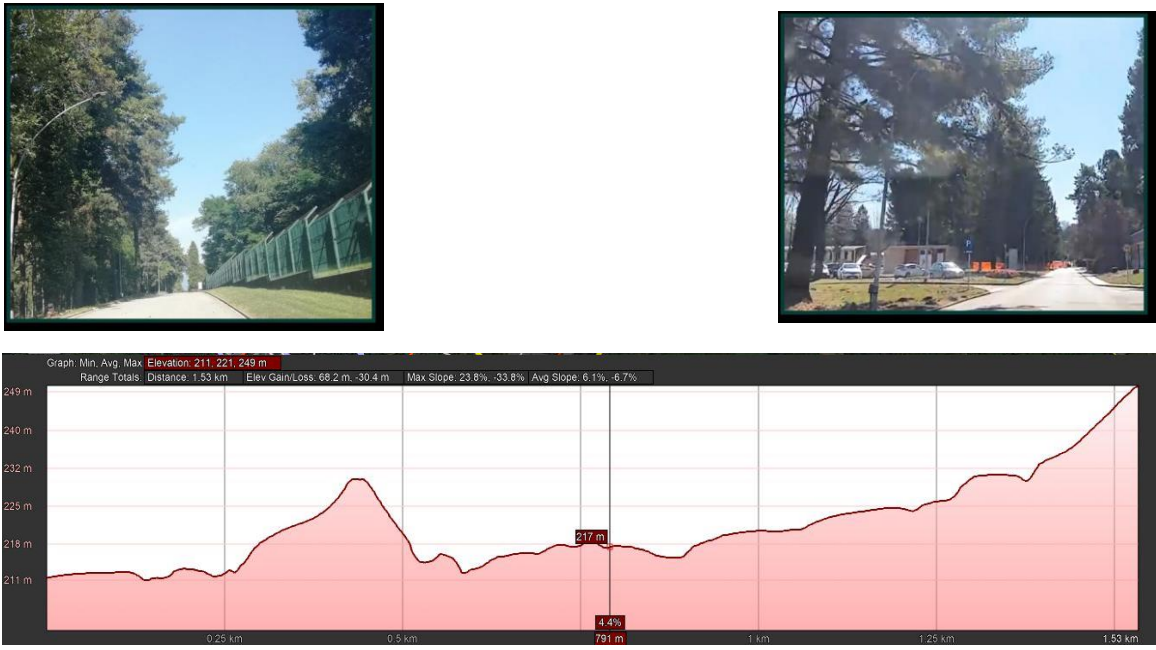


Figure 97. Examples of the test environments available on the JRC Ispra Campus.

- A flight zone up to 600 m is shown in Figure 98; the flight zone is under the control of the JRC Ispra Site Manager, and can be used for drone testing, as described in the following test case.

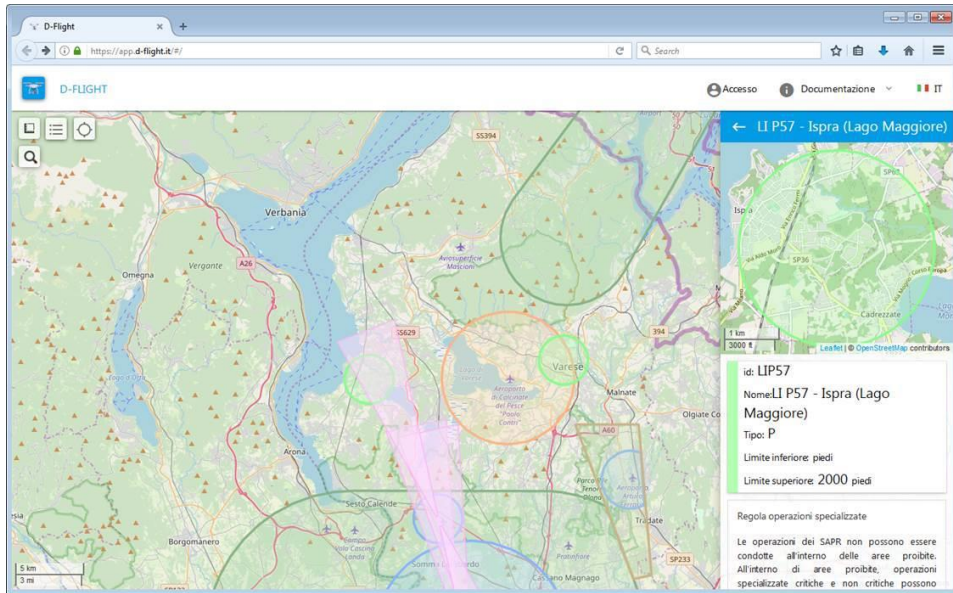


Figure 98. Representation of the LI P57 "No Fly Zone" on the ENAV aeronautical map. This spatial area is under the control of JRC Ispra Site Manager.

3.14.2 JRC Living Labs

Through the living labs [97], the JRC is opening its research sites to put new technologies and applications into practice, in real-life and control environments. Currently, a number of pilot projects for smart city solutions with focus on digital energy and future mobility are on-going. Access to the Living Labs is managed mostly through a call for expressions of interest. The selection of the project is carried out based on the scientific and technical value of the proposed project as well as the innovation and market applicability of the applications.

3.14.3 Test Cases

3.14.3.1 *SARA drone flight trials in the JRC Campus*

As part of the Living Labs initiative, a flight trial was carried out by the Search and Rescue Aid (SARA) project consortium at JRC Ispra [98]. Following the preparation of a test plan and its approval by the site management, several flights were carried out. In particular, two drones with different configurations were used to collect GNSS data, which was then post-processed by JRC in PPK mode using as a base a receiver installed on the campus. In addition to collecting GNSS data, the drones were used to record videos of the traffic on a portion of the campus road, to investigate the potential of drones in traffic monitoring. Some activities related to the SARA project are shown in Figure 99.



Figure 99. Tethered drone used in the flight trial (top-left), drone flying on the campus (top-right) and view from the on-board camera used for traffic monitoring (bottom). All photographs taken during the demonstration of the SARA Project in the campus of the JRC Ispra Site, on 1/10/2020.

3.14.3.2 *Testing of an indoor navigation app on a smartphone*

Seamless and continuous navigation is more and more a requirement for different applications and one of the most challenging environments for navigation is indoor. Indoor navigation is a challenging task which involves the solution of several problems such as signal attenuation, fading and measurements biases due to multipath propagation. Different solutions are currently available for indoor navigation exploiting WiFi signals,

fingerprinting, IMU and map constraints. Testing the solutions for indoor navigation is an even more challenging task, JRC has developed a testing environment in an office building to evaluate the performance of navigation systems in indoor environments. Two types of test can be performed: a repeatability test and an accuracy test. In the first case, a trajectory is repeated for several times in order to verify the consistency of the solutions obtained in the different laps. An example of such test is reported in Figure 100, during the test the user performed several loops around a large table present in a meeting room trying to always repeat the same trajectory. The quality of the navigation solution is assessed by comparing the different trajectories estimated for the different loops. A high consistency level of the navigation solution indicates the good performance of the system.

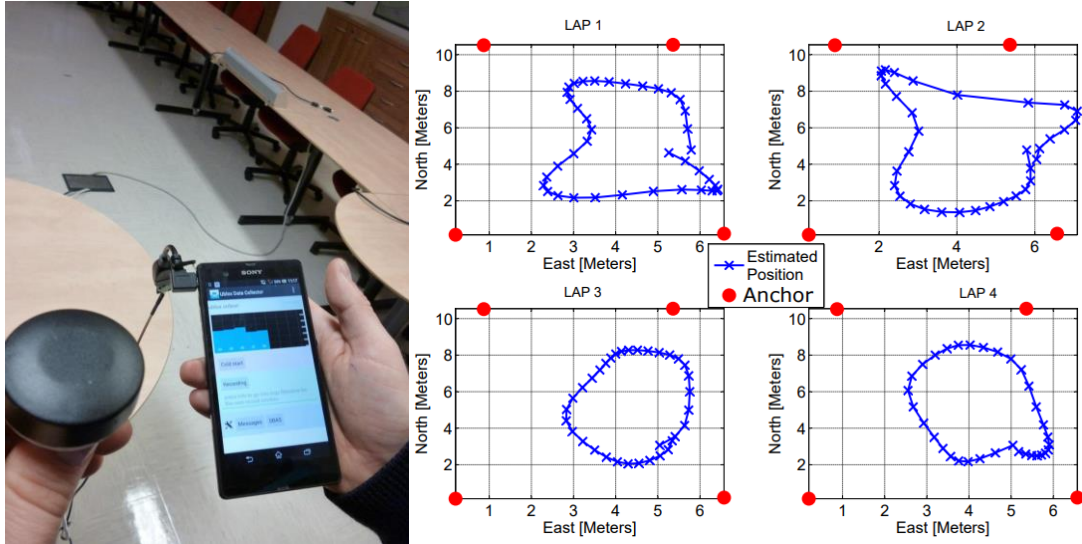


Figure 100. Example of repeatability test. On the left side the navigation device under test. On the right side, the reconstruction of the four laps performed by the user.

The accuracy evaluation is performed using a set of control points in a corridor. The coordinates of the control points are estimated using a total station. The example of the control points is shown in Figure 101. Using this test environment is possible to evaluate the trajectory of a user along the corridor. The corridor is characterised by a displacement of about 25 meters in the North-South direction and only 5 meters in the East-West direction.



Figure 101. Example of indoor accuracy test. On the left side the navigation device under test. On the right side, the displacement of the control points.

Using this approach, the user moves along the trajectory defined by the control points: the user can be also static on each control point for a specific time interval. In Figure 102, an example of the results obtained using the testing capacity presented. During the considered test, the user moved along the trajectory defined by the control points: the user was static on each control point for about 20 seconds. The test allowed to identify an anomalous behaviour of the navigation device in the correspondence of the control point number 7.

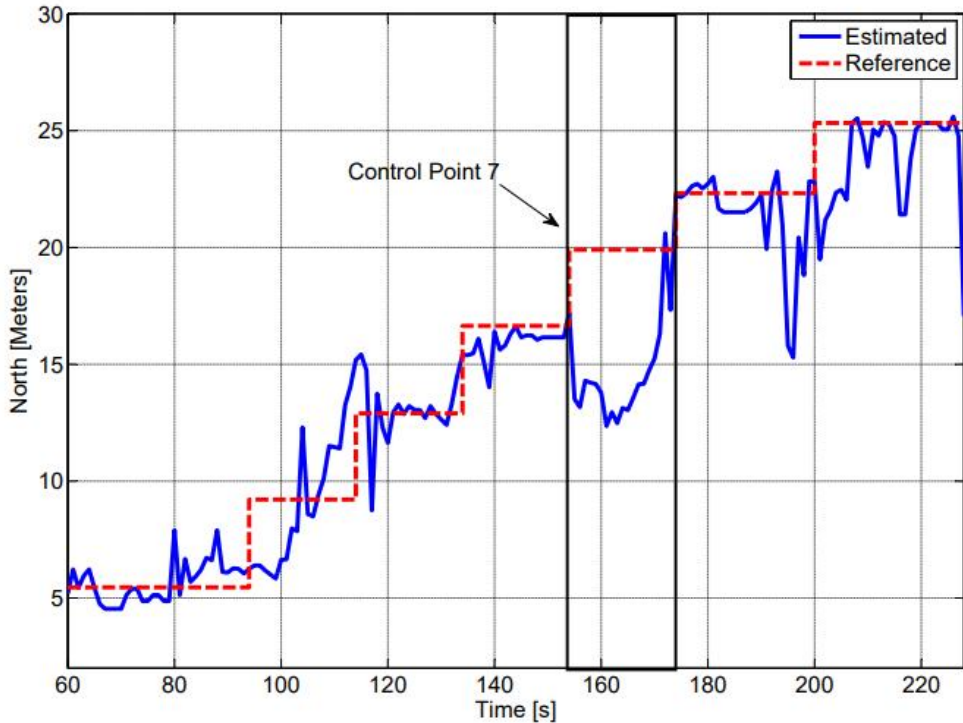


Figure 102. North coordinate evolution as a function of time. The red dotted line indicates the position of the control points.

3.14.3.3 VALOUR project

As part of the VALOUR project, the University of Modena has been using the JRC Ispra campus to investigate the generation of vehicle alert messages (VAMs) by vulnerable road users, such as bikers. The current algorithms used for the generation of these messages was reported to produce too many false alerts, potentially due to large errors in the reported positioning solutions. A dedicated test campaign to assess the dynamic of the bikes, the quality of the measurements and the potential use of alternative positioning solutions was carried out at the JRC in the frame of the Living Labs. As shown in Figure 103, a bike was equipped with the SPAN system and a reflector (tracked by the robotic total station) in order to get an accurate ground truth in all reception conditions. A record and replay device was used so that the GNSS signals could be replayed to the device under test using different configuration parameters. A smartphone was added to the set-up in order to assess whether it would provide a positioning solution accurate enough to generate the VAMs.

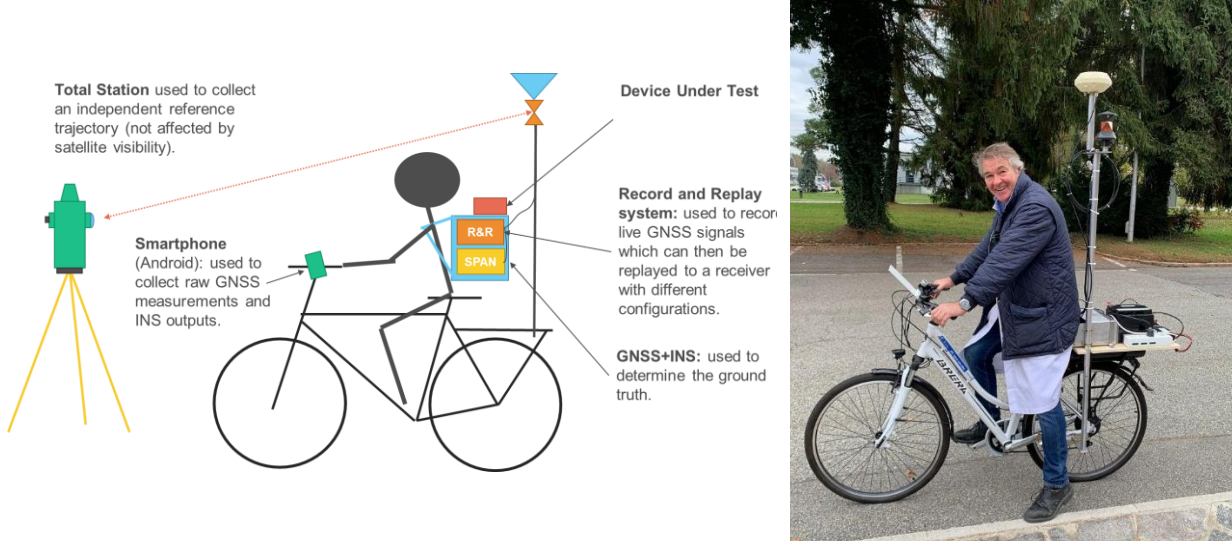


Figure 103. Set-up developed for the VALOUR project data collection (left) and installation of the bike (right).

4 Future Updates on the Inventory of GNSS Testing Capabilities

The current inventory report is an incremental update of its previous issue [1] in relation with the new and improved laboratory capability introduced in the previous Section 3. Following this approach, in the coming years this inventory will be subject to further updates of existing capabilities in relation with the exploiting of the new Galileo services, the development of instruments and measurement systems and the new advanced techniques in signal processing and measurement science. Therefore, this section presents a summary of the expected updates and additions for the future issue of the document, which are right now in preparation at the JRC.

The main expected updates and additions to this inventory are introduced in the following subsections.

4.1 LEO-PNT Test Bench

The new trend of LEO mega-constellations has the potential to revolutionize not only the access to broadband networks, but also that to Position, Navigation and Timing (PNT) services [99]. The potential to exploit LEO constellations for positioning as a signal of opportunity (SoP), as well as the potential enter into the scene of dual purpose and dedicated LEO-PNT systems, will introduce a new perspective for legacy GNSS users, which will have access to signals with different degrees of PNT capabilities from thousands of LEO satellites worldwide, with the promise of improved performance and robustness. The possibility to adapt pre-existent broadband telecom mega-constellation as well as the reduced cost of deploying dedicated PNT services through LEO platforms makes this technology an appealing solution to back-up or complement the conventional GNSS broadcasting signals from Medium Earth Orbit (MEO). The possibility to implement such GNSS-like services based on low cost LEO platform has generated more and more initiatives around the world. The Beijing Future Navigation Technology Co. Ltd is developing Centispace, a LEO-PNT system to provide positioning services. Another initiative is the one started by Xona Space Systems, which aims at developing PNT services based on 300 LEO satellites to provide secure GNSS augmentation and also an independent precise PNT service. In Europe there is also the on-going development of a future LEO-PNT constellation [68], which will complement Galileo with a LEO-layer improving performance and resilience of the GNSS services.

The JRC laboratory is working on extending its capabilities to a such a scenario by developing a LEO-PNT test bench allowing to preliminary test new LEO-PNT constellations and anticipate issues and advantage of upcoming commercial GNSS+LEO Receivers.

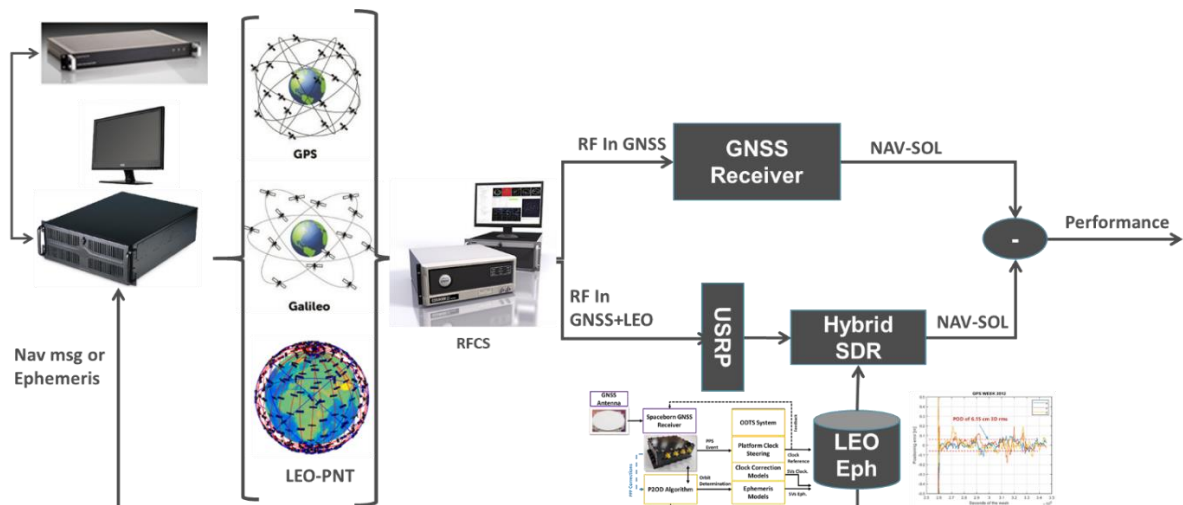


Figure 104. Preliminary LEO-PNT Test Bench Setup

The test bench is provided in Figure 104 and will include the following:

- 1) Compatibility with joint MEO and LEO simulation. This will be achieved by HW update of the RFCS simulators to support LEO-platform navigation and RF signal generation. Moreover, dedicated test will be performed in order to align LEO-SISRE with the expected on-board ODTs function [paper]. This approach will benefit of the P2OD characterization performed in Section 3.10.4 on LEO P2OD compatible spaceborne or COTS receivers in the SSV environment.
- 2) On the beginning a USRP+SDR approach will be developed in order to support general purpose GNSS-like LEO-PNT signals.

It will be possible to test and compare with respect to the same scenario the performances of the LEO-PNT augmentation with respect to the GNSS baseline

4.2 Norway Jammer Tests Scenarios

The increase usage of the GNSS signals in our daily lives has become indispensable in a large number of applications, from guiding aircraft and driverless cars to monitoring water supplies and responding to emergencies. However, GNSS signals are potentially vulnerable to the radio frequency interferences, such as jamming and spoofing attacks, due to their weak signal power received on the ground. In this context, the JRC's Galileo team participated to one of the world's largest jamming and spoofing testing campaigns in Bleik, Andoya, Norway between the 18th and 22nd of September 2023 [100]. The event called Jammertest 2023 brought together more than 200 participants from 80 companies and 19 countries worldwide (see Figure 105) and was organized by the Norwegian Public Roads Administration, Norwegian Communications Authority, Norwegian Defence Research Establishment, Norwegian Metrology Service and Norwegian Space Agency.



Figure 105. Jammertest 2023 participants.

The scope of this test campaign was to test the GNSS equipment resilience on the different types of attacks through several test cases stimulating GNSS signals in realistic conditions. In particular JRC activity was aimed to record, collect and validate the GNSS signals under these interference scenarios condition. The recording system considered is described in Section 3.12 while in Figure 106 a test setup with dual antenna configuration is shown. A test vector library will be shared to provide and support the interest of the GNSS community looking for any interference scenarios for research and/or testing activity.



Figure 106. Test Equipment: Antennas system (left) and Host PC with acquisition devices (right)

4.3 Radio Frequency Interference Detection from Space

In the framework of Jammertest 2023, JRC executed an experiment with the collaboration of ESA, Norwegian Communication Authority and Norwegian Defence Research Establishment (FFI) with the aim of monitoring the navigation L1 band from space. The main goal of this experiment was the collection of jamming data from space, i.e., from a LEO satellite. For this experiment, a custom jammer was designed by JRC and transmitted by FFI from a known location. Moreover, the jamming transmitter was engineered to steer part of the jamming power towards the space in order to enable the reception of a minimum level of jamming power at the satellite side.

The LEO satellite, used for data collection purposes, is OPS-SAT [101]. In 2019 OPS-SAT was injected into a circular, polar orbit at 515 km altitude and now is controlled from the European Space Operations Centre (ESOC) by ESA. JRC computed the time frame of the most convenient passages to record jamming data. Then, coordination with ESOC was established to start the collection at the pre-computed time instant. Previously, FFI started the transmission of the jamming signal from ground.

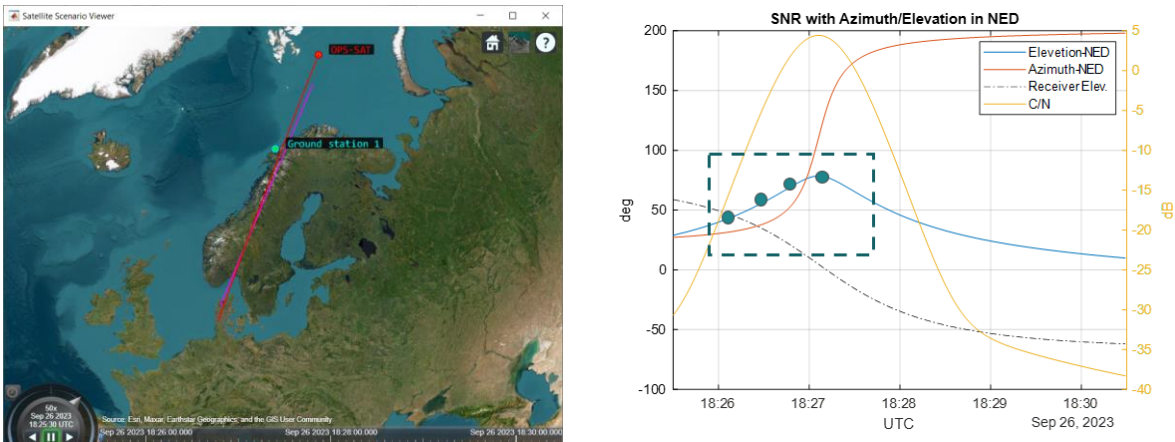


Figure 107. OPS-SAT trajectory and jammer location (left). Pre-computed elevation, azimuth and SNR for the given OPS-SAT passage (right)

Once the recorded data from OPS-SAT had been delivered from ESOC to JRC, the post-processing activity started. This activity was aimed at demonstrating the possibility to detect the presence of a GNSS jammer on ground from the LEO orbit. As an example of the results, Figure 108 below shows the spectrum of the transmit jammer signal from ground (on the left) and the PSD of the received samples recorded from OPS-SAT.

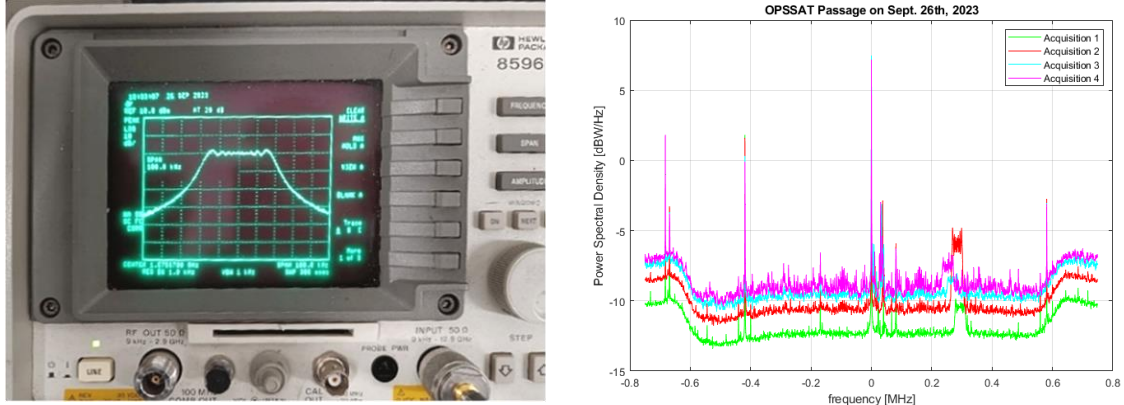


Figure 108. Power Spectral Density of the transmitted signal from ground (left) and recorded from OPS-SAT (right)

It is worth noting that the availability of these data is an asset for JRC, since it enables to design and implement a processing toolchain able to detect and geolocate the presence of jammers, observed in real-world environments. The knowledge of jammer signal structure and location could allow to assess the performance of the mentioned toolchain, in terms of detection capabilities and geolocation accuracy. This toolchain could be further improved and fine-tuned by means of hardware in the loop approach, by employing signal and scenario generations from Orolia Skydel [95].

4.4 CRPA Antenna Testing

Following the growing demand to characterize CRPA antennas in a controlled environment both in radiated and conducted modes, a major upgrade of the large anechoic chamber of the EMSL has been planned in 2024. In this upgrade, the installation of 8 RHCP transmit antennas on the dome will be made. The arrangement of the transmit antennas has been optimized to mimic the 3-D angles of arrival of the Galileo satellites, as seen from a reference location, in an optimal manner during a time window typically below 30 minutes. In Figure 109, a photograph of one of the transmit antennas on the dome and the polar plots of the RHCP and LHCP antenna gains at 1600 MHz are shown.

The radiated measurements on the CRPA antennas requires a GNSS simulator with multiple RF-output ports, each of them allocated to one of the 8 Galileo satellites of the scenario under test. The installation of an additional set of transmit antennas on the dome, which can radiate jamming or spoofing signals, is also foreseen. For the purpose of illustrating how a set-up of a radiated test on an CRPA antenna, two 3-D sketches showing, respectively, a possible arrangement of the transmit antennas (coloured in red) on the dome and a close view of the CRPA antenna on the measurement tower of the EMSL are shown in Figure 110. In this set-up, the CRPA antenna is tilted 35 degrees with respect to the vertical to have a more realistic distribution of the satellites in view.

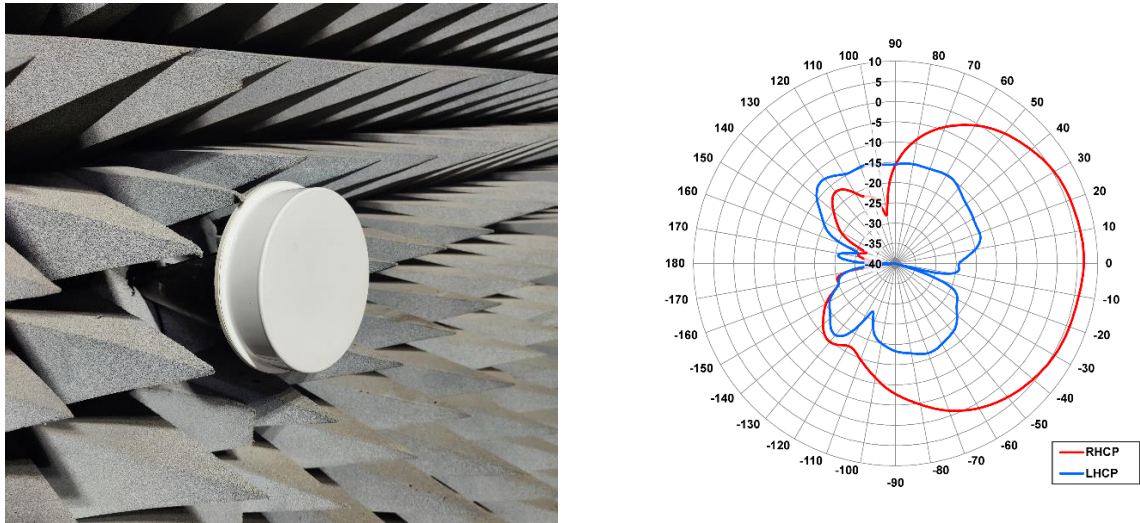


Figure 109. Photograph of one of the transmit antennas on the dome of the EMSL anechoic chamber (left); Polar plots of the RHCP and LHCP antenna gains at 1600 MHz (right).

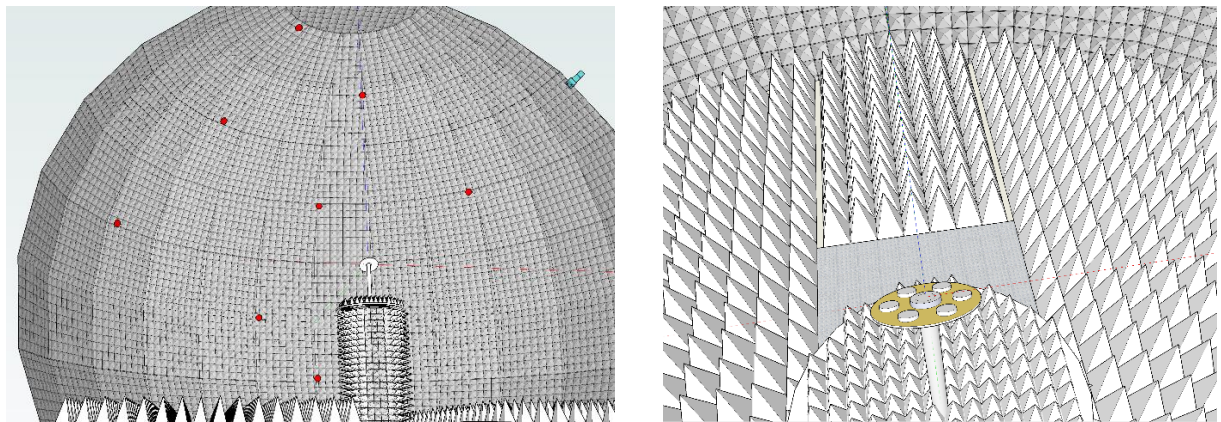


Figure 110. 3-D sketch showing a possible arrangement of the 8 transmit antennas (coloured in red) on the dome of the EMSL (left); Close view of a 3-D sketch of a 7-element CRPA antenna mounted on the measurement tower (right).

An additional testing capability that is under development is the possibility to characterize CRPA antennas in conducted mode bypassing the antenna-elements. The detailed specifications of these two testing configurations, i.e., in conducted and radiated mode, will be reported in the next release of this inventory.

4.5 GNSS Data Library

In relation with the mentioned test campaigns and laboratory activities in Section 3, the JRC has planned the implementation of an online GNSS Data Library freely accessible to the interested users. The main idea behind this activity is to support the GNSS community in its research and development activities by using reference data or test vectors of various kinds.

The current data sets under consideration for this online library implementation are:

- the estimation of the high-accurate reference trajectory and recorded data form the test drive in Milan, as described in Section 3.3.4
- the HAS correction or Test Vectors (ref. Section 3.4)
- the IF data samples recorded during the open air jamming and spoofing tests of Jammertest 2023 (ref. Section 4.2)

5 Conclusions

The EC Joint Research Centre (JRC) has established a long standing scientific and technical support activity with the Satellite Navigation Unit of the EC DG DEFIS and EUSPA. In this context, the JRC agreed to facilitate testing and demonstrations activities in R&D Actions under the EU GNSS Programmes in Horizon Europe. Over the last years, the scientific team at the JRC has kept on strengthening its portfolio of testing capabilities on the GNSS user-segment and, more specifically, those underpinning the adoption of Galileo and EGNOS. With the aim to document this evolution, a reference document providing an up-to-date inventory of the GNSS testing capabilities currently available at JRC has been produced. This report is a second issue and thus an update of a first release of the inventory published in 2021. The main upgrades and additions reported in this latest issue of the inventory were:

- A new testing capability aimed at characterising the phase center variation and phase center offset (PCV/PCO) of GNSS antennas was successfully developed and validated. This characterisation is important for the GNSS antennas used in high precision applications, including those in space in LEO and above.
- A test bench aimed at assessing the conformity of ship-borne SBAS receivers with respect to a new IEC standard was designed and tested thoroughly on a set of sample devices. This development was motivated by the planned deployment of the EGNOS Maritime Service.
- A data collection with a reference navigation system and multiple GNSS receivers on-board a vehicle driving in the city of Milan was completed. The associated datasets and reference trajectory, which are meant to help assess the performance of the Galileo HAS in an urban environment, will be shared with interested users in a near future.
- New capabilities supporting the performance assessment and implementation of the Galileo HAS on GNSS receivers were reported. An important new asset was a HAS testbed specifically designed to assess the performance of the HAS user algorithm in wide range of configurations.
- In view of the planned introduction of the Galileo Timing Service, a new testbed and new test procedures aimed at assessing the conformity of timing receivers against to the requirements set in a new CEN/CENELEC Galileo Timing Receiver Standard were implemented and reported.
- A thorough review of the capabilities supporting the Galileo OSNMA was made, introducing several new tools fully aligned with the latest specifications of the authentication scheme. Some illustrative results obtained during the tests facilitated to the BANSHEE and ASGARD projects were included.
- A Galileo ACAS testbed, developed under the PAULA project and later handed over to the JRC, was presented. Interestingly, the PAULA testbed is a multi-purpose platform that can also help assess the performance of Galileo OSNMA and HAS.
- A testing capability supporting the compliance check of GNSS receivers implementing the functionalities of the Galileo I/NAV improvements, specified in the latest ICD of the Galileo Open Service, was reported. Here, example results from a recent test campaign coordinated by EUSPA are included.
- In support of the tests and performance assessment studies of the ARAIM service for civil aviation, a novel horizontal ARAIM service implementation, based on the JRC's ARTEX ARAIM testbed that complies with the requirements of civil aviation and SoL service, was introduced.
- To facilitate the adoption of Galileo as a major component of the SSV service, a new integrated SSV test bench (ISSVTB) implementation, designed to test and benchmark the performance of GNSS receivers in space (i.e., LEO orbit and above) was developed and thoroughly validated. Here, some illustrative results obtained in H2020 GASPER project, which will be the first IOV/IOD mission exploiting the real-time P2OD and Galileo HAS, were presented.
- A set of testing capabilities developed to support the demonstrations of C-PNT technology platforms conducted in the Campus of JRC Ispra in 2021 and 2022, which included timing plus indoor and outdoor positioning technologies not relying on GNSS.
- An update of the record and replay testing capabilities of GNSS signals that are based on different HW platforms depending on the requirements on the sampling rate, number of simultaneous frequency bands, and bit depth of the recorded samples.

- A major extension of the testing capabilities with RFI and spoofing attack scenarios, including new GNSS signal simulation features and a library of representative spoofing and meaconer attacks, was reported. Although this library was originally conceived for drone operation scenarios, it can easily be adapted for other use-cases, such as those of relevance in the automotive or civil aviation domains.
- On the facilitation of tests and demonstrations in open air in the Campus of the JRC Ispra Site, some interesting results on a GNSS application aimed at protecting vulnerable road users and vehicles, planned in the frame of the VALOUR project at the Università degli Studi di Modena e Reggio Emilia, were added.

In addition to the above upgrades on the inventory, several testing capabilities that are under development were announced and briefly reported. These included the planned developments in the LEO-PNT test bench, the library of recorded spoofing and jamming scenarios during Jammertest 2023 campaign, an experiment aimed at geolocating the position of a ground based jammer with an SDR RF grabber embarked on ESA's OPS-Sat cubesat in the LEO orbit, the foreseen upgrade of the EMSL anechoic chamber to characterize CRPA antennas in radiated mode, and the planned JRC GNSS data library to be made publicly available online in a near future.

References

- [1] L. Cucchi *et al.*, "JRC Testing and Demonstration Hub for the EU GNSS Programmes - Inventory of GNSS Testing Capabilities," 2021, doi: 10.2838/93444, JRC125180.
- [2] "Detection, Evaluation and Characterization of Threats to Road Applications." Accessed: Apr. 06, 2021. [Online]. Available: <https://www.gsa.europa.eu/detection-evaluation-and-characterization-threats-road-applications>
- [3] A. J. Sieber, "The European Microwave Signature Laboratory," *EARSeL Advances in Remote Sensing*, vol. 2, no. 1, pp. 195–204, Jan. 1993.
- [4] J. M. Lopez-Sanchez and J. Fortuny-Guasch, "3-D radar imaging using range migration techniques," *IEEE Transactions on Antennas and Propagation*, vol. 48, no. 5, Art. no. 5, May 2000, doi: 10.1109/8.855491.
- [5] J. Fortuny-Guasch and J. M. Lopez-Sanchez, "Extension of the 3-D range migration algorithm to cylindrical and spherical scanning geometries," *IEEE Transactions on Antennas and Propagation*, vol. 49, no. 10, Art. no. 10, Oct. 2001, doi: 10.1109/8.954932.
- [6] S. R. Cloude, J. Fortuny, J. M. Lopez-Sanchez, and A. J. Sieber, "Wide-band polarimetric radar inversion studies for vegetation layers," *IEEE Transactions on Geoscience and Remote Sensing*, vol. 37, no. 5, pp. 2430–2441, Sep. 1999, doi: 10.1109/36.789640.
- [7] J. Fortuny, K. Boniface, C. Gioia, M. Susi, M. Paonni, and M. Sgammini, "GNSS RF Signal Testing and Evaluation at the EC Joint Research Centre: An enabler of the Galileo market uptake," in *2019 European Microwave Conference in Central Europe (EuMCE)*, Prague, Czech Republic: IEEE, May 2019, pp. 323–326.
- [8] "GSS9000 Series GNSS Simulator - Spirent." Accessed: Mar. 26, 2021. [Online]. Available: <https://www.spirent.com/products/gnss-simulator-gss9000>
- [9] J. T. Curran, M. Bavaro, and J. Fortuny, "Analog and Digital Nulling Techniques for Multi-Element Antennas in GNSS Receivers," in *Proceedings of the 28th International Technical Meeting of the Satellite Division of The Institute of Navigation (ION GNSS+ 2015)*, Institute of Navigation, Sep. 2015, pp. 3249–3261.
- [10] "FLIR PTU-D300E Pan/Tilt Unit for side-mounted payloads up to 70 lbs | FLIR Systems." [Online]. Available: <https://www.flir.com/products/ptu-d300e/>
- [11] R. Zhou *et al.*, "Consistency Analysis of the GNSS Antenna Phase Center Correction Models," *Remote Sens.* 2022, vol. 14, no. 3:540, 2022, doi: 10.3390/rs14030540.
- [12] "IGS Antenna Committee." Accessed: Feb. 29, 2024. [Online]. Available: <https://igs.org/wg/antenna/#charter>
- [13] B. Görres, J. Campbell, M. Siemes, and M. Becker, "New anechoic chamber results and comparison with field and robot techniques," presented at the IGS Workshop, Bern, Switzerland, Mar. 2004. [Online]. Available: http://igscb.jpl.nasa.gov/igscb/resource/pubs/04_rtberne/cdrom/Session10/10_1_Goerres.pdf
- [14] "GSA publishes eCall guidelines to facilitate GNSS compatibility tests." Accessed: Mar. 30, 2021. [Online]. Available: <https://www.gsa.europa.eu/newsroom/news/gsa-publishes-ecall-guidelines-facilitate-gnss-compatibility-tests>
- [15] *Commission Delegated Regulation (EU) 2017/79 of 12 September 2016 establishing detailed technical requirements and test procedures for the EC type-approval of motor vehicles with respect to their 112-based eCall in-vehicles systems, of 112-based eCall in-vehicle separate technical units and components and supplementing and amending Regulation (EU) 2015/758 of the European Parliament and of the Council with regard to the exemptions and applicable standards (Text with EEA relevance.)*. 2017. [Online]. Available: <https://eur-lex.europa.eu/legal-content/EN/TXT/PDF/?uri=CELEX:32017R0079>
- [16] K. Boniface, C. Gioia, M. Susi, J. Fortuny-Guasch, and F. Sbardellati, "Galileo and EGNOS Adoption in Automotive Emergency Call System (eCall)," in *Proceedings of the 32nd International Technical Meeting of the Satellite Division of The Institute of Navigation (ION GNSS+ 2019)*, Sep. 2019, pp. 1284–1294. doi: 10.33012/2019.17130.

- [17] "GSA/JRC ECALL Conformance Testing Campaign: ECALL Devices Assessment Report." Jan. 10, 2018. Accessed: Mar. 30, 2021. [Online]. Available: <https://www.gsa.europa.eu/sites/default/files/content/gsa-jrc-ecall-conformance-testing-campaign.pdf>
- [18] "Sub-Committee on Navigation, Communications, Search and Rescue (NCSR), 3rd session, 29 February-4 March." Accessed: Mar. 26, 2021. [Online]. Available: <https://www.imo.org/en/MediaCentre/MeetingSummaries/Pages/NCSR,-3rd-session.aspx>
- [19] "Maritime navigation and radiocommunication equipment and systems - Global navigation satellite systems (GNSS) - Part 3: Galileo receiver equipment - Performance requirements, methods of testing and required test results." International Electrotechnical Committee, Mar. 26, 2021. Accessed: Mar. 26, 2021. [Online]. Available: <https://webstore.iec.ch/publication/4517>
- [20] C. Gioia, L. Cucchi, J. Fortuny-Guasch, and M. L. Martinez, "Galileo Adoption in Shipborne Equipment," Sep. 2020, pp. 884–895. doi: 10.33012/2020.17730.
- [21] "European Union, 'European GNSS (Galileo) High Accuracy Service Signal-In-Space Interface Control Document (HAS SIS ICD).'" [Online]. Available: https://www.gsc-europa.eu/sites/default/files/sites/all/files/Galileo_HAS_SIS_ICD_v1.0.pdf
- [22] P. Pintor *et al.*, "Galileo High Accuracy Service (HAS) Algorithm and Receiver Development and Testing," in *Proceedings of the 35th International Technical Meeting of the Satellite Division of The Institute of Navigation (ION GNSS+ 2022)*, Denver, CO, Sep. 2022, pp. 836–851. doi: 10.33012/2022.18462.
- [23] O. Horst *et al.*, "HASlib: An Open-Source Decoder for the Galileo High Accuracy Service," in *Proceedings of the 35th International Technical Meeting of the Satellite Division of The Institute of Navigation (ION GNSS+ 2022)*, Denver, Colorado, Sep. 2022, pp. 2625–2633. doi: 10.33012/2022.18508.
- [24] O. Horst, "Implementation of an Open-Source Software Suite for the Galileo High Accuracy Service," M.Sc. (Tech.) thesis, Aalto University, School of Electrical Engineering, Espoo, Finland, 2021. [Online]. Available: <https://aaltodoc.aalto.fi/server/api/core/bitstreams/36554201-2090-434f-83ac-ff88748f5e5a/content>
- [25] L. Cucchi, C. Gioia, T. Senni, and M. Paonni, "Galileo High Accuracy Service: an automotive test," presented at the 2023 IEEE International Workshop on Metrology for Automotive (MetroAutomotive), Modena, Italy, 2023, pp. 122–126. doi: 10.1109/MetroAutomotive57488.2023.10219123.
- [26] L. Cucchi, S. Damy, C. Gioia, B. Motella, and M. Paonni, "Testing the Galileo High Accuracy Service in Different Operational Scenarios," in *Proceedings of the 36th International Technical Meeting of the Satellite Division of The Institute of Navigation*, Denver, Colorado, Sep. 2023, pp. 2712–2722. doi: 10.33012/2023.19286.
- [27] "GNSS Market Report Issue 6." Accessed: Mar. 26, 2021. [Online]. Available: <https://www.gsa.europa.eu/gnss-market-report-issue-6-october-2019>
- [28] "GSA celebrates 1 billion Galileo smartphone users." Accessed: Mar. 26, 2021. [Online]. Available: <https://www.gsa.europa.eu/newsroom/news/gsa-celebrates-1-billion-galileo-smartphone-users>
- [29] T. Jahn *et al.*, "Assessment of GNSS Performance on Dual-Frequency Smartphones," in *Proceedings of the 32nd International Technical Meeting of the Satellite Division of The Institute of Navigation (ION GNSS+ 2019)*, Institute of Navigation, Oct. 2019. doi: 10.33012/2019.16860.
- [30] "European Location As A Service Targeting International Commerce." Accessed: Mar. 26, 2021. [Online]. Available: <https://www.gsa.europa.eu/european-location-service-targeting-international-commerce>
- [31] "Raw GNSS Measurements," Android Developers. Accessed: Apr. 09, 2021. [Online]. Available: <https://developer.android.com/guide/topics/sensors/gnss>
- [32] *Directive (EU) 2018/1972 of the European Parliament and of the Council of 11 December 2018 establishing the European Electronic Communications Code (Recast)Text with EEA relevance*, vol. 321, no. 32018L1972. 2018. [Online]. Available: <https://eur-lex.europa.eu/legal-content/EN/TXT/PDF/?uri=CELEX:32018L1972>
- [33] *Commission Delegated Regulation (EU) 2019/320 of 12 December 2018 supplementing Directive 2014/53/EU of the European Parliament and of the Council with regard to the application of the essential requirements referred to in Article 3(3)(g) of that Directive in order to ensure caller location in*

emergency communications from mobile devices, vol. 055, no. 32019R0320. 2019. Accessed: Mar. 26, 2021. [Online]. Available: http://data.europa.eu/eli/reg_del/2019/320/oj/eng

- [34] “Project FANTASTIC: Field Aware Navigation and Timing Authentication Sensor for Timing Infrastructure and Centimeter level positioning,” FANTASTIC Project. Accessed: Mar. 26, 2021. [Online]. Available: <http://gnss-fantastic.eu/>
- [35] M. Pini, G. Marucco, G. Falco, M. Nicola, and W. De Wilde, “Experimental Testbed and Methodology for the Assessment of RTK GNSS Receivers Used in Precision Agriculture,” *IEEE Access*, vol. 8, pp. 14690–14703, 2020, doi: 10.1109/ACCESS.2020.2965741.
- [36] D. Egea-Roca *et al.*, “Design, Implementation and Validation of a GNSS Measurement Exclusion and Weighting Function with a Dual Polarized Antenna,” *vol. Sensor* 18, no. 18:4483, Dec. 2018, doi: 10.3390/s18124483.
- [37] M. Pini, G. Marucco, G. Falco, M. Nicola, and W. De Wilde, “Experimental Testbed and Methodology for the Assessment of RTK GNSS Receivers Used in Precision Agriculture,” *IEEE Access*, vol. 8, pp. 14690–14703, 2020, doi: 10.1109/ACCESS.2020.2965741.
- [38] “Project GAUSS – Galileo-EGNOS as an Asset for UTM Safety and Security.” Accessed: Mar. 26, 2021. [Online]. Available: <https://projectgauss.eu/>
- [39] “ATLAS | Air Trafic Laboratory for Advanced unmanned Systems.” Accessed: Apr. 09, 2021. [Online]. Available: <http://atlascenter.aero/en>
- [40] “European Union, Galileo Open Service Service Definition Document (OS SDD).” [Online]. Available: https://www.gsc-europa.eu/sites/default/files/sites/all/files/Galileo-OS-SDD_v1.3.pdf
- [41] “European Union, Galileo Open Service Signal-In-Space Interface Control Document (OS SIS ICD).” [Online]. Available: https://www.gsc-europa.eu/sites/default/files/sites/all/files/Galileo_OS_SIS_ICD_v2.1.pdf
- [42] “European Union Space Program Agency (EUSPA) (2020) Information note on Galileo high accuracy service.” [Online]. Available: https://www.gsc-europa.eu/sites/default/files/sites/all/files/Galileo_HAS_Info_Note.pdf
- [43] “European Union, ‘European GNSS (Galileo) High Accuracy Service Internet Data Distribution Interface Control Document (HAS Internet Data Distribution ICD).’” [Online]. Available: https://www.gsc-europa.eu/sites/default/files/sites/all/files/Galileo_HAS_SIS_ICD_v1.0.pdf
- [44] “European Union, ‘Galileo HAS Service Definition Document.’” [Online]. Available: https://www.gsc-europa.eu/sites/default/files/sites/all/files/Galileo-HAS-SDD_v1.0.pdf
- [45] I. Martini, M. Susi, L. Cucchi, and I. Fernández-Hernández, “Galileo high accuracy service performance and anomaly mitigation capabilities,” *GPS Solutions* 28, vol. 25, Nov. 2023, doi: 10.1007/s10291-023-01555-w.
- [46] L. Bonenberg, B. Motella, and J. Fortuny, *Assessing Alternative Positioning, Navigation and Timing Technologies for Potential Deployment in the EU*. 2023. doi: 10.2760/596229.
- [47] “European Union, ‘Galileo Open Service Navigation Message Authentication (OSNMA) Info Note.’” [Online]. Available: https://www.gsc-europa.eu/sites/default/files/sites/all/files/Galileo_OSNMA_Info_Note.pdf
- [48] “European Union, ‘Galileo Open Service Navigation Message Authentication (OSNMA) Signal-In-Space Interface Control Document (SIS ICD).’” [Online]. Available: https://www.gsc-europa.eu/sites/default/files/sites/all/files/Galileo_OSNMA_SIS_ICD_v1.1.pdf
- [49] R. Terris-Gallego, I. Fernández-Hernández, J. A. Lopez-Salcedo, and G. Seco-Granados, “Guidelines for Galileo Assisted Commercial Authentication Service Implementation,” *International Conference on Localization and GNSS (ICL-GNSS), Tampere, Finland*, pp. 01–07, 2022, doi: 10.1109/ICL-GNSS54081.2022.9797027.
- [50] D. Calle, S. Cancela, E. Carbonell, I. Rodríguez, G. Tobías, and I. Fernández-Hernández, “First Experimentation Results with the Full Galileo CS Demonstrator,” presented at the Proceedings of the 29th International Technical Meeting of the Satellite Division of The Institute of Navigation (ION GNSS+ 2016), Sep. 2016, pp. 2870–2877. doi: 10.33012/2016.14728.

- [51] C. Sarto *et al.*, "Implementation and Testing of OSNMA for Galileo," presented at the Proceedings of the 30th International Technical Meeting of the Satellite Division of The Institute of Navigation (ION GNSS+ 2017), Sep. 2017, pp. 1508–1519. doi: 10.33012/2017.15184.
- [52] "NACSET - Navigation Authentication through Commercial Service-Enhanced Terminals," Internal Market, Industry, Entrepreneurship and SMEs - European Commission. Accessed: Mar. 30, 2021. [Online]. Available: https://ec.europa.eu/growth/sectors/space/research/horizon-2020/nacset_en
- [53] "European Union, Galileo Open Service Navigation Message Authentication (OSNMA) Receiver Guidelines." [Online]. Available: https://www.gsc-europa.eu/sites/default/files/sites/all/files/Galileo_OSNMA_Receiver_Guidelines_v1.1.pdf
- [54] "Septentrio AsteRx-U Receiver." Accessed: Mar. 26, 2021. [Online]. Available: <https://www.septentrio.com/en/products/gnss-receivers/rover-base-receivers/integrated-gnss-receivers/asterx-u>
- [55] S. Damy, L. Cucchi, and M. Paonni, "Impact of OSNMA Configurations, Operations and User's Strategies on Receiver Performances," *Proceedings of the 35th International Technical Meeting of the Satellite Division of The Institute of Navigation (ION GNSS+ 2022)*, Denver, CO, pp. 820–827, Sep. 2022, doi: 10.33012/2022.18302.
- [56] S. Damy, L. Cucchi, and M. Paonni, "Performance Assessment of Galileo OSNMA Data Retrieval Strategies," *Proceedings of the NAVITEC 2022 conference, NL, 5-7 April 2022*, Apr. 2022, [Online]. Available: [https://www.researchgate.net/publication/365838628_Performance_Assessment_of_Galileo\(OSNMA\)_Data_Retrieval_Strategies](https://www.researchgate.net/publication/365838628_Performance_Assessment_of_Galileo(OSNMA)_Data_Retrieval_Strategies)
- [57] A. Galan, I. Fernández-Hernández, L. Cucchi, and G. Seco-Granados, "OSNMAlib: An Open Python Library for Galileo OSNMA," in *2022 10th Workshop on Satellite Navigation Technology (NAVITEC)* IEEE., Noordwijk, Netherlands: IEEE, Apr. 2022. doi: ISBN Information: Electronic ISBN:978-1-6654-1616-0 Print on Demand(PoD) ISBN:978-1-6654-1617-7 ISSN Information: INSPEC Accession Number: 21971157 DOI: 10.1109/NAVITEC53682.2022.9847548.
- [58] "Unlock Secure Navigation on Embedded Platforms with Rokubun's OSNMA Library." [Online]. Available: <https://www.rokubun.cat/unlock-secure-navigation-on-embedded-platforms-with-rokubun-osnma-library/>
- [59] I. Fernández-Hernández *et al.*, "Semiassisted Signal Authentication for Galileo: Proof of Concept and Results," *IEEE Transactions on Aerospace and Electronic Systems*, vol. vol 59, no. no 4, pp. 4393–4404, Aug. 2023, doi: 10.1109/TAES.2023.3243587.
- [60] R. Terris-Gallego, J. A. Lopez-Salcedo, G. Seco-Granados, and I. Fernández-Hernández, "Preliminary Evaluation of Galileo ACAS Using Existing E1-E6 Open Signals and a Low-Cost SDR Platform," *Proceedings of the 36th International Technical Meeting of the Satellite Division of The Institute of Navigation (ION GNSS+ 2023)*, Denver, Colorado, pp. 1388-1402, Sep. 2023, doi: 10.33012/2023.19319.
- [61] L. Cucchi, S. Damy, M. Paonni, M. Nicola, and B. Motella, "Receiver Testing for the Galileo E1 OSNMA and I/NAV Improvements," *Proceedings of the 35th International Technical Meeting of the Satellite Division of The Institute of Navigation (ION GNSS+ 2022)*, Denver, Colorado, pp. 808-819., Sep. 2022, doi: 10.33012/2022.18301.
- [62] U.S. EU, "EU-U.S. Cooperation on Satellite Navigation Working Group C - ARAIM Technical Subgroup - Milestone 3 Report," Feb. 2016. [Online]. Available: <https://www.gps.gov/policy/cooperation/europe/2016/working-group-c/ARAIM-milestone-3-report.pdf>
- [63] J. Blanch *et al.*, "Baseline Advanced RAIM User Algorithm and Possible Improvements," *IEEE Transactions on Aerospace and Electronic Systems*, vol. Volume 51, no. No. 1, pp. 713–732, 2015, doi: 10.1109/TAES.2014.130739.
- [64] "Advanced RAIM Reference Airborne Algorithm Description Document (ARAIM ADD)," presented at the Working Group-Advanced RAIM Technical Subgroup (WG-C-ARAIM TSG), to be published by ARAIM Technical Subgroup, 2023.

- [65] J. She *et al.*, "Implementation of the Reference Advanced RAIM User Algorithm," *Proceedings of the 36th International Technical Meeting of the Satellite Division of The Institute of Navigation (ION GNSS+ 2023)*, Denver, Colorado, Sep. 2023.
- [66] *United Nations, The Interoperable Global Navigation Satellite Systems Space Service Volume*, Second Edition. Vienna, 2021. [Online]. Available: https://www.unoosa.org/res/oosadoc/data/documents/2021/stspace/stspace75rev_1_0_html/st_space_75rev01E.pdf
- [67] J. Ventura-Traveset, "Lunar Pathfinder and Moonlight," presented at the Seventeenth Meeting of the International Committee on Global Navigation Satellite Systems (ICG), Madrid, Spain, Oct. 2023. [Online]. Available: <https://www.unoosa.org/documents/pdf/icg/2023/ICG-17/icg17.02.10.pdf>
- [68] "H2020-ESA-052 ELCANO Proof of Concept." [Online]. Available: <https://esastar-publication-ext.sso.esa.int/search?s=ELCANO>
- [69] F. Menzione, M. Sgammini, and M. Paonni, "Reconstruction of Galileo Constellation Antenna Pattern for Space Service Volume Applications," *Publications Office of the European Union*, Mar. 2024, doi: 10.2760/765842.
- [70] "Navstar GPS Space Segment/User Segment Interfaces." [Online]. Available: <https://www.gps.gov/technical/icwg/IS-GPS-200N.pdf>
- [71] "Navstar GPS Space Segment/User Segment L5 Interfaces." [Online]. Available: <https://www.gps.gov/technical/icwg/IS-GPS-705J.pdf>
- [72] J. E. Donaldson, J. J. K. Parker, M. C. Moreau, D. E. Highsmith, and P. D. Martzen, "Characterization of on-orbit GPS transmit antenna patterns for space users," *NAVIGATION-US*, vol. 67, pp. 411–438, Jun. 2020, doi: 10.1002/navi.361.
- [73] A. Piccolo, A. Zin, S. Zago, L. Badano, and L. Marradi, "Navigating in Geostationary Orbit With a GNSS Receiver: A Further Analysis to In-Flight Results," *2023 IEEE 10th International Workshop on Metrology for AeroSpace (MetroAeroSpace)*, Milan, Italy, pp. 615–620, 2023, doi: 10.1109/MetroAeroSpace57412.2023.10190030.
- [74] W. Marquis, "The GPS block IIR/IIR-M antenna panel pattern," *public release under LMCO*, no. rev 3, 2014, [Online]. Available: https://www.navcen.uscg.gov/sites/default/files/pdf/gps/GPS_Block_IIR_IIR_M_Antenna_Panel_Pattern_Marquis_Aug2015_revised.pdf
- [75] F. Menzione, J. P. Boyero, S. Wallner, and M. Ciollaro, "Space Service Volume (SSV) - Galileo Reference Antenna Pattern," presented at the Seventeenth Meeting of the International Committee on Global Navigation Satellite Systems (ICG), Madrid, Spain, Oct. 2023. [Online]. Available: https://www.unoosa.org/documents/pdf/icg/2023/ICG-17/icg17_LunarPNT_05.pdf
- [76] "Septentrio mosaic-X5." [Online]. Available: <https://www.septentrio.com/en/products/gps/gnss-receiver-modules/mosaic-x5>
- [77] "GAlikeo SSpace ReceivER for Horizon 2020 IOD/IOV Mission (GASPER) under In-Orbit Demonstration and Validation (IOD/IOV) [DEFIS/2021/OP/0002]." [Online]. Available: <https://etendering.ted.europa.eu/cft/cft-display.html?cftId=8112>
- [78] "European Commission, European Radio Navigation Plan 2023," 2023, doi: 10.2889/245554.
- [79] "Software Defined Radios, NI products catalogue." [Online]. Available: <https://www.ni.com/it-it/shop/category/software-defined-radios.html>
- [80] "USRP X Series, Ettus Research SDR products." [Online]. Available: <https://www.ettus.com/product-categories/usrp-x-series/>
- [81] "LabSat-3 Product Information." [Online]. Available: <https://www.labsat.co.uk/downloads/product-info/Flyers/LabSat-3-Flyer.pdf>
- [82] F. Dovis, Ed., *GNSS interference, threats, and countermeasures*. in Artech House GNSS technology and applications series. Boston: Artech House, 2015.

- [83] P. J. G. Teunissen and O. Montenbruck, Eds., *Springer Handbook of Global Navigation Satellite Systems*. in Springer Handbooks. Cham: Springer International Publishing, 2017. [Online]. Available: <http://dx.doi.org/10.1007/978-3-319-42928-1>
- [84] G. G. (Associate E. Y. Jade Morton Frank van Diggelen, James J. Spilker Jr., Bradford W. Parkinson (Editors), Sherman Lo, *Position, Navigation, and Timing Technologies in the 21st Century: Integrated Satellite Navigation, Sensor Systems, and Civil Applications, Set*. WILEY, 2021. [Online]. Available: https://www.ebook.de/de/product/37759883/position_navigation_and_timing_technologies_in_the_21st_century_integrated_satellite_navigation_sensor_systems_and_civil_applications_set.html
- [85] "STRIKE3 Project." Accessed: Apr. 12, 2021. [Online]. Available: <http://gnss-strike3.eu/>
- [86] "First Operational, Secured and Trusted galilEO Receiver for ITS." Accessed: Apr. 15, 2021. [Online]. Available: <https://www.gsa.europa.eu/first-operational-secured-and-trusted-galileo-receiver-its>
- [87] "Trusted multi-application receiver for trucks | European Global Navigation Satellite Systems Agency." Accessed: Apr. 07, 2021. [Online]. Available: <https://www.gsa.europa.eu/trusted-multi-application-receiver-trucks>
- [88] "Trusted Vessel Information from Trusted On-board Instrumentation | TRITON Project | FP7 | CORDIS | European Commission." Accessed: Apr. 07, 2021. [Online]. Available: <https://cordis.europa.eu/project/id/312687>
- [89] "Project GAMMA." Accessed: Apr. 13, 2021. [Online]. Available: <https://www.projectgamma.eu/>
- [90] C. O'Driscoll *et al.*, "Compatibility Analysis Between LightSquared Signals and L1/E1 GNSS Reception," presented at the Proceedings of IEEE/ION PLANS 2012, Apr. 2012, pp. 447–454. Accessed: Mar. 26, 2021. [Online]. Available: <http://www.ion.org/publications/abstract.cfm?jp=p&articleID=10113>
- [91] M. Rao, C. O'Driscoll, D. Borio, and J. Fortuny, "LightSquared effects on estimated C/N 0, pseudoranges and positions," *GPS Solut*, vol. 18, no. 1, Art. no. 1, Jan. 2014, doi: 10.1007/s10291-012-0304-6.
- [92] L. Cucchi, J. Fortuny, G. Baldini, I. Fernandez-Hernandez, B. Martinez, and G. Vecchione, "A GNSS Jamming/Spoofing Test Suite for Smart Tachograph Applications," in *Proceedings of the 33rd International Technical Meeting of the Satellite Division of The Institute of Navigation (ION GNSS+ 2020)*, Institute of Navigation, Oct. 2020. doi: 10.33012/2020.17759.
- [93] *Commission Implementing Regulation (EU) 2016/799 of 18 March 2016 implementing Regulation (EU) No 165/2014 of the European Parliament and of the Council laying down the requirements for the construction, testing, installation, operation and repair of tachographs and their components (Text with EEA relevance) C/2016/1597*, no. 32016R0799. 2021. Accessed: Mar. 26, 2021. [Online]. Available: <https://eur-lex.europa.eu/legal-content/EN/TXT/?uri=CELEX%3A32016R0799>
- [94] *Commission Implementing Regulation (EU) 2018/502 of 28 February 2018 amending Implementing Regulation (EU) 2016/799 laying down the requirements for the construction, testing, installation, operation and repair of tachographs and their components (Text with EEA relevance) C/2018/1116*, vol. 32018R0502. 2021. Accessed: Mar. 26, 2021. [Online]. Available: <https://eur-lex.europa.eu/legal-content/GA/TXT/?uri=CELEX%3A32018R0502>
- [95] "Skydel GSG-8 Advanced GNSS Simulator." [Online]. Available: https://safran-navigation-timing.com/product/gsg-8-advanced-gnss-simulator/?model_interest__c=Skydel&product_interest__single_select=GNSS+Simulation
- [96] "Certified E-GNSS Remote Tracking of Drone and Aircraft FLIGHTs." [Online]. Available: <https://cordis.europa.eu/project/id/101082484/it>
- [97] T. LANGE, "Pilot living labs at the JRC," EU Science Hub - European Commission. Accessed: Apr. 07, 2021. [Online]. Available: <https://ec.europa.eu/jrc/en/research-facility/living-labs-at-the-jrc>
- [98] "Search And Rescue Aid and Surveillance using High EGNSS Accuracy." [Online]. Available: <https://cordis.europa.eu/article/id/428504-drone-plays-lookout-for-sea-rescue>
- [99] F. Menzione and M. Paonni, "LEO-PNT Mega-Constellations: a New Design Driver for the Next Generation MEO GNSS Space Service Volume and Spaceborne Receivers," in *2023 IEEE/ION Position, Location and Navigation Symposium (PLANS)*, Monterey, CA, USA: IEEE, Apr. 2023, pp. 1196–1207. doi: 10.1109/PLANS53410.2023.10140052.

- [100] “Jammertest 2023 Information.” [Online]. Available: <https://rntfnd.org/wp-content/uploads/Jammertest-2023-information.pdf>
- [101] “OPS-SAT.” [Online]. Available: https://www.esa.int/Enabling_Support/Operations/OPS-SAT

List of abbreviations and definitions

ACAS	Assisted Commercial Authentication Service
ADC	Analog-to-Digital Converter
ADKD	Authentication Data and Key Delay
RAIM	Advanced RAIM
ARTEX	RAIM demonstrator for Testing and Experimentation
ATLAS	Air Traffic Laboratory for Advanced Systems
AWGN	Additive White Gaussian Noise
BER	Bit Error Rate
CAS	Commercial Authentication Service
CDF	Cumulative Distribution Function
CEN	European Committee for Standardization
CENELEC	European Committee for Electrotechnical Standardization
CfT	Call for Tender
CoG	Centre of Gravity
COG	Corse Over Ground
COTS	Commercial Off The Shelf
CRPA	Controlled Reception Pattern Antennas
CSTTFF	Cold Start Time-To-First-Fix
CW	Continuous Wave
C/No	Carrier-to-Noise Power Spectral density ratio
C-PNT	Complementary PNT
DAC	Digital-to-Analog Converter
DC	Direct Current
DEFIS	Defence Industry and Space
DHCP	Dynamic Host Configuration Protocol
DG	Directorate General
DNS	Domain Name System
DSM	Digital Signature Messages

DSSS	Direct-Sequence Spread Spectrum
DUT	Devices Under Test
EC	European Commission
ECS	Encrypted Code Sequence
EGNOS	European Geostationary Overlay System
EKF	Extended Kalman Filter
EMSL	European Microwave Signature Laboratory
ERNP	European Radio Navigation Plan
ESOC	European Space Operations Centre
E2E	End-to-End
ETRF	European Terrestrial Reference Frame
EU	European Union
EUSPA	European Union Agency for the Space Programme
FANTASTIC	Field Aware Navigation and Timing Authentication Sensor for Timing Infrastructure and Centimeter level positioning
FDE	Fault Detection and Exclusion
FFI	Norwegian Defence Research Establishment
FOC	Full Operational Capability
G1G	Galileo 1 st Generation
GASPER	GAlikeo SSpace ReceivER for Horizon 2020 IOD/IOV Mission
GAUSS	Galileo-EGNOS as an Asset for UTM Safety and Security
GDOP	Geometrical Dilution of Precision
GEO	Geosynchronous Earth Orbit
GFE	Galileo Fundamental Elements
GGA	Global Positioning System Fixed Data
GGTO	Galileo to GPS Time Offset
GNSS	Global Navigation Satellite System
GSA	GNSS DOP and Active Satellites
GSC	GNSS Service Centre

GSV	GNSS Satellites in View
GUI	Graphical User Interface
HAS	High Accuracy Service
HE	Horizon Europe: The EU Research and Innovation Programme in the Multi-Annual Financial Framework 2021-2027
HEO	High Eccentric Orbit
HGA	High-Gain Antenna
HW	Hardware
H2020	Horizon 2020: The EU Research and Innovation Programme in the Multi-Annual Financial Framework 2014-2020
ICD	Interface Control Document
ICG	International Committee on GNSS
IEC	International Electrotechnical Committee
IEEE	Institute of Electrical and Electronics Engineers
IF	Intermediate Frequency
IGS	International GNSS Service
INRiM	Istituto Nazionale di Ricerca Metrologica
IMO	International Maritime Organisation
IMU	Inertial Measurement Unit
IOD	Issue Of Data
JRC	Joint Research Centre
ISSVTB	Integrated SSV Test Bench
J/S	Jammer over Signal
KPI	Key Performance Indicator
LEO	Low Earth Orbit
LG	Low-Gain
LHCP	Left Hand Circularly Polarised
MAS	Mission And Services
MEMS	Micro Electro Mechanical System
MEO	Medium Earth Orbit

MGEX	Multi-GNSS Experiment
MISE	Ministero dello Sviluppo Economico
NAS	Network Attached Storage
NMA	Navigation Message Authentication
NMEA	National Marine Electronics Association
NTP	Network Time Protocol
OBU	On-board Unit
OPNT	Optical Positioning, Navigation and Timing
OSNMA	Open Service Navigation Message Authentication
OTA	Over The Air
PATROL	Position Authenticated Tachograph foR OSNMA Launch
PCI	Peripheral Component Interconnect
PCO	Phase Center Offset
PCV	Phase Center Variation
PDOP	Position Dilution Of Precision
PLC	Programmable Logic Controller
PNT	Position Navigation Timing
POD	Precise Orbit Determination
PPP	Precise Point Positioning
PPK	Post Processing Kinematic
PPS	Pulse Per Second
PSAP	Public Safety Answering Point
PVT	Position Velocity and Time
P2OD	Precise On-board Orbit Determination
RAIM	Receiver Autonomous Integrity Monitoring
RedCED	Reduced Clock and Ephemeris Data
RECS	Re-Encrypted Code Sequences
RF	Radio Frequency
RFCS	RF Constellation Simulator

RFI	Radio Frequency Interference
RHCP	Right Hand Circularly Polarised
RINEX	Receiver Independent Exchange
RMS	Root Mean Squared
RS	Reed Solomon
RTK	Real Time Kinematic
RX	Receive
R&R	Record & Replay
SAR	Synthetic Aperture Radar
SARA	Search and Rescue Aid
SBAS	Satellite Based Augmentation System
SCER	Security Code Estimation and Replay
SDR	Software Defined Receiver
SGP4	Standard General Perturbations Satellite Orbit Model 4
SIS	Signal In Space
SOG	Speed Over Ground
SoL	Safety-of-Life
SPAN	Synchronous Position Attitude and Navigation
SPO	Spaceopal
SP3	Standard Product 3
SSP	Secondary Synchronization Patterns
SSR	State Space Representation
SSV	Space Service Volume
STD	STandard Deviation
ST	Smart Tachograph
SW	Software
TC	Test Case
TCP/IP	Transmission Control Protocol / Internet Protocol
TESLA	Timed Efficient Stream Loss-Tolerant Authentication

TLE	Two Lines Element
TTFF	Time-To-First-Fix
TX	Transmitter
UA	User Algorithm
UNOOSA	United Nations Office for Outer Space Affairs
USRP	Universal Software Radio Peripheral
VNA	Vector Network Analyser
WG	Working Group

List of figures

Figure 1. 3-D sketch of an exploded view of the EMSL with a car on top of the rotating tower (left). A photograph of the rotating tower with an antenna under test (right)	7
Figure 2. Close view of the antennas, video camera and laser pointer in the sleds A (left) and B (right) of the EMSL laboratory.....	8
Figure 3. Sketch of the side view (left) and top view (right) of the two circular scans in an antenna measurement in the EMSL, which correspond to the zenith and azimuth angles.....	9
Figure 4. 3D sketches identifying the four mechanical axes of the EMSL (left) and the spherical grid of measurement points in an antenna measurement with combined azimuth/zenith scans (right).....	9
Figure 5. Sketches of the set-up of a calibration measurement with the vector network analyser: reference antenna with known gain on transmit (left) and receive (right) modes	10
Figure 6. Two vertical cuts of the LHCP and RHCP gain of a Javad choke-ring antenna at the frequency of 1578.0 MHz: vertical cuts at azimuth 0 deg (left) and azimuth 90 deg (right).	11
Figure 7. Photograph of the Trimble Zephyr Type 2 (left), and RHCP gain versus frequency of a Trimble Zephyr Type II antenna measured at boresight in the EMSL (right)	11
Figure 8. Sketch of the laboratory set-up to characterise an antenna using a GNSS simulator as a signal source (left) and photograph of the GNSS simulation rack behind the dome of the EMSL (right).....	12
Figure 9. A sketch of the multi-port microwave switch (left) and a photograph of a 7-element antenna array mounted on the measurement tower of the EMSL (right).....	13
Figure 10. Close view of the 7-element antenna array and the ground plane (left); vertical cuts of the RHCP gain pattern of the central and a peripheral element at azimuth 0deg (center); horizontal cuts of the gain of the central and a peripheral element at 40 deg elevation (right).....	13
Figure 11. 3-D sketch of the signal routing network of the array of the 36 fixed antennas on the outer surface of the dome (top), and photograph showing the arrangement of the fixed probe antennas as seen inside the anechoic chamber (bottom).....	14
Figure 12. Photographs of the pan-tilt antenna positioner mounted on the measurement tower of the EMSL during one of the integration tests; (left) side and (right) front views of the pan-tilt antenna positioner.....	15
Figure 16. Test bed setup for compliance assessment of SBAS-enabled maritime receivers.....	19
Figure 17. Example of EGNOS-based horizontal positioning performance for a maritime receiver	20
Figure 19. Tracking sensitivity analysis of dual-frequency multi-constellation SBAS receivers.....	21
Figure 20. Photograph of the set-up used in the measurement campaign of the ship-borne receivers. The movable platform holds an RF signal generator and an antenna to generate RF interference signals.....	23
Figure 21. Sketch illustrating the calibration of the GNSS signal power levels in the radiated tests. Using the amplified RF output of the simulator and a programmable attenuator, C/N0 values observed with a reference receiver in the radiated tests (left) are fully aligned with those measured with the same receiver in conducted mode (right) using the calibrated RF output of the simulator.....	24
Figure 22. Two photographs with a close view of the set-up used with the programmable vector signal generator and a TX standard gain horn antenna on the movable platform of the EMSL	24
Figure 23. Pseudorange ramps and horizontal positioning error as a function of the time in the RAIM/FDE test case.....	25
Figure 24. Working Flow of the processing scheme.....	26
Figure 25. JRC van equipped for the kinematic test aimed at assessing the performance of a HAS-enabled user terminal.....	27
Figure 26. Mean horizontal (upper box) and vertical (bottom box) error.....	27

Figure 27. Standard deviation of the horizontal (upper box) and vertical (lower box) error.....	28
Figure 28. Setup developed for vehicular (left) and pedestrian (right) tests using smartphones	29
Figure 29. Sketch of the RF testing environment with the smartphone in an anechoic chamber.....	30
Figure 30. Schematic representation of the test set-up for smartphone testing using simulated GNSS signals.	30
Figure 31. Views of the actual set-up for smartphone testing using simulated GNSS signals, in the RF shielded room (left) and in the control room (right).....	30
Figure 32. Novatel PwrPak7-E2, the reference navigation system available at the JRC.....	32
Figure 33. (Left side) Experimental set-up of the cart used for the dynamic test in the frame of the FANTASTIC project; (Right Side) Picture of the cart used for the dynamic tests carrying the SPAN-CPT system on the top (Extracted from FANTASTIC White Paper).....	33
Figure 34. Cart carrying the devices under test during a dynamic data collection in a vineyard (Pini et al., 2020b).....	33
Figure 35. Reference trajectory obtained by post processing the SPAN-CPT and the reference station data.	34
Figure 36. CDF of the horizontal position errors estimated for different devices under test and using the provided post-processed SPAN-CPT trajectory as reference (Pini et al., 2020b).....	34
Figure 37. (Left Side) High-end geodetic antenna placed under open sky at the ATLAS facility, connected to a high geodetic receiver to serve as reference station during flight tests with drones (Right Side) Tucan drone used in the frame of the GAUSS Project (images courtesy of the GAUSS project).....	35
Figure 38. Reference trajectory computed for one of the flight performed by the Tucan drone with Novatel Inertial Explorer.....	35
Figure 39. Surveying of the measurement points using a GNSS receiver (left) and the total station (right). ..	36
Figure 40. Survey results for the test carried out with the total station in the JRC Campus.....	37
Figure 41. Tracking of a drone using a multi-station (left) and a reflector mounted on the drone (left)	37
Figure 42. Dynamic test scenario in the Milan metropolitan area.....	38
Figure 43. Galileo HAS data broadcasting scheme.....	39
Figure 44. HAS UA Testbed currently deployed at JRC.....	40
Figure 45. Comparison of Galileo (top) and GPS (bottom) SISE errors and components of Broadcast (left) and HAS (right) ephemeris w.r.t. IGS final products.	41
Figure 46. HAS solution for a static solution at JRC location with OS and HAS ephemeris.....	42
Figure 47. Calibration setup, with JRC time reference visible on top.....	44
Figure 48. Results of INRIM 46 days calibration campaign.....	44
Figure 49. Record/replay setup for testing Galileo timing receivers	45
Figure 50. Timing test equipment in JRC laboratory.....	46
Figure 51. OSNMA testing capabilities.....	48
Figure 52. TESLA chain parameters retrieved from the JRC OSNMA parser	49
Figure 53. Schematic representation of the ACAS concept at the system (a) and receiver level (b).....	52
Figure 54. Paula UT modules options.....	52
Figure 55. Fault Detection Flowchart (figure taken from (She et al., 2023))	56
Figure 56. Fault Detection and Exclusion Flowchart (figure taken from (She et al., 2023))	57
Figure 57. Horizontal Protection Level Coverage @99.5% of RNP 0.1	57

Figure 58. Space Service Volume and beyond.....	58
Figure 59. JRC-ISSVTB Block Diagram.....	59
Figure 60. SSV user mission profile example	60
Figure 61. RFCS Signal Calibration Setup.....	61
Figure 62. GNSS Receiver Low-Gain (Patch) and High-Gain profiles example.....	61
Figure 63. EIRP of Galileo E1-BC (Menzione et al., 2023)	62
Figure 64. Multiple GNSS Receivers testing hardware-in-the-loop	63
Figure 65. Galileo and GPS Visibility (left) and SSV user ground track (right).....	64
Figure 66. GPS L1C/A and L5 Pseudoranges (left) and Carrier Phases (right)	65
Figure 67. Galileo E1C and E5a Pseudoranges (left) and Carrier Phases (right)	65
Figure 68. Navigation Solution Performance, ECEF position error (left) and ECEF velocity error (right)	65
Figure 69. GASPER configuration for EtE test with the GNSS receiver antenna	66
Figure 70. Results of the link frequency stability test (Bonenberg et al., 2023)	68
Figure 71. Satelles antenna on the roof of the building 72C in the Campus of JRC Ispra.....	68
Figure 72. Results of 101 day of time generation and OTA test on the Satelles platform.....	69
Figure 73. Example of referenced permanent points at the JRC site for kinematic tests.....	69
Figure 74. Outdoor (left hand side) and indoor (right hand side) experimental set up.	70
Figure 75: Block diagram of the JRC recording system for GNSS signals.....	72
Figure 76. Illustrative photographs capturing the interior and exterior of the JRC's van, showcasing the record and replay system employed in OSNMA test drives. These images depict the laptop, the NI-USRP 2944r device, the rubidium clock, and the PCI-to-Thunderbolt 3 adapter, highlighting their integration within the van's setup.	73
Figure 77. Detailed diagram depicting the record and replay system's configuration as a GNSS repeater with an adaptable time delay.....	74
Figure 79. Photograph of the setup used in the EMSL for the compatibility assessment with LightSquared (left). Observed loss of C/No versus power of the LTE signals with the three receivers tested and one of the proposed band allocations (right).	76
Figure 80. Snapshot of the real time spectrum analyser showing the narrow-band pulse interference signal, its power spectrum, power versus time, and power spectrogram.	77
Figure 81. Timeline showing the time intervals where the wide-band interference signal was present.....	77
Figure 82. Snapshot of the real time spectrum analyser showing the wide-band AWGN signal, its power spectrum, power versus time, and power spectrogram.	78
Figure 83. Spectrogram and power spectral density of a narrow-band sawtooth FM waveform, with a bandwidth of 10 MHz and a sweep time of 20 usec.	78
Figure 84. Spectrogram and power spectral density of a wide-band sawtooth FM waveform, with a bandwidth of 40 MHz and a sweep time of 20 usec.	79
Figure 85. Spectrogram and power spectral density of a narrow-band triangular FM waveform, with a bandwidth of 10 MHz and a sweep time of 20 usec.	79
Figure 86. 2D nominal-genuine trajectory with a rectangular shape.	81
Figure 87. Nominal-genuine Speed profile versus time.	81
Figure 88. Nominal-genuine heading versus time.	81

Figure 89. 3D genuine trajectory and meaconer location	82
Figure 90. Galileo spoofer signals power advance versus time.	83
Figure 91. Genuine trajectory, spoofer location and counterfeit trajectory.	84
Figure 92. Genuine and counterfeit speed profiles.....	84
Figure 93. Genuine and counterfeit trajectories.	85
Figure 94. Genuine and counterfeit speed profiles.....	86
Figure 95. Galileo spoofer signals power advance	86
Figure 96. Satellite high-resolution image of the campus of JRC Ispra Site (source: Google Earth).....	88
Figure 97. Examples of the test environments available on the JRC Ispra Campus.	89
Figure 98. Representation of the LI P57 "No Fly Zone" on the ENAV aeronautical map. This spatial area is under the control of JRC Ispra Site Manager.....	89
Figure 99. Tethered drone used in the flight trial (top-left), drone flying on the campus (top-right) and view from the on-board camera used for traffic monitoring (bottom). All photographs taken during the demonstration of the SARA Project in the campus of the JRC Ispra Site, on 1/10/2020.....	90
Figure 100. Example of repeatability test. On the left side the navigation device under test. On the right side, the reconstruction of the four laps performed by the user.	91
Figure 101. Example of indoor accuracy test. On the left side the navigation device under test. On the right side, the displacement of the control points.	91
Figure 102. North coordinate evolution as a function of time. The red dotted line indicates the position of the control points.....	92
Figure 103. Set-up developed for the VALOUR project data collection (left) and installation of the bike (right).	93
Figure 104. Preliminary LEO-PNT Test Bench Setup	94
Figure 105. Jammertest 2023 partcipants.....	95
Figure 106. Test Equipment: Antennas system (left) and Host PC with acquisition devices (right)	96
Figure 107. OPS-SAT trajectory and jammer location (left). Pre-computed elevation, azimuth and SNR for the given OPS-SAT passage (right).....	96
Figure 108. Power Spectral Density of the transmitted signal from ground (left) and recorded from OPS-SAT (right)	97
Figure 109. Photograph of one of the transmit antennas on the dome of the EMSL anechoic chamber (left); Polar plots of the RHCP and LHCP antenna gains at 1600 MHz (right).	98
Figure 110. 3-D sketch showing a possible arrangement of the 8 transmit antennas (coloured in red) on the dome of the EMSL (left); Close view of a 3-D sketch of a 7-element CRPA antenna mounted on the measurement tower (right).	98

List of tables

Table 1. Typical interactions between JRC and the project consortium requesting the facilitation of testing and demonstration activities.....	5
Table 2. Specification of the positioning ranges and accuracies of the four mechanical axes of the EMSL.....	8
Table 3. JRC-ISSVTB Scenario Configuration Overview.....	63
Table 4. NI and Ettus Research USRP devices list.....	71

GETTING IN TOUCH WITH THE EU

In person

All over the European Union there are hundreds of Europe Direct centres. You can find the address of the centre nearest you online (european-union.europa.eu/contact-eu/meet-us_en).

On the phone or in writing

Europe Direct is a service that answers your questions about the European Union. You can contact this service:

- by freephone: 00 800 6 7 8 9 10 11 (certain operators may charge for these calls),
- at the following standard number: +32 22999696,
- via the following form: european-union.europa.eu/contact-eu/write-us_en.

FINDING INFORMATION ABOUT THE EU

Online

Information about the European Union in all the official languages of the EU is available on the Europa website (european-union.europa.eu).

EU publications

You can view or order EU publications at op.europa.eu/en/publications. Multiple copies of free publications can be obtained by contacting Europe Direct or your local documentation centre (european-union.europa.eu/contact-eu/meet-us_en).

EU law and related documents

For access to legal information from the EU, including all EU law since 1951 in all the official language versions, go to EUR-Lex (eur-lex.europa.eu).

Open data from the EU

The portal data.europa.eu provides access to open datasets from the EU institutions, bodies and agencies. These can be downloaded and reused for free, for both commercial and non-commercial purposes. The portal also provides access to a wealth of datasets from European countries.

Science for policy

The Joint Research Centre (JRC) provides independent, evidence-based knowledge and science, supporting EU policies to positively impact society



EU Science Hub

joint-research-centre.ec.europa.eu



@EU_ScienceHub: ec.europa.eu/jrc



EU Science Hub – Joint Research Centre



EU Science, Research and Innovation



EU Science Hub



@eu_science



Publications Office
of the European Union